UNIVERSITÀ
DEGLI STUDI
DI PADOVA

UNIVERSITÀ DEGLI STUDI DI PADOVA

DIPARTIMENTO DI INGEGNERIA INDUSTRIALE

CORSO DI LAUREA MAGISTRALE IN INGEGNERIA MECCANICA

SET-UP AND CALIBRATION OF A TEST ROOM FOR INDOOR ENVIRONMENTAL QUALITY ANALYSIS

Relatore: Prof. Antonino Di Bella

Correlatori: Prof. Michele De Carli

Ing. Giulia Alessio

Laureando: TOMMASO SASSONE

ANNO ACCADEMICO 2018/2019

INDICE

ABSTRACT

In the summer of 2016 the "Unified Indoor Climate Group" was founded, composed by the Departments of Engineering and Psychology of Padua, with the purpose of studying, setting up and measuring thermal and interactive indices within a climate chamber destined to be used as a working environment (office). This project represents the beginning of an activity aimed at recognizing the effects of environmental parameters on the productivity of people and their perception of the working environment, according to different typical parameters of a room (such as furniture, natural and artificial lighting, climatic devices, etc.). Conditions of a workplace will be reproduced considering the engineering aspects (structures, climate, indoor air quality, etc.), accompanied by statistical and psychological analyses. To this end, a climate chamber was created on the 3rd floor of the Technical Physics building in the University of Padua. The present work represents the first step of the research for evaluating the Indoor Environmental Quality in this test room.

The thesis consists of three macro-topics:

- Research review;
- Detailed description of the laboratory and the technical room;
- Creation of a simulation model for the calibration of radiant systems.

The purpose of the review work is to provide a wide and exhaustive overview of the research carried out in terms of thermal comfort and Indoor Environmental Quality (IEQ), in particular focusing on the research methods used and on the parameters taken in account. Moreover, in parallel with the analysis of the most used research methods and the most evaluated parameters, a climate chambers research was carried out during the review.

The second part of this thesis consists of a detailed description of the laboratory and the technical room, analysing the geometry and the systems with which they are equipped. All the drawings represented were made using the software AUTOCAD®, after having personally carried out measurements inside the two rooms. Radiant systems (floor, ceiling and walls), mechanical ventilation system and all the hydronic systems for managing flow rates and supply temperatures are carefully described and

their main characteristics analysed. All the components present in the two rooms were designed, provided and installed by more than 20 companies from northern Italy.

Finally, following the method of the detailed energy balance of a room, the third part of this work aims at creating a simulation model in steady-state conditions that allows to determine the internal surface temperatures of the climate chamber (floor, ceiling, walls and windows) and the internal air temperature as a function of the external temperature, temperatures of the water into the six radiant systems and solar radiation (transmitted and absorbed). Furthermore, this model has been realized to carry out an analysis of the radiant asymmetry that occurs at different thermal conditions (hot / cold floor and hot / cold ceiling, according to the season considered). To do this, the hourly profile of the water temperature that flows inside floor or ceiling radiant systems was determined (depending on the thermal condition considered), respecting some conditions to be simulated, such as keeping constant the operative temperature inside the room, equal to the set-point value (26 °C in summer season, 20 °C in winter season).

RIASSUNTO

Nell'estate 2016 è stato fondato il "Gruppo Unificato di Climate Indoor", composto dai Dipartimenti di Ingegneria e Psicologia di Padova, con lo scopo di studiare, allestire e misurare gli indici termici e interattivi all'interno di una camera climatica destinata ad essere adibita ad ambiente lavorativo (ufficio). Tale progetto rappresenta l'inizio di un'attività volta a riconoscere gli effetti dei parametri ambientali sulla produttività delle persone e la loro percezione dell'ambiente lavorativo in funzione di diversi parametri tipici di una stanza (come il mobilio, l'illuminazione naturale e artificiale, i dispositivi climatici, ecc.). Verranno riprodotte le condizioni di un luogo di lavoro considerando gli aspetti ingegneristici (strutture, clima, qualità dell'aria indoor, ecc.), accompagnati da analisi statistiche e psicologiche. A questo scopo, è stata realizzata una camera climatica al 3° piano dell'edificio di Fisica Tecnica dell'Università di Padova. Questo lavoro di tesi rappresenta il primo passo della ricerca focalizzata sull'analisi della qualità ambientale interna (IEQ) della camera.

La tesi si compone di tre macro-argomenti:

- Revisione delle ricerche in materia di comfort;
- Descrizione dettagliata del laboratorio e del locale tecnico;
- Creazione di un modello di simulazione per la calibrazione dei sistemi radianti.

Lo scopo del lavoro di revisione è quello di fornire una panoramica ampia ed esaustiva delle ricerche effettuate in termini di comfort termico e qualità ambientale interna, in particolare concentrandosi sui metodi di ricerca utilizzati e sui parametri presi in considerazione. Di tutti gli articoli letti, 74 sono stati selezionati per un'analisi più dettagliata. Dalla ricerca letteraria è emerso che effettuare delle misurazioni in camere climatiche o in uffici esistenti in presenza di soggetti umani non è il metodo più comunemente utilizzato per valutare il comfort. La maggior parte delle ricerche predilige la simulazione numerica e si concentra solo ed esclusivamente sull'analisi del comfort termico, trascurando altri aspetti come il comfort acustico, il comfort luminoso e la qualità dell'aria. Tuttavia, dobbiamo tenere a mente che per una valutazione globale della qualità dell'ambiente interno, anche l'analisi dei parametri igrometrici, acustici e di qualità dell'aria è fondamentale, perché sono strettamente correlati al benessere e ai problemi di salute delle persone (ad es. *sindrome*

dell'edificio malato). Gli aspetti psicologici e produttivi degli occupanti non vengono quasi mai presi in considerazione. Pertanto, l'approccio multidisciplinare proposto non riscontra alcuna similarità con tutte le ricerche indagate. Grazie a questo progetto, infatti, l'obiettivo è colmare la lacuna emersa in letteratura, a causa della specificità delle ricerche svolte fino ad ora. Parallelamente all'analisi dei metodi di ricerca più utilizzati e dei parametri più valutati, durante la revisione è stata condotta una ricerca sulle camere climatiche. L'obiettivo di questa indagine è confrontare le dimensioni caratteristiche (superficie in pianta e volume) della nostra sala prove con le altre descritte negli articoli analizzati, e quindi selezionare quelle geometricamente simili al fine di determinare possibili termini di paragone per i risultati che si otterranno in futuro. Da questo confronto sono state identificate cinque camere climatiche geometricamente simili a quelle costruite a Padova, quattro esistenti e una simulata.

La seconda parte di questa tesi consiste in una descrizione dettagliata del laboratorio e del locale tecnico, analizzandone la geometria e gli impianti di cui sono equipaggiati. Tutti i disegni rappresentati sono stati realizzati utilizzando il software AUTOCAD®, dopo aver effettuato personalmente le misurazioni all'interno delle due sale. Gli impianti radianti (pavimento, soffitto e pareti), il sistema di ventilazione meccanica e tutti i sistemi idronici per la gestione delle portate e delle temperature di alimentazione sono descritti accuratamente e le loro principali caratteristiche analizzate. Tutti i componenti presenti nelle due stanze sono stati progettati, forniti e installati da più di 20 aziende del nord Italia. Per questo motivo, nelle università italiane ed europee non esistono corrispettivi simili al laboratorio realizzato, grazie anche alla multidisciplinarietà degli aspetti affrontati simultaneamente.

Seguendo il metodo del bilancio energetico dettagliato di una stanza, la terza parte di questo lavoro mira a creare un modello di simulazione in condizioni stazionarie che permetta di determinare le temperature superficiali interne della camera climatica (pavimento, soffitto, pareti e finestre) e la temperatura interna dell'aria in funzione della temperatura esterna, delle temperature dell'acqua nei sei impianti radianti e della radiazione solare (trasmessa e assorbita). Inoltre, questo modello è stato realizzato per effettuare un'analisi dell'asimmetria radiante che si verifica in diverse condizioni termiche (pavimento caldo / freddo e soffitto caldo / freddo, a seconda della stagione considerata). Per fare ciò, è stato ricavato il profilo orario della temperatura dell'acqua che scorre all'interno degli impianti radianti a pavimento o a soffitto (in base alla

condizione termica considerata), rispettando alcune condizioni in fase di simulazione, come ad esempio mantenere la temperatura operativa all'interno della stanza costante e pari al valore nominale (26 °C nella stagione estiva, 20 °C nella stagione invernale).

È stato deciso di selezionare tre giorni per effettuare le simulazioni del modello, caratterizzati dalle seguenti condizioni:

- Giorno estivo: 18 luglio (5.00-20.00). Alte temperature e alta radiazione solare;
- Giorno invernale: 15 febbraio (7.00-19.00). Basse temperature e alta radiazione solare;
- Giorno invernale: 28 dicembre (7.00-19.00). Basse temperature e bassa radiazione solare.

Ripetendo sistematicamente alcune operazioni di inserimento dati nel foglio di calcolo Excel, sono stati determinati i profili orari della temperatura dell'acqua, utili per una futura calibrazione degli impianti radianti. Questo profilo di temperatura dell'acqua infatti rappresenta sostanzialmente i valori delle temperature di compensazione al fine di soddisfare le condizioni iniziali imposte al modello (ad esempio temperatura operativa costante). Confrontando i valori e gli andamenti dei profili ottenuti, è possibile notare l'elevata influenza che la radiazione solare ha sulla temperatura dell'acqua, tanto che, nella simulazione del secondo giorno, le temperature scendono al di sotto della condizione di neutralità di una superficie (in riscaldamento condizione pari a 20 °C) per un breve periodo di tempo.

Per quanto riguarda l'analisi dell'asimmetria della temperatura radiante, tutti i valori ottenuti rientrano nei limiti stabiliti dalla norma EN ISO 7730, in particolare la condizione di soffitto caldo, considerata come la causa di massimo discomfort. Il passo successivo sarà quello di determinare la differenza di temperatura massima che è possibile raggiungere nella condizione soffitto caldo / pavimento freddo, mantenendo la temperatura operativa costante al valore di set-point, al fine di eccedere i valori limite previsti dalla normativa.

I risultati ottenuti dal modello teorico saranno verificati mediante misurazioni non appena sarà garantito il funzionamento della camera climatica. Inoltre, saranno utilizzati per calibrare e impostare i diversi impianti radianti al fine di eseguire test

sperimentali in presenza di persone sull'asimmetria radiante e sulla qualità dell'ambiente interno.

In futuro infatti, la sala sarà adibita ad ufficio per 4 persone al fine di testare il comfort e la qualità dell'ambiente percepito dagli occupanti al variare dei parametri ambientali. Ai partecipanti sarà richiesto di svolgere determinate mansioni, tipiche di un ambiente lavorativo (ad esempio attività al computer, ecc.) al fine di valutarne la produttività, e di dare un loro giudizio sulle condizioni ambientali a cui sono sottoposti.

Nell'immagine sottostante è rappresentata un'ipotetica configurazione della camera climatica adibita ad ufficio.

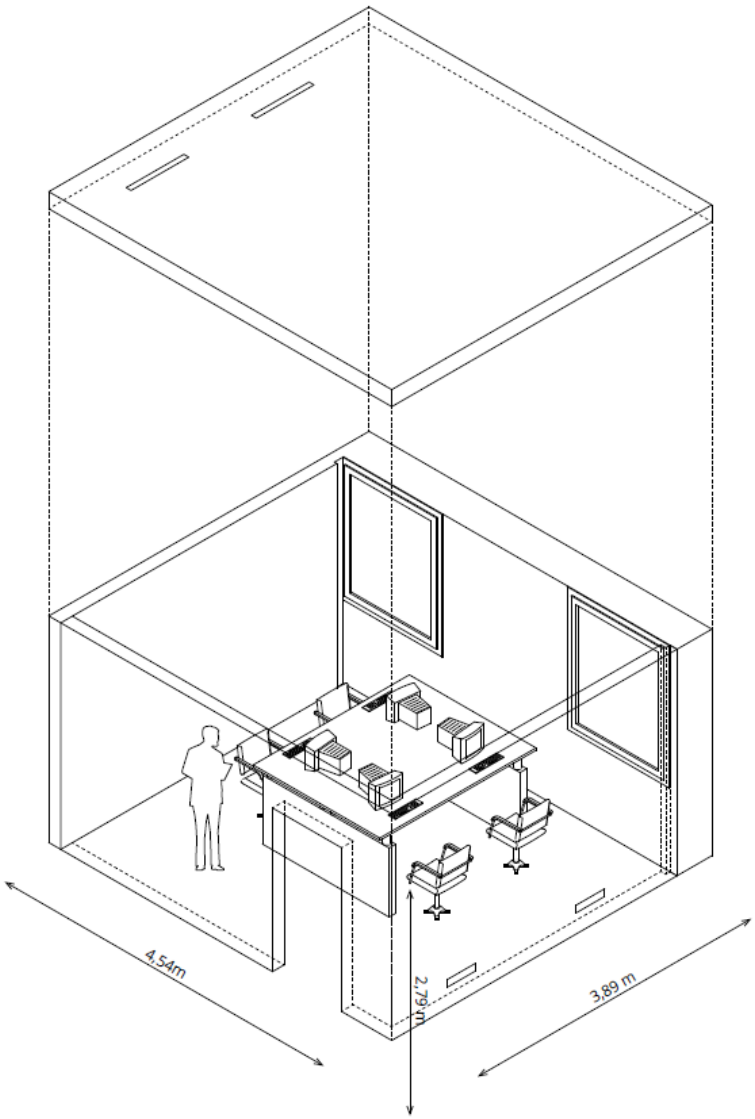

Fig. 0. *Ipotetica configurazione della camera adibita ad ufficio*

Chapter 1

RESEARCH REVIEW

1.1. Introduction

Thermal comfort is an important aspect regarding the satisfaction of occupants with their environment, and it is considered as an important building performance indicator. This term is used to describe a satisfactory, stress-free thermal environment in buildings, but also, according to Health and Safety Executive (HSE) [1], it describes a person's state of mind in terms of whether he/she feels hot or cold. Therefore, thermal comfort is a complex phenomenon and a subjective concept. This is due to the large differences between persons, both psychological and physiological; moreover, environmental factors (such as humidity and sources of heat, wind, etc.), combined with personal factors (such as clothing and work-related factors), influence the thermal comfort feeling [1]. The interaction of these factors makes the term "thermal comfort" difficult to define. However, during the design phase of a building it is useful to predict the thermal comfort of the occupants in advance, because humans spend 80-90% of the day indoors [2], and it is necessary that buildings be designed in such a way that sufficient comfort is provided. Infact, the main function of a building is to create a healthy and comfortable indoor environment for its occupants. The good building design characteristics might be summarized as follows [3]:

- meets the purpose and needs of the building's owners and occupants;
- meets the requirements of health, safety and environmental impact as prescribed by codes and recommended by standards;
- achieves good indoor environment quality, which consists of high quality in the following dimensions: *thermal comfort, indoor air quality, acoustical comfort, visual comfort*;
- creates an emotional impact on the building's occupants and beholders.

In the early 21th century, building systems, i.e. heating, ventilation, air-conditioning (HVAC) and lighting, have been developed to provide and maintain a comfortable environment for human occupancy. As a consequence, today, the energy required for this, contributes to about 30-40% of the total energy consumption of buildings

[4]. Reducing energy demand through optimal operation is the subject of building control research, while human satisfaction in buildings is studied in the thermal comfort community. Thus, balancing the two is necessary for a sustainable and comfortable building stock. Both research fields are inherently multidisciplinary, but have been generally analyzed independently, or focused on specific examples. However, energy efficient operation cannot be achieved without considering human comfort. Nevertheless, building systems and technology focuses predominantly on energy-savings rather than incorporating results from thermal comfort.

The purpose of this review is to provide a wide and exhaustive overview of the research carried out in terms of thermal comfort and Indoor Environmental Quality (IEQ), in particular focusing on the research methods used and on the parameters taken in account.

The publications based on the research methods used have been classified in five categories:

- Physical measurements in laboratory test (climate) chamber;
- Physical measurements in building;
- Building performance numerical simulation;
- Human subject testing;
- Occupant-based survey.

This classification scheme has been used because it allowed us to distinguish simulated, measured and subjectively perceived comfort. When one article had more than one method, it has been decided to classify the publication in more than one single category. Moreover, for each of these articles, it has been analyzed which parameters have been taken in account to evaluate the indoor environmental quality, the year of publication and the country in which the research has been performed.

The parameters that have been considered are the following:

- Thermal;
- Hygrometric;
- Acoustic;
- Indoor Air Quality (IAQ);

- Physiological;
- Comfort/Discomfort;
- Productivity.

1.2. Research overview

1.2.1. Review method

For the literature review, papers published from 1972 to 2018 were searched, using predominantly Google Scholar database. The most used keywords for the search were the following: “thermal comfort”, “indoor thermal comfort”, “thermal comfort assessment”, “indoor environment”, “IAQ (indoor air quality)”, “IEQ (indoor environmental quality)”, “thermal satisfaction”, “thermal sensation”, “radiant systems”, “local discomfort”, “radiant asymmetry”, “occupant comfort and productivity”. With this method, a large number of research articles were collected as reference list. From this reference list, the articles that have a direct relation with thermal comfort and possibly radiant systems were choosen, based on title, abstract and conclusions. After that, the most interesting 74 papers were selected for more detailed analysis.

1.2.2. Historical and regional distribution of researches trend

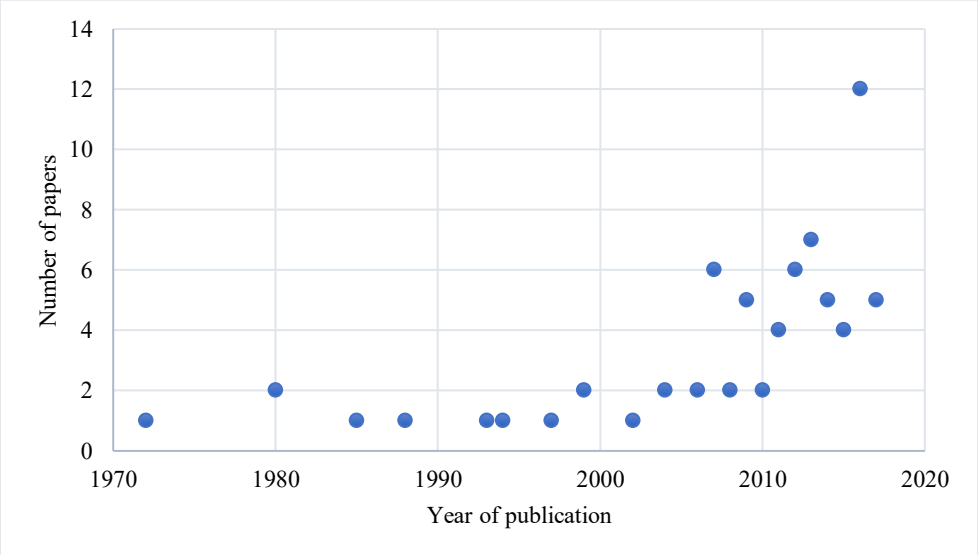

Fig. 1. *Annual number of published articles*

Before focusing on the key aspects related to the problem of thermal comfort, it is important to analyze the historical research trend and the regional distribution of researches. As stated previously, in the early 21th century, building systems have been developed in order to improve indoor environment for human occupancy. Consequently, there has been a growing interest in studying and characterizing the heat transfer performances and the thermal comfort provided by such systems [5]. This trend is confirmed by the analysis of the annual number of published articles, as shown in Fig. 1, which demonstrates the growing interest in recent years. This growing is also confirmed by the results of two review articles analyzed during the selection: Rhee and Kim (2015), Park and Nagy (2017). Instead, regarding the most active nations in the research and development of systems that guarantee thermal comfort in buildings, the regional distribution of research is shown in Fig. 2. As we can see, the thermal comfort researches are widespread in European countries, North America and East Asia. For this reason, it is possible to state that the study and analysis of this problem, although not yet particularly widespread, has been dealt with in different climatic conditions, even in the presence of hot and humid climates that may represent a limitation regarding problems of condensation.

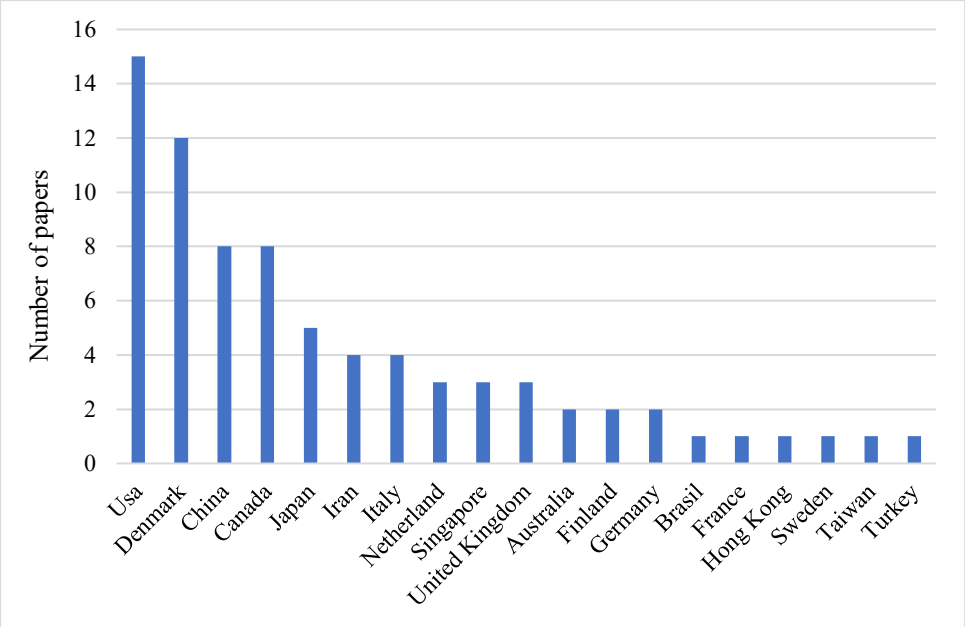

Fig. 2. *Regional distribution of researches*

1.3. Research methods classification scheme

As stated previously, the publications based on the research methods used have been classified in five categories:

- Physical measurements in laboratory test (climate) chamber;
- Physical measurements in building;
- Building performance numerical simulation;
- Human subject testing;
- Occupant-based surveys.

This classification scheme has been used because it allowed us to distinguish simulated, measured and subjectively perceived comfort.

For *physical measurements in laboratory test (climate) chamber* are considered those measurements made in a certified and controlled test facility, without the presence of any human subject. Very often these rooms are configured in such a way as to simulate a common office, equipped with a heating/cooling system and in which there are numerous internal loads (occupants, PC and lighting). In order to simulate the presence of occupants are used heated dummies with simplified geometry or thermal manikins with realistic body geometry.

For physical measurements in building are considered those measurements consisting of continuous monitoring campaigns carried out in real office buildings for long periods of time (a year or more) and in different climate conditions.

For *building performance numerical simulation* are considered those measurements made with the aid of computational fluids dynamics (CFD) software or whole building energy simulation software (e.g., EnergyPlus or TRNSYS). This type of measurements are made by creating a model of the analyzed environment in the calculation software. Once realized, it is possible to vary the different parameters of the environment (size and materials, temperature, heating/cooling system, ventilation system, internal loads) in order to carry out a quick and complete study in different conditions and configurations. Generally, numerical simulations are a useful analysis tool when it is not possible to performe physical measurements or in order to validate an experimental model.

For *human subject testing* are considered those measurements made in a laboratory test chamber or in existing office with the presence of human subjects, in different environmental conditions. Thanks to the presence of occupants, not only objective measurements but also physiological are carried out. This research method is generally coupled with subjective measurements through the use of surveys and questionnaires, but sometimes it is also used to compare the results with simulation models.

For *occupant-based surveys* are considered those measurements carried out in order to investigate subjective sensations on the surrounding environment through the compilation of questionnaires. This research method is particularly useful because it allows to correlate objective measurements with the subjective perception of indoor environment and thermal comfort. Generally, in these tests, the occupants are exposed to different experimental conditions for predetermined time intervals. During these periods, they are asked to fill out a series of questionnaires related to their satisfaction with indoor environment and sometimes to perform different tasks in order to investigate the influence of environmental conditions to the productivity.

1.4. Evaluated parameters classification scheme

Standards ISO 7730 [6] and EN 15251 [7] recommend maximum values for the indoor thermal climate parameters (for both whole body thermal sensation and local thermal comfort, air and operative/mean radiant temperature, air velocity, etc.) for winter and summer conditions in order to achieve thermally comfortable indoor environment for occupants. Nevertheless, it is necessary to consider the delicate question of which metrics can be used to assess thermal comfort. In this section we analyze the comfort metrics that are relevant for our review. Metrics are classified into two categories: *objective metrics* (based on physical measurements) and *subjective metrics* (based on occupant feedback).

1.4.1. Objective metrics

One common way to quantify thermal comfort is consider *temperature parameters*, through the measure of dry-bulb air temperature, globe temperature, mean radiant temperature (MRT) (derived from the globe temperature), and operative temperature (calculated using dry-bulb air temperature and MRT). However, sometimes more specific parameters are

considered, such as cooling capacity, thermal response time and heat transfer.

Another commonly used method is the *predicted mean vote (PMV)*, a comfort model established to predict thermal sensation from "cold" to "hot". This objective metric was developed by Fanger [8], in 1972, which studied the thermal conditions necessary to achieve thermal comfort. His studies resulted in the PMV index, expressed as the predicted thermal sensation on the 7-point ASHRAE thermal sensation scale (ranges from -3 [cold] to +3 [hot] with the value of 0 set as neutral) [9], under uniform environmental conditions for a group of persons. This index is based on the heat balance equation on the human skin [10] and correlated to environmental parameters (air temperature, mean radiant temperature, air speed, humidity), activity level (metabolic rate) and clothing insulation. The PMV model is complemented with the Predicted Percentage of Dissatisfied (PPD) people model [10], and the combined PMV-PPD model is currently used in standards, such as ASHRAE-55 [9] and ISO 7730 [6]. In particular, in the ISO 7730 as well as in the EN 15251, this model is used to define three categories of thermal requirements for mechanically cooled buildings: *category I* (or *class A*) (PPD < 6%, i.e. -0.2 < PMV < +0.2), *category II* (or *class B*) (PPD < 10%, i.e. -0.5 < PMV < +0.5) and *category III* (or *class C*) (PPD < 15%, i.e. -0.7 < PMV < +0.7).

The PMV and the PPD express the thermal comfort for the human body as a whole. However, thermal dissatisfaction can also be caused by a thermal discomfort of a part of the body. For this reason, in the standards are indicated *four local discomfort factors* that are particularly relevant for radiant systems:

- *Draft risk* is defined as an unwanted local cooling of the body caused by air movement. This kind of discomfort depends on three variables: air temperature, mean air velocity, and turbulence intensity. Based on human subject testing, this model was converted into percentage of dissatisfied for draft (PD_{Draft}) and is applied to people who perform light activity, especially sedentary with a global

thermal sensation close to neutrality. Infact, the discomfort is less for activities with higher energy metabolism than the sedentary lifestyle and for subjects who feel a sensation of heat rather than neutrality. Finally, this model predicts well the draft risk in the neck, but instead it could overestimate the prediction of discomfort for arms and feet; this is the reason why it has been removed from ASHRAE 55 [9].

- *Vertical air temperature difference* (*stratification*) is another local factor that can cause discomfort. Its evaluation is made throuht the percentage of dissatisfied for vertical air stratification ($PD_{Vertical}$), a correlation established to consider vertical air temperature difference between head and ankles. This model, described in stardards EN ISO 7730 [6] and ASHRAE 55 [9], is valid for temperature differences between head and feet below 8 °C. In particular, the EN ISO 7730 [6] proposes as a limit a gradient of 3 °C/m (*class B*), which corresponds to a dissatisfied percentage less than 5%. Finally, this metric only applies for head temperature being higher than feet temperatures (people are less sensitive under opposite conditions).
- *Radiant asymmetry* is defined as the difference between the plane radiant temperature of the two opposite sides of a small plane element (*the plane radiant temperature is the temperature coming from the perpendicular direction to the measuring surface*). It is usually evaluated comparing temperatures of two opposing surfaces of a room. This kind of discomfort can derive from the presence of surfaces with a temperature different from the environmental one, as in the case of glazing, non-insulating walls, machinery, hot or cold radiant panels on walls, floors or ceilings. In particular, both EN ISO 7730 [6] and ASHRAE 55 [9] define limits of radiant asymmetry when using radiant walls, floors and ceilings based on percent dissatisfied curve.
- *Floor temperature* can be too low or too high and then cause discomfort. The cause of this is due to the heat exchange between the body and the floor through the feet. The factors that influence this

discomfort are the floor temperature, the thermal conductivity and the thermal capacity of the material of which the floor is covered, the type of footwear worn and the time spent. The model for the determination of the percentage of dissatisfied for hot and cold floors described in standards (EN ISO 7730 [6] and ASHRAE 55 [9]) has been obtained from studies on people standing and / or in a sedentary state with footwear. The limits proposed by both standards in winter season range between 19 °C and 29 °C (*class B*), which corresponds to a dissatisfied percentage that is less than 10%. There are no limits for summer season.

It is important to underline that this type of local discomfort was not taken into consideration in the review analysis carried out, because in many of the articles analyzed the focus was mainly on problems related to vertical air stratification or radiant asymmetry between walls.

Human physiological measurements have been also taken into account. Infact in the review, we found laboratory studies focusing on different body part temperatures (i.e. skin temperature, core (intestinal) temperature, rectal temperature) or diagnostic tests as electrocardiogram (ECG to determine HRV) and electroencephalograph (EEG). These measurements can be used as input to detailed comfort models (such as the Advanced Thermal Comfort Model [11]), which can then be used to predict local and overall thermal comfort.

Not only the overall and local thermal comfort of occupants, but also *indoor air quality (IAQ)* is an important aspect, in particular regarding ventilation system design. Continuous and spot measurements of the main indoor air pollutants have been performed in some of the experiments analyzed. The most evaluated parameter has been the carbon dioxide (CO_2) concentration, but it has been also consider the total volatile organic compounds (TVOCs), respirable suspended particles (RSP) and the Air Change Effectiveness (ACE), related to the contaminant removal efficiency.

Finally, *acoustic* and *hygrometric measurements* have been investigated. Generally, these parameters have never been taken into consideration individually, but to complete the overall analysis of indoor environment quality (IEQ). When we talk about acoustic measurements, we mainly refer to equivalent sound level (L_{eq}), equivalent sound absorption area (A - Sabin formula) and reverberation time, parameters that contribute to guarantee good acoustical comfort. On the other hand, the most considered hygrometric parameter is relative humidity, that is the percentage of water vapor present in the air. Proper dehumidification is essential, as it can sometimes reduce the sensation of heat without lowering the temperature too much. However, the reduction of humidity should not be excessive: the optimal values of relative humidity are between 40% and 60% in order to avoid the risk of diseases caused by excess moisture, but the percentage must not fall below 35%.

1.4.2. Subjective metrics

A common way to investigate general perception of indoor environment and thermal comfort is throught surveys, in which occupants can express their subjective sensations.

Thermal Sensation Vote (TSV) is a 7-point ASHRAE interval scale going from -3 (cold) to +3 (hot), with the value of 0 set as neutral, to rate thermal sensation. Vote refers to human subjects filling out a thermal sensation scale during the exposure to certain thermal conditions at a given point in time. It's important to specify that TSV can be conducted for whole body (global) sensation as well as for local sensation.

Another commonly used method is the *Thermal Comfort Vote (TCV)*, a scale to rate thermal comfort from "uncomfortable" to "comfortable". This vote is commonly set on the ISO-defined 4-point scale ("uncomfortable", "slightly uncomfortable", "slightly comfortable", "comfortable"), where the value of 0 is unavailable, but however in some publications is assumed a 5-point scale that included a "neutral" comfort vote. This type of metric is generally used in right-now survey (at a given point in time) or background surveys (in general). Finally, as the previous one, TCV can be

conducted for whole body (global) as well as for local body parts.As we realized in the review carried out, sometimes the subjective evaluation of an environment is not only limited to thermal comfort, but also concerns the general perception of the indoor environmental quality (IEQ) of a building. For this reason, in many publications typical surveys on thermal comfort include questions on *perceived indoor air quality*, *acoustical comfort* (noise level), *visual comfort* (lighting) and *health problems* (Sick Building Syndrome symptoms). Moreover, one particular aspect that is often investigated is the relationship between *self-reported performance/productivity* and the indoor environment. Some research results infact, showed that the indoor environment has the biggest influence on productivity in relation to the job stress and job dissatisfaction [12]. This relationship can be estimated in terms of motivation and well-being of office workers, or above all in terms of task performance. In many publications in fact, the effect of indoor environment on productivity of office workers has been systematically and comprehensively assessed by

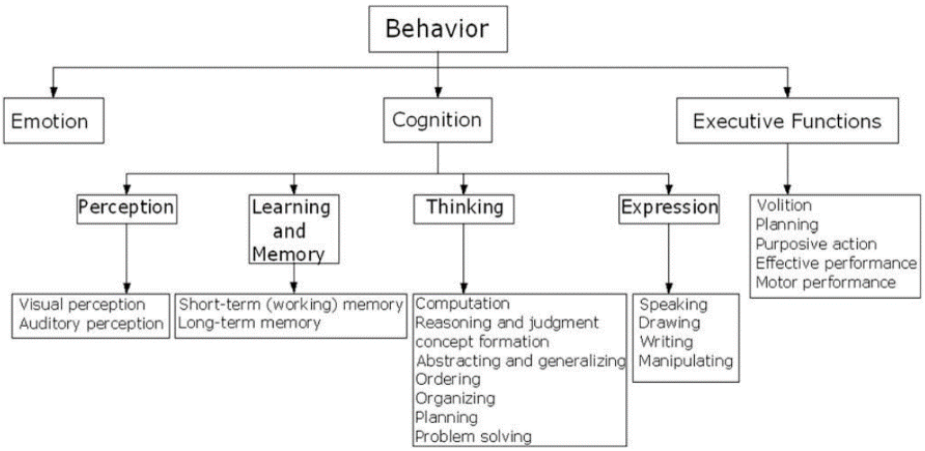

***Fig. 3**. A neurobehavioral framework for evaluation of productivity of office work*

testing their neurobehavioral functions, with different test batteries performed during the experimental procedures. In these tests, has been evaluated different capacities of human being, cognitive and executive functions, as perception, thinking, memory and learning. From the results obtained, various considerations have been subsequently extrapolated regarding the impact of the indoor environment in decision-making

performance. A descriptive framework of these neurobehavioral functions is illustrated in Fig. 3 [13].

1.5. Classifications results

As stated previously, of the all papers reviewed, 74 were selected. In this section we analyze the results of the research methods classification and the evaluated parameters classification that we have obtained in our review. Moreover, remember that when one article had more than one method, it has been decided to classify the publication in more than one single category.

1.5.1. Research methods classification

In Fig. 4, results of the research methods classification are summarized. As we can see, the most used method is the numerical simulation (*29 references*), while the least taken into consideration is the physical

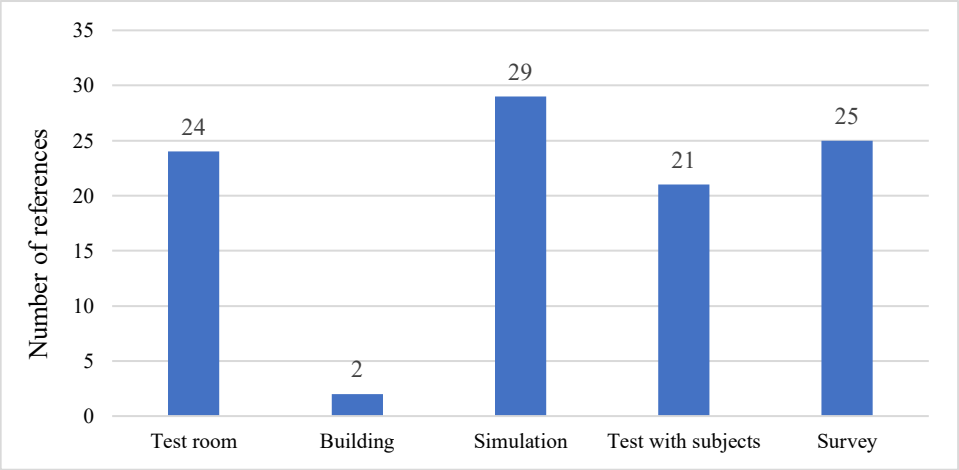

Fig. 4. *Research methods classification*

measurements in existing buildings (*2 references*). The remaining three methods instead attest to the first, with numerous references. The main reasons for this disparity are certainly attributable to their different analysis procedure. Performing a numerical simulation, in fact, allows to obtain the results in a short period of time and above all to carry out a complete study in different configurations and environmental conditions, through the variation of multiple parameters. Conversely, continuous monitoring campaigns require particularly long periods of time (a year or more) in order to obtain the same results.

1.5.1.1. Physical measurements in laboratory test chamber

We found 24 studies that were fully or partially based on physical measurement in laboratories. Dominguez et al. [14] conducted an experimental and numerical study in order to quantify the effects of horizontal and vertical free-hanging sound absorbers on the cooling performance of TABS (Thermally Active Building Systems) and on the thermal indoor environment. The experiments were carried out in a climate chamber configured as a two-person office room located at the Technical University of Denmark (DTU), equipped with floor and ceiling TABS decks to obtain realistic conditions of a multi-story building with TABS. The room had a balanced ventilation system that was capable of providing airflow at a defined flow rate and temperature. Different ceiling coverage ratios were tested. The results showed that the use of vertical sound absorbers has a less pronounced effect on the cooling performance of TABS and, therefore, a lower effect on the thermal indoor environment. Cold air stagnation in the plenum and the consequent decrease in convective heat exchange between the occupied zone of the room and the TABS has been identified as the major cause of the reduction in cooling performance of TABS when horizontal panels were used. The developed simulation model compared to experimental measurements, was able to predict closely the cooling performance reduction of TABS, the ceiling surface temperature, and the thermal indoor environment in most cases. Olesen et al. [15] conducted an experiment of a small office (or study room) with one simulated outside wall. Nine heating systems were tested, including: radiant ceiling, radiant floor, air distribution system, convectors and radiators. The test room was located at the Laboratory of Heating & Air Conditioning of the Technical University of Denmark. Four tests were made with each heating method. The results revealed that all nine heating systems proved in all tests to be capable of creating a remarkably uniform thermal environment (PPD ≈ 5%) in the entire occupied zone. In all tests, vertical air temperature differences, radiant temperature asymmetry and floor temperatures were inside established

comfort limits. There was a risk of mean air velocities higher than 10 cm/s along the floor in the occupied zone nearest to the frontage when the down-draft along the window and from the air infiltration was not counteracted by an upward convection from the heating system. Kulpmann et al. [16] performed thermal comfort and air quality experiments in a laboratory chamber equipped with a radiant ceiling and displacement ventilation (DV) system. The aim of this study was to investigated the effect of varying the cooling capacity shares of the cooled ceiling and the ventilation system. The vertical profile of the room temperature was more pronounced when the load was covered with the ventilation system. Air quality investigation instead, showed that combination of DV with cooled ceiling induced a mixing of air within the space and could not ensure a safe displacement of air-transported pollution into the respiration area. Schiavon et al. [17] tested a similar combination of radiant ceiling and DV. The purpose of this study was to conduct laboratory experiments for a typical U.S. office to investigate how room air stratification is affected by the ratio of cooling load removed by a chilled ceiling to the total cooling load, for two different chilled ceiling configurations. The experiments were carried out in a climatic chamber equipped with radiant panels installed in the suspended ceiling. The authors observed that room air stratification in the occupied zone decreases when a larger portion of the cooling load is removed by the chilled ceiling. In all cases, the temperature difference between head and ankle stayed below 3° C, which satisfies standards requirements. In a second paper [18], the same authors conducted laboratory experiments to investigate the influence of high cooling load (91.0 W/m2) and two different heat source heights (at floor level and at 1.52 m) on thermal stratification and air change effectiveness. The experiments were carried out in a climatic chamber located at Center for the Built Environment, University of California, Berkeley. The results showed that displacement ventilation with a chilled ceiling is able to provide a stable thermal stratification and improved ventilation effectiveness compared to mixing ventilation for a wide range of configurations. In particular, stratification and air change effectiveness

decreases when a larger portion of the cooling load is removed by the chilled ceiling. Finally, increasing the height of heat sources has the potential to reduce energy use and improve indoor air quality. Corgnati et al. [16] used a combination of experimental and numerical methods to assess an all-air mixing ventilation system alone or coupled with radiant ceiling panels in an office environment. The experiments were carried out in a test room configured as a two-person office, equipped with an all air mixing ventilation system (the radiant system was not part of the experimental set-up) and realised inside the Highly-Insulated Full Scale Test Room of the Building Technology and Structural Engineering Department at Aalborg University (DK). The results obtained from the experimental campaign were used to validate a CFD model. These numerical studies were then extended to the coupled mixing ventilation and cold radiant ceiling panels. In particular, attention was drawn on the evaluation of the main supply jet properties (throw and penetration length) and on the draft risk caused by the cold air drop into the occupied zone. The results obtained demonstrate that the use of a primary air mixing and cold radiant ceiling panels coupled systems lead to an improvement of comfort in comparison to a system without radiant panels. Infact, there was an increase of the jet longitudinal throw and smaller vertical drop, and significant decrease of the draft risk (PDdraft) due to the jet direct drop. Mustakallio et al. [19] conducted laboratory experiments in order to compare the performance of four systems based on radiant and convective cooling with regard to the generated thermal environment and human response. These cooling variants tested were: chilled beam (CB), chilled beam with radiant panel (CBR), radiant ceiling panels with ceiling installed mixing ventilation (CCMV) and four desk partition-mounted local radiant cooling panels with ceiling installed mixing ventilation (MVRC). Measurements were performed in a climate chamber, modeled as a 2-person office and as a 6-person meeting room, in which the presence of six occupants was simulated by four heated dummies with simplified geometry and by two thermal manikins with realistic female body geometry. Two cooling conditions were simulated: design (maximum) heat load-64 W/m^2

(office room) and 85 W/m^2 (meeting room), and usual heat load-37 W/m^2 (office room) and 71 W/m^2 (meeting room). The results revealed that the differences in the thermal conditions achieved with the four systems were not significant. The air temperature and globe (operative) temperature differed up to 0.2 °C. Vertical temperature in all systems was less than 1 °C and radiant temperature asymmetry less than 5 °C in all systems. CB and CBR provided slightly higher velocity level in the occupied zone. The operative temperature in the studied cases with chilled ceiling in operation with mixing ventilation was almost the same as the operative temperature obtained with the active chilled beam (i.e. only convective cooling). The heat load distribution played major role for the airflow pattern in all studied systems. Jia et al. [20] conducted laboratory experiments in order to characterize the behavior of radiant cooling systems in a typical office environment, including the effect of ceiling fans on stratification, the variation in comfort conditions from perimeter to core, control on operative temperature vs. air temperature and the effect of carpet on cooling capacity. The goal of this study was to limit both the first cost and the perceived risk associated with such systems. The experiments were carried out in one of the test cells of the Facility for Low Energy eXperiments (FLEXLAB) at the Lawrence Berkeley National Laboratory (LBNL). Two types of radiant systems, the radiant ceiling panel (RCP) system and the radiant slab (RS) system (floor), were investigated. In total, ten test cases (five for RCP and five for RS) were performed, covering a range of operational conditions (the ventilation system was not used in this study). The results of this reported study showed that both radiant ceiling panel (RCP) and radiant slab (RS) cooling systems can provide thermal comfort at the moderate zone cooling loads. In cooling mode, the air stratification effect was significantly greater in the RS system than in the RCP system The use of ceiling fans was able to reduce any excess stratification and provide better indoor comfort. Modest variations in comfort conditions were observed near unshaded south-facing windows. In the RCP system, the difference between the operative temperature and air temperature is quite small if the loads can be met by the RCP system; for this reason, it

is possible to use air temperature as the controlled variable input to the zone temperature controller instead of the operative temperature, with significant cost savings. In the RS system, the use of thin carpet requires the supply chilled water temperature to be reduced by ∼1.0 K, with a corresponding reduction in the opportunities for free cooling and an increase in condensation risk. Karmann et al. [21] conducted two laboratory studies in order to experimentally assess the effect on radiant ceiling system cooling capacity for various coverage areas of free-hanging acoustic clouds and determine the change in sound absorption for the same configuration. The cooling capacity experiments was carried out in a certified controlled climatic chamber (Price Industries in Winnipeg, Manitoba, Canada), while the sound absorption experiments in a certified reverberant chamber (Armstrong World Industries in Lancaster, PA, USA). For the first part of analyss, the test room was modeled as a 4-person office, equipped with twelve radiant ceiling panels but without any ventilation system. The main conclusions of this study were that the cooling capacity coefficient slightly decreases when the ceiling cloud coverage increses. This reduction is on average 4–5 times less than the percentage coverage. The difference observed between air temperature and mean radiant temperature is less than 1 °C. This implies that measuring operative temperature or mean radiant temperature may not be needed in radiantly conditioned buildings. The acoustical clouds exhibited the greatest sound absorption between 200 and 2500 Hz. The sound absorption per cloud slightly decreases with increasing number of clouds. Compared to exposed concrete, our tested cloud variants resulted in a substantial reduction of reverberation time. The acoustic results showed that if the clouds covered 30% of the ceiling in a private office or 50% in an open plan space, acceptable sound absorption at the ceiling was achieved. To sum up, this study demonstrated that good acoustic quality can be achieved with only a minor reduction of cooling capacity. Ning et al. [22] conducted an analysis of the cooling capacity and surface temperature distribution for cooling radiant ceiling panel (CRCP) systems with CFD method for heat transfer simulation and experimental data to verify the reliability of

the simulation propose. Moreover, they proposed three improved panel types with reduced air thickness to elevate the cooling capacity and retain uniform temperature distribution. The experiments were conducted in a controlled environment chamber in Zhuhai, China, equipped with a ventilation system. The results were that when maintaining the same minimum surface temperature for condensation control, cooling capacities of the improved panels were found to be increased by over 40% compared to the original one and larger (18.9%) than general CRCP type, while the surface temperature distribution were very uniform. Bauman et al. [23] reviewed current cooling load calculation methods and then described the results of simulation and experimental studies addressing the sensible zone cooling load differences between radiant and air systems. In this article, published in the ASHRAE journal, the authors described the energy simulation analysis conducted by Feng et al. [24] (*section 1.5.1.3*) and the experimental studies conducted by the same authors [25], in which they investigated how the dynamic heat transfer in rooms conditioned by a radiant system is different from an air system, and how such differences affect the sensible cooling load and cooling load calculation methods for radiant systems. Four tests with two heat gain profiles were carried out in a standard climatic chamber, located in the Center for the Built Environment, University of California, Berkeley. For each profile, two separate tests were carried out to maintain a constant operative temperature: one with radiant chilled ceiling panels (12 aluminum radiant panels) and a second with an overhead mixing air distribution system. The experimental results confirmed that radiant system cooling rates are different from air systems even when similar thermal comfort conditions are maintained. In fact, the instantaneous cooling rate for the radiant system was on average 18%-21% higher than the air system for the tested conditions. Moreover, the radiant system removed 75-82% of total heat gains during the period when the heater was on, while the air system removed 61-63%. This differences were caused by the amount of energy stored in the non-active thermal mass. Miriel et al. [26] conducted an experimental study in order to evaluate the performances

and thermal comfort of a water ceiling panel in heating and cooling mode, and subsequently developed a simulation study (TRNSYS) with the aim of validate the experimental model. The experiments were carried out in one room in a T5 experimental house, built in Rennes (France), equipped with four ceiling water panels incorporated into the false-ceiling. The test campaign and the simulated study showed that water ceiling panels may be used as the heating and cooling system of buildings with a good thermal insulation. They guaranteed satisfactory thermal comfort conditions in terms of indoor air temperature profile and PPD (the GRES test protocol was used). Their power was limited and the building's heating and cooling loads had to be low. The heating mode gave good results with a reduction of the setpoint temperature during the night. Finally, this cooling technique was suitable for office buildings with low thermal loads and for which no additional air treatment system was provided. Causone et al. [27] conducted experimental studies in order to evaluate the heat transfer coefficients between radiant ceiling and room in typical occupancy conditions of an office or residential building and typical set point values of system parameters. The experiments were carried out in a test chamber, equipped with a hydronic radiant ceiling composed of eight radiant panels with a water circuit in each, a hydronic radiant floor and hydronic radiant panels on three of the vertical walls (six panels on the wider wall and four panels on each of the narrower walls). The forth wall is used to enter the room through a door and to check measurements through a window. In these studies only the radiant ceiling was evaluated. Besides, the chamber was equipped with four metallic cylinders to simulate occupant loads inside the room. These cylinders were also used to simulate internal gains during cooled radiant ceiling tests, while the vertical radiant walls were used to simulate heat losses during heated radiant ceiling tests. The obtained values of heat transfer coefficients (radiant, convective and total) confirm tendencies found in the literature, indicating limitations and possibilities of radiant ceiling systems improvement. Rahimi and Sabernaeemi [28] conducted a set of experiments to investigate the participation of radiation and free

convection in the heat transferred from the ceiling surface of a room to other internal surfaces. In order to do this, a cubical enclosure which represents a simplified model of a room was constructed and equipped with a radiant ceiling heating system. In the different studies carried out, the inlet water temperatures of the radiant ceiling heating system ranged from 45 °C to 70 °C. The results showed that the radiation is the substantial mechanism in the heat transferred from the warm surface of the ceiling to the other surfaces of the enclosure using a radiant ceiling heating system. The participation of the radiation increases slightly when the ceiling surface temperature is increased and it is almost the only heat transfer mechanism when the ceiling temperature is high. D'Ambrosio Alfano et al. [29] conducted a critical review on the typical measurement methodologies of mean radiant temperature combined with a comparative analysis of the metrological performances exhibited by the more common practice instruments on the market. To this purpose, a special room-test has been designed aiming to reproduce the typical microclimatic conditions can be encountered in workplaces both in summer and in winter conditions. The effect of the measurement methodology and used instruments on the thermal comfort (global and local) and the thermal stress assessment has been finally discussed. Obtained results showed that the use of different instruments consistent with ISO Standard 7726 requirements resulted in values of the mean radiant temperature compatible with each other, but the consequences on thermal environment assessment appeared often ambiguous. The experimental results focused on the need for starting an in-depth discussion on the measurements' protocols and the instruments leading to a possible reduction of the required accuracy levels reported in the ISO Standard 7726. Mustakallio et al. [30] conducted experimental tests in order to analyze the differences in thermal conditions between radiant ceiling (integrated into the false ceiling tiles) with mixing ventilation, chilled beam and chilled beam with integrated radiant panels. Measurements were performed in a meeting room at two levels of heat loads (86 and 71 W/m^2), in which the presence of six occupants was simulated by four heated dummies with simplified geometry and by two

thermal manikins with realistic female body geometry. Air temperature, operative temperature, velocity and turbulent intensity were measured and draft rate levels calculated at 8 heights in the room. The results showed that the identified differences in the thermal conditions in the room provided by the studied systems are not big. Moreover, the difference between operative temperature and room air temperature was at most 0.4 °C in all studied cases. Finally, the velocity and draft rate levels in the occupied zone were a bit higher in both chilled beam cases. Casale et al. [31] conducted laboratory studies in order to make a comparison between the measurements of the mean radiant temperature and the radiant asymmetry determined throught different methods (direct and indirect). In particular, a characterization and validation of the thermographic technique (indirect) was carried out comparing the measurement results obtained with those obtained through the classical technique of the globometer (direct). Finally, the use of a numerical code was proposed in order to evaluate the mean radiant temperature and the radiant asymmetry when the observer's spatial position varies. The analysis of the results showed that the indirect measurement by thermography is a very interesting technique since it allows real-time measurements suitable for measurements in non-stationary conditions and in non-uniform thermal environments. The measurement of mean radiant temperature with the thermographic technique results in good agreement with that obtained through the globometric method. The numerical code developed for the post-processing of the thermographic results allows an accurate calculation of the factors of view, the simulation of test conditions slightly different from those detected, the calculation of the mean radiant temperature for different positions of the observer through a single thermographic survey and the simulation of different emissivity of the test surfaces. Yang et al. [32] conducted an evaluation of the performance of a brushless direct current (DC) stand fan in 100 experiments that measured manikin-based equivalent temperature, fan power consumption and cooling fan efficiency (CFE) index at four different dry-bulb temperatures (24, 26, 28, and 30 °C), fan speed settings (corresponding to centreline speeds in the range 0.6-

2.5 m/s at 1 m distance), two fan-manikin distances (1 and 2 m) and two fan-manikin orientations (front and side). The experiments were carried out in the Field Environmental Chamber (FEC) at National University of Singapore (NUS). Room air temperature was controlled by a variable air volume (VAV) air conditioning system. The CFE index is defined as the ratio of the whole-body cooling effect generated by non-uniform airflow from the fan to its power consumption (°C/W). The experimental results showed that the CFE index was influenced by dry-bulb temperature, fan speed setting, and fan-manikin distance, but not by fan-manikin orientation. The lower the temperature and the closer the fan, the higher was the CFE index. Increasing fan speed setting simultaneously enhanced whole-body cooling and increases power use. Consequently, the CFE had a non-monotonic relationship with fan speed setting and the peak value was reached for an intermediate speed. As a complement to air-conditioning, the tested stand fan was a suitable energy-efficient technology for providing thermal comfort in warm environments. Klemke et al. [33] conducted experimental studies in order to analyze electrical energy savings, reduce heat up time and validate simulation models. The experiments were carried out in a climate chamber located in the Technical University of Berlin with two office working environments modeled in order to provide realistic internal heat sources. Two floor heating systems were tested: a conventional system with heating tubes installed in a counter flow spiral pattern and a state of the art capillary tube system installed in a parallel tube pattern with a reduced concrete layer thickness. Different supply temperatures and mass flow rates were investigated concerning their applicability for an unsteady operation. Obtained results showed that with rising supply temperatures and decreasing mass flow rates the specific energy demand in both systems could be reduced by around 82 % at a supply temperature of 55 °C. The heat-up time to increase the operative temperature from 18 to 22 °C could be reduced by a factor of up to 4.6 using the capillary tube system and up to 2.6 using the conventional tube system. Finally, after the experimental studies, in order to simulate the unsteady operation of a floor heating system and

evaluate its effect on the dynamic thermal behavior of the room, a Modelica model was created. The simulations models were validated with experimental data from the measurements of operative room temperature and the median floor surface temperature. Rees and Haves [34] conducted a series of experiments regarding displacement ventilation with and without chilled ceiling panel systems in order to analyze air mixing condition and distribution in the room. The characteristics of this type of systems were studied by making temperature and air flow measurements in a test chamber configured as a two-person office, over a range of operating parameters typical of office applications. The results showed that linear temperature gradients in the lower part of the room were found, in all cases, to be driven by convection from the adjacent walls. Moreover, significant mixing, indicated by reduced temperature gradients, was evident in the upper part of the room in the chilled ceiling results at higher levels of heat gain. Visualization experiments, velocity measurements and related numerical studies indicated that with greater heat gains the plumes have sufficient momentum to drive flow across the ceiling surface and down the walls. At last, in cases with moderately high internal gains, comparison of the temperature gradients indicated that the effect of ceiling surface temperature on the degree of mixing and the magnitude of the temperature gradient were of secondary importance. These findings are in contrast to the view that it is natural convection at the ceiling that causes enhanced mixing. Behne [35] conducted experimental studies in order to evaluate air quality and thermal comfort provided by two different ventilation systems, combined with a radiant cooled ceiling. The test chamber was vented by either a displacement ventilation system with the supply air inlet along one of the walls and on the floor or by a mixing ventilation system having two slot diffusers mounted in between the cooled ceiling panels. Considering the obtained results, none of the ventilation systems investigated could be recommended to supplement a cooled ceiling without carefully considering the pros and cons. If the air quality in the occupied zone was top priority a cooled ceiling could be combined with a displacement

ventilation system. Pollutants released by persons were removed from the occupied zone to a great extent and good air quality could be achieved associated with comfortable thermal conditions. However, the portions of cooling load removed by both of the components have to be adjusted properly. If the favorable characteristics of a radiant cooled ceiling with respect to thermal comfort were most important, an air-conditioning concept could be realized with mixing ventilation and a cooled ceiling. But, in that case, had to make sure that the supply air diffusers were properly designed, situated and adjusted to avoid any draft problems. Kim et al. [36] conducted experimental and numerical studies in order to analyze the thermal environment of an office space air-conditioned by a cooling panel system. By comparing both the results of the field measurement and the simulation, the expected precision of the CFD for an indoor space with a cooling panel was examined from a practical point of view. Moreover, three types of HVAC system (cooling panel system, all-air cooling system, and hybrid air cooling system composed of cooling panel and natural ventilation) were analyzed using CFD to examine the effectiveness of the cooling panel system. The space considered was on the ground floor of a six-storey reinforced concrete building located in Shibuya Ward, Tokyo, Japan. The office was equipped by a cooling panel system, installed in one of the vertical wall, and without any ventilation system. Inside, four occupants were simulated. From the obtained results, the indoor vertical temperature distribution showed relatively large deviations during operation of the cooling panel. This system removed more heat from the human model by radiant heat transfer and caused the mean radiant temperature and operative temperature to be lower than the all-air system, which resulted in better cooling efficiency. Furthermore, the prediction of indoor thermal environment by the CFD method corresponded with the results of field measurements, with a reasonable error. Therefore, this method proved to have sufficient accuracy from a practical point of view. Saber et al. [37] conducted experimental studies to evaluate the performance of a decentralized dedicated outdoor air system (decentralized DOAS) combined with a radiant cooling system

in terms of occupant thermal comfort and indoor air quality for the tropical context. Different sets of operational scenarios (experiments) were carried out in the test bed of low exergy ventilation technologies (BubbleZERO) in Singapore, located near the campus of NUS, in order to realize the impact of system related parameters, like ventilation rate and supply water temperature to radiant ceiling panel, on thermal comfort and indoor air quality. The results showed that supply chilled water temperature and space cooling load have strong impacts respectively on the capacity of decentralized units and cooling panel, which consequently influence indoor air condition. Indoor air was predicted to be in comfort range ($-0.2 < PMV < 0.2$) only at specific periods of the day and an automatic control was required to modulate the system under various indoor and outdoor conditions. For a certain range of ventilation rates, a reduction of supplied fresh air flow rate does not have a considerable influence on the air temperature of the conditioned space. However, to keep CO2 level within the limits set by air quality standards, ventilation rate should be at least 70% above the minimum ventilation requirements of local standard. Main challenges of implementing DDOAS coupled with radiant cooling in the tropics include the condensation risk on the radiant panels, nonuniformity of panel surface temperature and low air movement inside the space.

1.5.1.2. Physical measurements in building

We found 2 studies that were fully based on physical measurement in buildings. Pfafferott et al. [18] conducted indoor monitoring campaigns over 2 or 3 years (between 2001 and 2005) in 12 low-energy office buildings located in three different summer climate zones in Germany (summer-cool, moderate, summer-hot). Cooling strategies used in these structures were different: most buildings used night ventilation for pre-cooling, some buildings used TABS with ground cooling, and some others used earth-to-air heat exchangers for air-cooling. No building had a mechanical driven chiller. The purposes of these studies were to discuss the existing thermal comfort standards, analyzing room temperature as function of the ambient air temperature and determining

the frequency of exceeding standard requirements, and show crucial points for the building design and operation according to thermal comfort and energy saving. The results of data evaluation showed that passively cooled low-energy office buildings provided a good thermal comfort in moderate European summer climate. These monitoring campaigns demonstrated that, during a moderate summer or a commonly warm summer, prevalent criteria for thermal comfort in buildings without mechanical cooling were exceeded for less than 5% of the building operation time, considering the real building operation and the actual user behavior. However, only TABS using ground cooling provided a good thermal comfort even in extreme weather conditions. Moreover, these results were compared with post occupancy evaluations with regard to occupant satisfaction. Occupants rated their thermal sensation, their satisfaction with the room temperature and their satisfaction with the perceived change of indoor environment after their interaction. The processing of results revealed that the occupant satisfaction with the room temperature correlated strongly with the possibility of the occupants to change their working environment (e.g. operable windows or temperature control of heating or cooling system) and their sensation that the environment actually changed (e.g. perceived temperature increases or decreases). On the other hand, the occupant satisfaction correlated poorly with the actual room temperature and the temperature sensation. Kolarik et al. [38] conducted a monitoring campaigns in order to analyse operative temperature drifts and occupant satisfaction with thermal environment in three office buildings (Denmark, Spain and Italy) utilizing embedded radiant heating/cooling systems. Continuous measurements of operative temperature were conducted at four workplaces in each building for one year. The results showed that the limit for 4-hour operative temperature drift (0.8 K/h) was exceeded in all studied buildings, with a range of percentage of occupied time with exceeded limit between 2% and 52%. On the other hand, limits for hourly and 2-hour drifts were exceeded in about 2% of occupied time. Moreover, in order to evaluate occupants' satisfaction with indoor environment, an internet based survey was

distributed among employees in investigated buildings. The employees were requested to answer a questionnaire consisting of 23 questions within a week, referring to one month period prior to the survey. In this, occupants were asked to assess their satisfaction with temperature conditions at their workplace, air quality, acoustic and lighting conditions as well as local thermal discomfort and building related health symptoms. The results obtained showed that temperature satisfaction slightly decreased when rate of temperature change increased, thus higher temperature drifts seemed to lead to higher dissatisfaction.

1.5.1.3. Building performance numerical simulation

We found 29 studies that were fully or partially based on computer simulation programs. Rage et al. [39] conducted numerical studies in order to validate a new TRNSYS component (Type Ecophon Acoustic Elements) developed to simulate partially covered suspended ceilings such as hanging sound absorbers. The tool was validated by numerically modelling a set of similar experiments carried out by Pittarello's previous studies [40] in a TABS test facility located at the Technical University of Denmark, equipped with floor and ceiling TABS decks. A total of 12 scenarios was modeled, varying suspended ceiling coverage ratios, type of suspended ceilings, internal heat gains and TABS water supply temperatures. The results obtained from the simulations were very close to the experimental results. The first set of measurements analyzed the effect of the above-mentioned parameters in the heat flow from TABS; the difference between the numerical results and measurements is in the range of -6.9% to +5.2%. The second evaluated the impact on TABS cooling capacity coefficient and room temperatures. The simulated cases led to absolute differences of +4.3% higher in average for the cooling capacity coefficient. On the other hand, the operative temperature in the room was particularly well estimated, with a maximum relative difference of +0.3°C. The same authors [41] conducted similar studies in order to better quantify the impact of soffit-hanging sound absorbers on the cooling performance of

TABS, assessed by means of the cooling capacity coefficient of the ceiling deck. The influence of different ceiling coverage ratios (0-30-45-60 and 80%) as well as the influence of the distance at which the absorbers were placed were studied by numerical simulations using TRNSYS (Type Ecophon Acoustic Elements). Tests were performed in a test room simulating a two-person office of 20 m^2, with a typical cooling load of 42 W/m^2. As in the previous study, the numerical model reproduced the same geometrical and thermal properties as a TABS test facility located at the Technical University of Denmark, equipped with floor and ceiling TABS decks. Besides, a constant ventilation rate of 1.35 ACH is set for mechanical ventilation, with a supply temperature of 20°C. The results showed that adding soffit-hanging sound absorbers in a room conditioned by TABS impacted the performance of this latter, as the sound absorbers shielded some of the radiation from the chilled surface, as well as prevented some of the hot air plume generated by the internal heat sources to reach the ceiling. In fact, covering 60% of the soffit surface with sound absorbers hanging at 300 mm from the ceiling active deck was expected to reduce the cooling capacity coefficient of TABS by 15.8%. This dropped to 25.4% with a coverage of 80%. The distance at which panels were placed from the slab instead had a moderate impact on the results, but it was clearly better to place them as far as possible from the slab, both for acoustic and thermal reasons. The presence of acoustic panels also affected the thermal comfort: the operative temperature in the room increased by 0.9°C in the former case and up to 1.6°C in the latter. Dominguez et al. [4] (*section 1.5.1.1*). Chowdhury et al. [42] conducted an analysis and prediction of thermal comfort using DesignBuilder in order to evaluate the actual thermal conditions of the Information Technology Division (ITD), an air-conditioned multi-storeyed building at Central Queensland University in the city of Rockhampton (Australia), during winter and summer seasons. Thermal comfort was assessed and compared using three alternative low-energy cooling technologies: radiant ceiling panels (33% ceiling area), economizer (mixed air-control) and pre-cooling (cooling of the thermal mass through air-conditioning during off-peak

hours). The metric used was the predicted mean vote (PMV) index, calculated using the effective indoor temperature and relative humidity for those cooling techniques. Simulated results showed that systems using a chilled ceiling offered the best thermal comfort for the occupants during summer and winter. Although economiser and pre-cooling offered less thermal comfort due to subtropical climate, however, they satisfied the existing thermal comfort standards. The validity of the simulation results was checked with measured values of temperature and humidity for typical days in both summer and winter. The predicted results showed a reasonable agreement with the measured data. Olesen and Mattarolo [43] conducted numerical studies using EnergyPlus in order to compare ten different radiant system configurations (TABS, radiant panel, and ESS located on either floor or ceiling) to a reference (conventional) variable air volume (VAV) system with active heating and cooling. The simulation model reproduced a 4-story building located in Copenhagen, Denmark. The metric used was the percentage of time during which indoor conditions (operative temperature) exceeded comfort limit of EN 15251 [44]. The obtained results revealed that all radiant system variants enhanced the thermal comfort conditions. Salvalai et al. [45] conducted a comprehensive analysis of an office building performances in terms of energy consumption and thermal comfort related to different cooling concepts in six different European climate zones (Stockholm, Hamburg, Stuttgart, Milan, Rome, and Palermo). A total of 17 environment for a typical office building was modeled with TRNSYS and five cooling technologies was simulated: natural ventilation (NV), mechanical night ventilation (MV) without heat recovery systems, fancoils (FC), suspended ceiling panels (SCP), and concrete core conditioning (CCC). In the first two strategies, the cooling system was absent (only ventilation). Moreover, simulations were carried out for the summer period and comfort was evaluated by analysing the operative temperature of the office space (also ceiling surface temperature was taking into account). The main results obtained from dynamic simulations highlighted that if the buildings and control strategies are

carefully and adequately designed, the passive cooling by ventilation strategies can be successfully employed in Northern and Central Europe. On the other hand, in climate such that of Milan, Rome and Palermo, the ventilation strategies showed low cooling capacity. For this reason, the use of the right windows openings control strategy is crucial in order to increase the thermal comfort. However, this study showed favourable thermal comfort for radiant systems compared to air systems. The water based radiant systems in fact, coupled with ground heat pump source, represented a good compromise between comfort and energy consumption even in hot climates like Rome and Palermo, reducing considerably the energy consumption in comparison with FC scenario. Corgnati et al. [46] (*section 1.5.1.1*). Ning et al. [47] conducted numerical studies in order to evaluate the dynamic thermal performance of radiant systems. Instead of considering the most common steady-state thermal parameters, as cooling or heating capacity and thermal resistance, the index selected to characterize the thermal performance of radiant systems was the response time (τ_{95}). The response time was defined as the time it takes for the surface temperature of a radiant system to reach 95% of the difference between final and initial values when a step change in control of the system is applied as input. A large number of simulations (56,874) were performed using Computational Fluid Dynamics (CFD) method and an adapted state space method (SSM) for different radiant system types (RCP/ESS/TABS) with a variety of configurations and boundary conditions. What emerged from the numerical results allowed the authors to purpose a preliminary radiant system classification scheme which helped to describe clearly the dynamic thermal performance of radiant systems. By using response time in fact, the radiant systems could be classified into fast response ($\tau_{95} < 10\ min$, like RCP), medium response ($1\ h < \tau_{95} < 9\ h$, like ESS) and slow response ($9\ h < \tau_{95} < 19\ h$, like TABS). Ning et al. [22] (*section 1.5.1.1*). Jin et al. [48] conducted a numerical analysis in order to establish a relationship between occupant productivity and multi-variant IEQ (thermal comfort, aural comfort, visual comfort and air quality). The basis of this relationship consisted

of creating a link between two existing studies, described in subsequent sections (*Wong et al. [49] – section 1.5.1.5; Kawamura et al. [50] – section 1.5.1.4*). In order to test the potential of the relationship, it was compared with the results of seven independent studies. Besides, limits of applicability were identified and the sensitivity of productivity to different IEQ aspects was also investigated. Finally, the "multi-variant IEQ – productivity" relationship was applied to a simple façade design example to illustrate the economic value of façade-related IEQ. The simulation model reproduced a notional office room in the city of London with a partly glazed façade, conditioned by a forced air unit (heating and cooling) and configured as a two-person office room. For the calculation, the main parameters related to IEQ (as light level, CO_2 concentration and PPD) were obtained from computational building performance simulation (EnergyPlus). The results revealed that the occupant productivity-loss was an important factor in selecting an efficient façade design option. The relationship in fact, could serve as a guideline for façade design and plant sizing. The results also showed that in some cases it was possible for the plant size to be intentionally undersized or the façade to underperform in order to achieve maximum economic value. Wang et al. [51] conducted numerical studies in order to provide graphs that allow designers to directly determine, for a representative room geometry, the acceptable range of surface temperatures of radiant floor and ceiling systems as a function of air temperature. In fact, the surface temperature limits specified by current standards do not vary with air temperature, and in particular, the limits for ceiling temperature are specified in terms of radiant temperature asymmetry, which is difficult to convert into surface temperatures. The graphs were generated using the Berkeley Thermal Comfort Model (BCM), a multisegment model able to predict skin and core temperatures, thermal sensation and comfort, for the whole body as well as for 16 local body parts, for a wide range of environmental conditions. These acceptable and optimal floor or ceiling temperatures were found simulating a large size model room, chosen in order to represent open plan offices. It's important to specify that acceptability was defined as

the absence of whole-body discomfort. Before determing graphs however, in order to check the ability of the BCM to predict thermal comfort with radiant systems, simulated results were compared with several previous human subject tests. In general, the obtained results were in good agreement with experiments, given a number of uncertainties in reproducing the laboratory conditions and matching a variety of different comfort voting scales. In particular, what emerged from simulations was that, depending on the air temperature, comfort could be provided with radiant floor temperatures of 15-40°C, which was a wider range than that specified in ASHRAE Standard 55 and ISO 7730 (19-29°C). Besides, comfort could also be provided with ceiling temperatures of 15-50°C (corresponding to radiant temperature asymmetry for cool ceiling as 8°C, and for warm ceiling 15°C), also wider than values contained in Standard 55 and ISO 7730 for warm ceiling (radiant asymmetry less than 14°C for a cool ceiling, and less than 5°C for a warm ceiling). Vamshi Gooje [52] conducted a research focused on thermal comfort as a result of radiant asymmetry in a space. In order to validate the simulation output, an actual data set from an Adobe house at Carefree, Arizona was used. This ASHRAE funded project consisted on a high-mass adobe residence with insulation on the exterior and radiant panels in both the ceiling and the floor supplied by a hydronic source (the west zone of the building was simulated for the study). To compare and validate the data acquired from the case study house, Radtherm™ was used, a thermal modelling program that predicted the full temperature distribution. Moreover, the validated outputs from the simulation program was used to create a thermal comfort model. The results obtained from this research emphasized the need in the green building industry to focus on the effects of radiant asymmetry on thermal comfort instead of average space temperature. Feng et al. [24] conducted a series of energy simulation analysis in order to investigate whether the same design cooling load calculation methods could be used for radiant and air systems by studying the magnitude of the cooling load differences between radiant and air systems over a range of configurations and to suggest potential

improvements in current design guidelines. For the comparison between the systems, two single zone models with no interior partitions were developed in EnergyPlus v7, one conditioned by an air system and one by radiant system. From the radiant side, all three radiant systems (RCP/ESS/TABS) were studied, both on the ceiling and on the floor. In total, 74 simulation cases were configured, including 13 (11 for RCP) variations for the three types of radiant systems and their equivalent air systems. The numerical results showed that zone level 24-hour total cooling energy of radiant systems can be 5-15% higher than air systems due to differences in conduction load through the building envelope and peak cooling load at the radiant system hydronic level can be 7-31% higher than air system for zones without solar load. Moreover, emerged that these cooling load differences between the two systems originated due to the following phenomena: radiant cooling surfaces directly removed part of the radiant heat gain and reduce heat accumulation in the building mass; only part of the convective heat gain became instantaneous cooling load. These results highlighted that simplified methods were not appropriate for cooling load calculation in radiant system design. Radiant systems had to be modeled using a dynamic simulation tool that was capable of capturing radiant heat transfer for cooling load calculation. Atmaca et al. [53] conducted a thermal comfort study in order to investigate the local differences between the body segments caused by high radiant temperature and to analyze the interior surface temperatures and its effect on human thermal comfort of different wall and ceiling constructions. For the first aim, thermal interactions between human body and its environment were simulated to predict skin temperature of the individual body segments. The simulations were conducted by appropriately modifying Gagge 2-node model to multi-segment case to demonstrate the local differences. In order to simplify the calculation of radiant temperature, only three radiant surfaces (the two walls and ceiling) were treated in these simulations. Finally, also PMV index was calculated to evaluate thermal comfort or discomfort. The results of this first part of the study were found to be in good agreement with experimental and simulation values

reported in the literature and showed that a high radiant temperature caused an increase in the PMV, and so a local thermal discomfort especially in body parts which were close to the warm surfaces. For the second aim instead, the sol–air temperature approach was used to calculate the interior surface temperatures of the wall and ceiling. It's important to specify that the sol–air temperature is defined as the equivalent outdoor air temperature that gives the same rate of heat flow to a surface as would the combination of incident solar radiation, convection with the ambient air, and radiation exchange with the sky and the surrounding surfaces. As in the previous part, thermal comfort or discomfort was discussed with PMV index obtained from the simulations. The results of this second part showed that interior surface temperatures of un-insulated walls and ceilings exposed to a strong solar radiation reached high levels, causing thermal discomfort for the occupants in buildings. Miriel et al. [26] (*section 1.5.1.1*). Tye-Gingras and Gosselin [5] conducted a hybrid numerical optimization study of a heating ceiling and wall hydronic radiant panel system in a typical residential building located in Quebec City, Canada. In particular, the purpose of the reseach was to show the impact of the size, position, and fluid inlet temperature of the panels on thermal comfort and energy consumption of the system. The problem was assessed in the form of a multi-objective optimization procedure to minimize heat losses through the envelope and predicted percentage of dissatisfied people (PPD), in order to maximize comfort. The room modeled was heated by hydronic radiant panels that could be embedded in the ceiling and/or the right wall (in the left wall there was a window). In particular, eight panel arrangements were simulated. A commercial finite volume code ANSYS FLUENT was used for the 2D CFD calculations, coupled with a semi-analytic radiant panel model specially developed for coupling with CFD. This strategy allowed considering the real room geometry, while providing at the same time accurate temperature profiles of the radiant panels and detailed temperature and comfort data field in the room. The results showed that comfort and energy consumption were contradictory objectives, which means that there was no single optimal

design but a family of optimal designs that were good trade-offs between the two objectives. Moreover, thermal comfort was more sensitive than the energy consumption to the design variables. Finally, adjusting correctly the fluid inlet temperature, it was also possible to achieve nearly optimal solutions, even when reducing the total panel surface by 66%. This meant that the temperature control of the fluid was the most important parameter for maximizing comfort and minimizing energy consumption of hydronic heating radiant panels. Klemke et al. [33] *(section 1.5.1.1)*. Moslehi et al. [54] conducted a series of calculations in order to numerically assess the compatibility of heating-cooling radiant ceiling panels with different climatic conditions of Iran, using EnergyPlus simulation program together with a Visual Basic code, for mean radiant temperature calculation across the space, developed by authors. Evaluated parameters in these studies were the energy performance, thermal comfort using Predicted Mean Vote (PMV) and Predicted Percentage of Dissatisfied (PPD) indexes, risk of condensation and asymmetric radiation caused by radiant ceiling panel for a typical residential building. The numerical model reproduced a typical residential room with a double glazed window facing south and one occupant inside it. Moreover, five different climatic conditions were simulated. The obtained results indicated that for dryer regions, with less risk of condensation, the radiant systems could help home owners to save around 11.3% on heating energy and 9.1% on cooling energy use. Besides, decreasing the room thermal loads might eliminate the asymmetric radiation dissatisfaction in the heating mode and drastically reduce the risk of condensation in the cooling mode. Hao et al. [55] conducted numerical studies in order to investigate the feasibility of combining chilled ceiling (CC), displacement ventilation (DV) and desiccant dehumidification, and above all, to determine if this integrated system configuration could realize desirable levels of IAQ, thermal comfort, and energy savings in the hot and humid climate of China. Parameters as IAQ, thermal comfort, and energy saving potential of the combined system were estimated using a mathematical model of the system described in this paper. The model was employed to analyze a

case study of the proposed system and compare it with a conventional all-air system. The environment in which simulations were developed was a typical office building in Beijing. The results obtained from the comparison showed that the combined system was able to save 8.2% of total primary energy consumption and above all to achieve better IAQ and thermal comfort. Chilled ceiling, displacement ventilation and desiccant dehumidification responded consistently to cooling source demand and complemented each other on indoor comfort and air quality. In fact, the room air temperature with the CC + DV system might be 2 K higher than all-air system for identical comfort level and there was no draft risk when the cooling load removed by CC was less than 100 W/m^2. Chiang et al. [56] conducted computational fluid dynamics (CFD) simulation studies in order to examine the thermal comfort performance of a radiant cooling panel system for subtropical region. Extensive CFD studies were performed based on an experimental radiant cooling ceiling system installed in a typical office where CFD simulation of a typical condition was validated by comparing the results to the field measured data in the actual room. The test chamber, modeled as a typical office environment, was located on the ground floor of a nine-storey reinforced concrete building at the National Taiwan University of Science and Technology (NTUST), Taipei (Taiwan). The room was equipped by 44 radiant cooling ceiling panels and integrated with a mechanical ventilation system to analyze the indoor air temperature distribution and an air dehumidification control system to prevent possible condensation phenomena on the cold surface of the ceiling. Simulations were carried out with/without air exchange as supplementary cooling (MV). Moreover, during the simulation, particular attention was given to the relationship between the panel and diffuser, analyzing parameters as the panel surface area and temperature, diffuser positions, and air temperature. The obtained results from the studies showed that in hot and humid climate, the lowest permissible ceiling temperature (18 °C) and the maximum panel area (60% of ceiling) could not achieve thermal comfort if there was no supplementary air cooling. Whereas the presence of air cooling could

achieve a thermal comfort (PMV within ±1), even when supply air temperature was as high as 24 °C. These considerations could serve as a design guideline for installing a radiant cooling ceiling system integrated with a mechanical ventilation system in hot and humid regions. In fact, they could be used in order to propose solutions alongside limitations on improving indoor thermal comfort and energy efficiency. Besides, they also revealed how the two systems could affect or complement each other. Myhren and Holmberg [57] conducted thermal comfort comparisons between different heating systems and focused on how their position affected the indoor climate in an exhaust-ventilated office under Swedish winter conditions. The heat emitters used were a high and a medium–high temperature radiator, a floor heating system and large wall heating surfaces at low temperature. Computational fluid dynamics (CFD) simulations were used to investigate possible cold draught problems, differences in vertical temperature gradients, air speed levels and energy consumption. Two different office rooms were modeled in order to include comparisons between an old-fashioned office and a room with a different ventilation system and better insulated walls and windows. Moreover, two different types of exhaust ventilation were used together with all heating systems. The general conclusions from this study were that low temperature heating systems might improve indoor climate, giving lower air speeds and lower temperature differences in the room than a conventional high temperature radiator system. The disadvantage with low temperature systems was a weakness in counteracting cold down-flow from ventilation supply units. For that reason the location of heat emitters and the design of ventilation systems proved to be of particular importance. Niu and Kooi [58] conducted a thermal comfort and indoor contaminant distributions analysis through the combined use of thermal dynamic behaviour simulation and CFD techniques for a room equipped with three typical cooling strategies: a conventional displacement ventilation system, a cooled water-ceiling with a displacement ventilation system, and an air-ceiling with a ceiling diffuser system. The advantages and disadvantages of the different systems was highlighted by comparison.

Thermal comfort problems, such as risks of local draft and vertical temperature stratification, and indoor air quality (IAQ) problems, such as odour distributions and ventilation effectiveness were investigated through the analysis of the following parameters: velocity vectors, temperature distributions (isotherms), distribution of the pollutant concentration and the percentage of dissatisfied people due to draft and odours. The numerical simulation results indicated that a cooled ceiling in combination with a displacement ventilation gave a good performance in thermal comfort and ventilation effectiveness at the cooling load of 50 W/m^2 floor area. On the other hand, the air-ceiling system created a flow pattern more close to well mixed situations, with a ventilation effectiveness still higher than the one at the cooling load of 50 W/m^2 floor area. However, the free-falling ventilation air stream, enhanced by the downward convective flow from the cooling panels, tended to increase draft risks along the floor, and also reduce the ventilation effectiveness. Khorasanizadeh et al. [59] conducted a two dimensional numerical study to compare the performance of a floor heating system and a common radiator heating system, in terms of air movement and temperature distribution. Applying different physical boundary conditions such as air absorptivity, floor temperature, wall temperatures and window dimension, the flow and temperature distributions in a two-dimensional enclosure were investigated with CFD simulations, and results for floor heating were compared with those obtained for concentrated heating. The analysis of simulations showed that the temperature distribution in a floor heating system was more uniform than a centralized heating system. This allowed to provide better thermal comfort for occupants. Moreover, obtained results showed that in a floor heating system the vertical temperature distribution in the middle of the room was closer to ideal conditions and required less power to achieve that conditions, with a consequently significant reduction of energy consumption. Maerefat et al. [60] conducted a numerical and laboratory study in order to evaluate the physiological responses and thermal comfort of sleeping persons in an eastern-style bed on a heated floor. For this purpose, thermal sensation

of sleeping occupants on the heated floor was compared with that of sleeping persons on the conventional beds. In the first part of the analysis, the conformity of floor heating systems with sleeping in the eastern-style beds was investigated by using the simplified 3-node model (based on Gagge's standard model). In the second one, the thermal sensation and physiological parameters of the human body was evaluated in a room equipped with floor heating system for the two different conditions of sleeping (eastern-style bed and conventional bed). As stated previously, not only the global thermal sensation (TSENS) was investigated, but also adaptation indices such as core temperature, skin temperature and skin wettedness was taking into account. The results revealed that under similar thermal conditions, thermal sensation and skin wettedness of the sleeping persons were obviously higher on the eastern-style beds than on the conventional beds. Therefore, sleeping in an eastern-style bed caused the person to feel more thermal discomfort. Furthermore, the results indicated that to get the same level of thermal and wettedness pleasantness on both aforementioned beds, the thermal insulation value of the blanket had to be about 0.4 clo lower in the eastern-style bedding arrangement than in the conventional bed. Le Dréau and Heiselberg [61] conducted a sensitivity analysis in order to characterise the advantages and drawbacks of four types of terminals (active chilled beam, radiant floor, wall and ceiling) and to determine the parameters influencing their thermal performance. Steady-state simulations of a typical European office room was performed, with internal dimensions chosen similar to the PASSYS test cell. All four types of terminals were associated with a ventilation system (Dedicated Outdoor Air System) to ensure an acceptable indoor air quality (not equipped with heat recovery). The parameters varied wer related to the outdoor conditions (outdoor temperature, part of direct to total solar radiation), the type of ventilation system (air change rate,air temperature gradient, convective flow in the room), the room properties (emissivity and absorptivity of the internal surfaces) and the position of the person/sensor in the room. The obtained results showed that the air change rate, the outdoor

temperature and the air temperature stratification had the largest effect on the cooling need (maintaining a constant operative temperature). Due to their higher dependency on the air change rate and outdoor temperature, convective terminals were generally less energy effective than radiant terminals. The global comfort level achieved by the different systems was always within the recommended range, but differences was observed in the uniformity of comfort. In fact, the radiant ceiling achieved the most uniform comfort conditions in the space, whereas the least uniform conditions was obtained with the cooled floor. Leung and Ge [62] conducted a numerical and field study in order to establish the desired thermal environment for sleep thermal comfort and investigate the potential energy savings achieved by reducing the operative temperature at night in heating season. The methods employed in this research included a multisegment single node heat transfer model to correlate the indoor thermal environment to the human body thermal conditions during sleep, field measurements of the thermal environment of a radiant ceiling heated to compare with simulation model and estimations of energy saving potential by reducing night-time temperature set-points. The building studied was a single family dwelling, located in North West of Bolton, Ontario. The residence was thermally maintained by radiant heated and cooled ceiling where hydronic pipes were embedded in sprayed concrete. Ventilation was provided to the building through a 100% outdoor air system delivering ventilation air into each occupied space. The results showed that the thermal environment represented by the operative temperature of the room could be reduced to around 15 °C to maintain sleep thermal comfort, significantly less than the thermal environment required by the building codes and ASHRAE comfort standard. Consequently, this finding led to potential energy savings and improved quality of thermal environment for sleep thermal comfort. Kim et al. [36] (*section 1.5.1.1*). Zmeureanu and Fazio [63] conducted a technical study of the thermal performance of a hollow core concrete floor system for passive cooling of a Montreal office building, while maintaining the thermal comfort within acceptable limits. A mathematical models was

implemented in the CBS-MASS computer program to estimate the hourly variation of the sensible cooling load, the room air temperature and the thermal comfort index for a given configuration of the space and for a particular day. Computer simulations for a warm and sunny day showed that, during occupancy, the hollow core floor system provided thermal comfort without mechanical cooling. In particular, emerged that the hollow core slab led to PMV values between -0.3 and 0.3, just satisfying comfort conditions. Moreover, it was also revealed that higher ventilation rate in the hollow core and thicker concrete plate were good for thermal comfort.

1.5.1.4. Human subject testing

We found 21 studies that were fully or partially based on tests with human subjects. Nkurikiyeyezu et al. [64] conducted an experimental study in order to propose heart rate variability (HRV) as an alternative indicator of thermal comfort status. To test this hypothesis, statistical, spectral, and nonlinear HRV indice of 17 human subjects doing light office work in a cold, a neutral, and a hot environment was analyzed. In detail, seventeen male university students voluntarily participated in the study (healthy and without any cardiovascular or respiratory illness), placed inside three different climate chambers whose thermal settings were similar to a cold, a neutral and a hot thermal sensation on the PMV index scale. During the experiment, subjects were seated and asked to type randomly selected news articles to simulate office work, while their electrocardiograms (ECG) were recorded. Right after the experiment, subjects were requested to rate their thermal comfort sensation on Visual Analog Scale (VAS) consisting of a 10 equal intervals line with numerical ranges from 0 (representing the lowest sensation) on the left side to 10 (the highest sensation) on the right side of the line. The processing of obtained results showed that HRV was distinctively altered depending on the thermal environment and that it was possible to reliably predict each subject's thermal state (cold, neutral, and hot) with up to a 93.7% accuracy. The result of this study suggested that it could be possible to design automatic real-time thermal

comfort controllers based on people's HRV. Schellen et al. [65] conducted an experimental research in order to study the effects of different cooling principles (convective, in terms of increased air velocity, and radiant, in terms of applying a cold radiant panel) on human local and whole body thermal comfort, physiological responses and productivity. Moreover, emphasis was on gender differences since several studies showed that thermal perceptions significantly differ between males and females. Twenty healthy subjects (10 males and 10 females) were exposed one by one to two different experimental conditions: cooling through convection (CC) and cooling through radiation (RC). Convective cooling occurred through an increased air velocity, where the supply temperature equaled the room temperature, while radiant cooling occurred through applying a cold radiant ceiling panel. Both cases were designed to achieve a predicted neutral thermal sensation (PMV≈0). The test room was situated at the laboratory of the unit Building Physics and Services of the department of the Built Environment at the Eindhoven University of Technology. The dimensions of the room were similar to a standard office room. During the experiments physiological responses, thermal comfort and productivity were measured. Every 30 minutes, the test subjects filled out a questionnaire. Thermal sensation votes, both global and local for each body part, were asked on a continuous 7-point ASHRAE thermal sensation interval scale. Moreover, productivity was assessed using the Remote Performance Measurement (RPM) method. Within this method, the productivity was estimated by two simulated office tasks: text typing and addition. The results of this research indicated that under non-uniform conditions, the actual mean thermal sensation votes (TSV) significantly differed from the PMV for both genders. In fact, subjects were feeling significantly colder than predicted. Females were more uncomfortable and dissatisfied under the same environmental conditions compared to males. Besides, for females, local thermal sensation and skin temperature of the extremities (hands and arms) were of high importance for whole body thermal sensation. On the other hand, for males, local thermal sensation and skin temperature of the extremities

were less important. Finally, in terms of cooling, the operative temperatures for females needed to be increased by ≈1.2 K to improve satisfaction with the thermal environment. In a second paper [66], the same authors conducted an investigation of the effects of different cooling techniques (passive and active, convection and radiation) and different ventilation principles (mixing and displacement ventilation) on subjective and physiological responses. Furthermore, emphasis was on the influence of non-uniformity (temperature stratification, radiant asymmetries and local increased air velocities) on local effects (local skin temperatures and local thermal sensations) and subsequently whole body thermal assessment. Ten male subjects were placed one by one in a climate chamber (the same described previously) for six different experimental conditions. In summary the following cases were studied:

1. PC-C-M: *passive* cooling through *convection* by *mixing* ventilation;
2. AC-C-M: *active* cooling through *convection* by *mixing* ventilation;
3. AC-C-D: *active* cooling through *convection* by *displacement* ventilation;
4. AC-R-M-C: *active* cooling through radiation by the *ceiling* and *mixing* ventilation;
5. AC-R-M-F: *active* cooling through *radiation* by the *floor* and *mixing* ventilation;
6. AC-R-D-F: *active* cooling through *radiation* by the *floor* and *displacement* ventilation.

As in the previous research, every 30 minutes during the experiments, the subjects filled out a questionnaire. Thermal sensation votes, both global and local for each body part, were asked on a continuous 7-point ASHRAE thermal sensation interval scale. Although all cases were designed at PMV≈0, subjective data indicated significant differences between the cases. For the prediction of thermal sensation and thermal comfort under non-uniform conditions, the operative temperature only was not sufficient. Combined local discomfort factors and local effects

(local thermal sensations and local skin temperatures) played an important role in the comfort assessment. Furthermore, non-uniform environments, as case 6, could achieve a comparable or even a more comfortable assessment compared to uniform environments. Imanari et al. [67] conducted a comparison between a radiant ceiling panel system and a conventional air-conditioning system in terms of thermal comfort, energy consumption, and cost in order to investigate the various characteristics of a radiant ceiling panel system and its practical applications. Thermal environments, along with human responses, were investigated by using a meeting room equipped with radiant ceiling panels (56% of the total ceiling area). Air Handling Unit (AHU) was equipped to handle latent load and ventilation, and used to simulate the conventional all-air system. Fresh air was introduced into the room through the sensible and latent heat recovery unit (total heat exchanger). To compare thermal environments and comfort, seven male/female subjective experiments were carried out. Tests with male subjects were carried out while the meeting room was used normally, for the purpose of the meetings. Occupants, who were not informed of the type of air-conditioning system being operated, were asked to fill out a question form at the end of the meeting. On the other hand, tests for female subjects were carried out for the purpose of subjective experiments. During these tests in fact, occupants voted on thermal comfort and sensations every 15 minutes. Obtained results showed that the radiant ceiling panel system was capable of creating smaller vertical variation of air temperature and a more comfortable environment than conventional systems. Moreover, since part of the sensible thermal load was handled by radiant ceiling panels, the volume of supplied air could be reduced. Draughts were eliminated and lower energy consumption for air transport was achieved. Lin et al. [68] conducted an experiment in order to compare the thermal comfort performance of radiant heating system with convective heating system through objective measurements and subjective survey. To achieve this goal, both the subjective response and the objective parameters was measured and collected. Firstly, the overall thermal satisfactory of radiant and convective

heating terminals were investigated through subjective survey. Three typical heating terminals were compared in this research: Air Source Heat Pump (ASHP), radiator and Floor Heating (FH). The experiment was performed in three individual but consecutive office rooms, located in the northeast part of the Architecture Building of Tsinghua University (Beijing, China), under three experimental conditions (warm,moderate and cool condition). 97 healthy college students partecipated in the experiment (group of 3/4). Every subject consecutively experienced all the three rooms heated by different systems to the same condition, staying in each room for half an hour and voting every 15 minutes on six thermal comfort related aspects (thermal sensation, humidity, draught, local discomfort, overall thermal satisfaction and overall preferences) plus the acoustic environment. Secondly, the reasons behind the overall thermal satisfactory level and occupants' preference between these three typical terminals were explored through the measurement of physical parameters including the Mean Radiant Temperature (MRT), humidity, air movement, A-weighted sound level, temperature fluctuation and vertical temperature difference. The results revealed that no significant difference between radiant and convective heating system was observed in the Mean Radiant Temperature (MRT), indoor humidity and noise issue. Though radiant heating systems resulted in lower draught risk and less local discomfort complains in the feet region due to the less significant temperature fluctuations and vertical temperature gradients, radiant heating did not have significantly higher overall thermal satisfaction votes and was not significantly more preferred by occupants. Akimoto et al. [69] conducted a research in order to investigate the influence of the worker's behavior and task conditioning on worker's thermal comfort and productivity. For this purpose, thermal environment and worker's behavior were measured, and questionnaires to occupants, who worked as usual, were conducted on thermal and comfort sensation. The experiment was performed in a new office building of the M Company. The office was an open space with no pillars, where universal layouts could be installed, equipped with task/ambient

conditioning (TAC). TAC systems were being studied and developed to respond to the increased requirements for local control of indoor heat load, and to meet the thermal preferences by individuals. To understand the thermal environment in work zones in an office, various physical factors of thermal environment were measured, such as horizontal temperature and humidity distributions, vertical temperature distribution, airflow speed, and radiant temperature. Moreover, to understand the activity state of the workers, details of workers behavior were monitored, including state of seating, number of steps taken when they walked around and metabolic rate during work hours. Finally, questionnaire surveys were filled out at arriving the office/during work/at leaving the office, using thermal sensation vote scale and comfort sensation vote scale, while intellectual productivity of the workers was assessed by subjective evaluation. Obtained results showed that both activity level of occupant and exposed thermal environment was greatly different one by one. Besides, emerged that an increase in metabolic rate according to worker's behavior influenced on their thermal comfort. Finally, under the TAC control condition, the thermal sensation was neutral, and the percentage of people who felt uncomfortable was small. The workers' votes were ''comfortable'' even at values of 29–30 °C, showing that the TAC system enhanced the cool feeling perceived by the workers. Kawamura et al. [50] conducted a subjective experiment in order to evaluate the effects of improvement of indoor environmental quality on occupant's performance. The analysis was carried out in a climatic chamber at Waseda University, conditioned as the conceivable environments in office, in which eight different environmental conditions were simulated (operative temperatures, lighting and with or without traffic noise). Ten male college-aged subjects performed multiplication tasks and voted satisfaction with indoor environment and subjective symptoms of fatigue before and after each session of task. In order to estimate effects of improvement of thermal, lighting and acoustic environment on productivity, the "Predicted-performance-vote" was proposed in this study. The processing of results highlighted that subjects gave priority

to improve thermal and acoustic environment rather than lighting environment. The self estimated performance was related to occupants' satisfaction with indoor environment and was inversely related to fatigue. Therefore, subjects evaluated themselves well-performed when satisfaction with indoor environment was higher and fatigue was lower. Boerstra et al. [70] conducted a laboratory study in order to investigate how having or not having control over one's thermal environment affected end-user responses, in particular perceived comfort, the incidence of SBS symptoms and task performance. The central idea was to compare comfort, health and performance responses in two situations that were the same from a physical and physiological point of view but different from a psychological point of view. The study was carried out at the International Centre for Indoor Environment and Energy (ICIEE) at the Technical University of Denmark. The experimental room had a Constant Air Volume (CAV) system that allowed for very precise conditioning of the room temperature (28°C). Six workstations were placed in the room, including a chair, a table, a desktop computer and an adjustable table fan. A total of 23 subjects (12 males and 11 females) were exposed twice for about 2.5 h. During the first session (A) occupants were able to fine-tune their local thermal environment at any given time with the personal desk fan with continuous, stepless adjustable control. During the second session (B) subjects still had the desk fans, but this time the fans were controlled from an adjacent room by the researchers who adjusted the individual air speed profiles so they were identical to those recorded during the first session. Moreover, during both experimental sessions occupants had to answer online questions and conduct performance tests. The questionnaire consisted of eight different sections that were filled in at different times during experiments: occupants' overall assessment of the indoor environment, perceived air quality, thermal comfort, satisfaction with the environment, self-assessed performance, perceived control over different environmental aspects and prevalence of building related (SBS) symptoms (7-point Likert scales were used). Instead, the computerized performance tests involved addition, multiplication, Tsai-

Parrington numbers tests and text typing. Obtained results showed that perceived control over temperature, air movement and ventilation was significantly higher during session A. Comfort scores during session A and B were similar and also the incidence of SBS symptoms did not differ significantly between the two sessions. On the contrary, both self-assessed and objectively measured performance was significantly better during session B. Finally, about two-thirds of the subjects indicated to prefer the session A type situation (with manual control) over a situation B type situation (with 'automatic control'). Shan et al. [71] conducted a field experiment in two identical tutorial rooms in order to quantitatively compare human subjects' thermal comfort, sick building syndromes (SBS), and short-term performance under mixing ventilation (MV) system and passive displacement ventilation (PDV) system. The experiment was conducted in two side-by-side tutorial rooms on Nanyang Technological University, Singapore. The two rooms were identical except for their ventilation systems. In particular, both rooms did not have exhausts, so the indoor air was driven out through natural leaking. Moreover, the PDV system did not mechanically pump the cool fresh air into the room through outlets at ground level, but let the temperature gradient in the room to drive the fresh air. Thirty-nine healthy university students (male-female ratio was 6:7) were recruited as human subjects to participate the experiment. During the experimental session occupants had to answer subjective questionnaires and perform computerized task-based tests. The survey used to investigate subjective feeling of occupants towards the environment was compiled from ASHRAE Standard 55 and used 7-point scale to rate different aspects of indoor environment (thermal and draft) and SBS. On the other hand, the work performance evaluation questions used in the experiment were compiled from cognitive psychology, behavioral psychology and neuropsychology. Main results revealed that MV could lead to significantly larger overall draft sensation than PDV due to high air velocity from the overhead diffusers. On the other hand, PDV led to significantly higher draft and colder sensation in the lower body level because the diffusers in the PDV room were located at the ground level,

while draft distribution was perceived relatively homogenous in the vertical direction in the MV room. Seat arrangement (e.g. location and orientation) could lead to inhomogeneous sensations in the horizontal direction in both the MV and PDV rooms. Higher CO_2 concentration was the main factor causing SBS related to head, while both higher CO_2 concentration and lower relative humidity (RH) contributed to SBS related to eyes. As a consequence, SBS resulted from high CO_2 concentration and low RH could lead to decrease in short-term performance. Lan et al. [72] conducted a laboratory experiment in order to investigate the effects of thermal discomfort on office workers' productivity. In particular, the object was to evaluate the effects of thermal discomfort on occupants' workload, emotion, well-being, and motivation, and also the relationship between these activities and their neurobehavioral performance. The experiment was carried out in an ordinary but low-polluting office, in which participants sat at seven workstations and the room temperature was controlled by an air-conditioner. Three thermal conditions were created (indoor air temperature of 17 °C, 21 °C, and 28 °C). Twenty-one volunteered (6 females and 15 males) participants were recruited for this experiment. During exposures in the lab, occupants performed computerized neurobehavioral tests and their physiological parameters, including electrocardiogram (ECG to determine heart rate variation HRV) and electroencephalograph (EEG), were also measured. Several subjective rating scales were used to investigate participant's comfort, emotion, well-being, motivation and the workload imposed by tasks. The results of this laboratory study indicated that the warm discomfort negatively affected participants' well-being and increased the ratio of low frequency (LF) to high frequency (HF) of HRV. In a moderately uncomfortable environment, the workload imposed by tasks increased and participants had to exert more effort to maintain their performance. Moreover, results showed that thermal discomfort caused by high or low air temperature had negative influence on office workers' productivity and the subjective rating scales were useful supplements of neurobehavioral performance measures when evaluating the effects of

IEQ on productivity. Lan et al. [73] conducted an attempt to establish a quantitative relationship between thermal environment (thermal sensation votes) and human performance, examining the effect of thermal discomfort on a wide range of performance tasks. The experiments were carried out in a normal office, ventilated by 100% outdoor air using the mixing principle and equipped with six workstations. Twelve volunteers (6 females and 6 males) partecipated and two different thermal conditions were created (22°C and 30°C). Each experimental session lasted for 4.5 hours. During exposure in the room, subjects conducted tasks performance, as text typing, simulated office work and neurobehavioural tests. The processing of results showed that human performance was negatively affected by thermal discomfort caused by elevated air temperature. Furthermore, a quantitative relationship between thermal sensation votes and performance tasks was established to predict productivity loss due to thermal discomfort in the cost-benefit calculations pertaining to indoor environments. This relationship suggested that the optimum performance was achieved when people feel slightly cool, thereby it makes sense to set the PMV limits in workplaces in the range between −0.5 and 0 instead of between −0.5 and 0.5 as stipulated in the present standards. Lan et al. [13] conducted a laboratory test in order to propose a neurobehavioral approach for the evaluation of the effect of indoor environment quality on office workers' productivity quantitatively and comprehensively. In particular, the effect of room temperature on performance of neurobehavioral tests was investigated in the laboratory. The experiment was carried out in an ordinary but low-polluting office, equipped with six workstations, and the room temperature was controlled by an air-conditioner. Twenty-four participants (12 females and 12 males) were recruited to participate and were exposed to four different thermal conditions (19 °C, 24 °C, 27 °C and 32 °C) based on the thermal sensation from cold to hot. Four neurobehavioral functions, including perception, learning and memory, thinking, and executive functions were measured with nine representative psychometric tests. Besides, during exposure, a questionnaire was used to obtain subjective

sensations included questions regarding perceived air quality, general perceptions of the environment and thermal comfort (TSV and TCV). From the analysis of results it was found that the neurobehavioral approach could be worked to quantitatively and systematically evaluate office workers' productivity. Motivated people could maintain high productivity for a short time under adverse (hot or cold) environmental conditions when they were trying to do their best. Moreover, room temperature affected task performance differentially, depending on the type of tasks, because of different tasks were accomplished by different dominant hemispheres and different brain cortexes. Lan and Lian [74] conducted a field laboratory study to investigate the effect of indoor air temperature on productivity. The experiment was carried out in the same ordinary but low polluting office described in the previous research [13], controlled by an air-conditioner but equipped with seven workstations. Twenty-one students (6 females and 15 males) were recruited to participate and were exposed to three thermal conditions (17 °C, 21 °C and 28 °C). Participants' performance was evaluated with 13 computerized neurobehavioral tests, which assessed different neurobehavioral functions including visual perception, working memory, reasoning, executive functions etc. On the other hand, occupants' emotion was assessed with the Profile of Mood States (POMS), which consisted of six identifiable mood states: tension, depression, anger, vigor, fatigue, and confusion. After each neurobehavioral test was completed, participants filled in a questionnaire that included questions regarding general perceptions of the environment (TSV and TCV), emotion, and self-rate effort. The results revealed that more information could be provided when subjective questionnaires were utilized together with neurobehavioral performance measures. The POMS showed high reliability to investigate the relationship between thermal environment and occupant productivity. The performance of neurobehavioral tests decreased when the thermal environment deviated from neutral condition. Furthermore, participants experienced more negative emotions and had to exert more effort to maintain their performance under moderately adverse (slightly

warm or slightly cool) environmental conditions. Hodder et al. [75] conducted a field experiment in order to determine the effect of ceiling temperatures on the vertical radiant temperature asymmetry within a chilled ceiling/displacement ventilation office environment and its effect on the thermal comfort of sedentary office workers. A typical chilled ceiling/displacement ventilation office was created within a laboratory test room, in which the ceiling temperature could be varied over a range of typical operating values. The chilled ceiling had a 90% active area, consisting of six individual circuits connected in parallel. Finally, the room was equipped with a window to overlook the external environment. Eight female subjects took part in the study, over four ceiling temperatures selected for investigation (22 °C, 18 °C, 14 °C and 12.5 °C). Each subject completed a total of 22 sensation questionnaires at various stages throughout the experiment, and was asked to give details about her current thermal condition, about how she would prefer to feel, about whether she felt any local discomfort and about the freshness of the air in the test room. Obtained results showed that the vertical radiant temperature asymmetry experienced within a typical chilled ceiling/displacement ventilation environment did not significantly affect the thermal comfort of the desk-seated occupant. Moreover, The sensation of "freshness" appeared to be correlated with increasing vertical radiant temperature asymmetry and it might also be related to an increased downward movement of cool air. Olesen et al. [76] conducted a study in order to estimate experimentally the limit of the asymmetric thermal radiant field to which persons in thermal neutrality could be exposed without considering the surroundings uncomfortable. The experiments were carried out in the environmental chamber at the Laboratory of Heating and Air Conditioning, Technical University of Denmark. The ceiling, floor and side walls were covered with high gloss aluminium plates, which made it possible to regulate the radiant temperature. In fact, a pair of opposite walls could be held at different temperatures, while keeping the mean radiant temperature constant. Sixteen healthy college-age subjects (8 females and 8 males) were tested individually. Each subject, virtually naked, selected that

uniform environment which rendered him thermally neutral. The asymmetry was then increased in steps at half-hour intervals until the temperature difference between opposite walls was 40 °C. Judgements of perception of asymmetry and discomfort from asymmetry were obtained for three orientations of the occupants. The main conclusions were that for subjects in thermal neutrality no significant difference was found between female and male reaction to asymmetric radiation. 50% of participants were able to sense the asymmetric radiation when the difference in radiant temperature between two half-rooms was 7.4 °C, independent of the direction in which the naked subjects were facing. Finally, a formula was derived for estimating the limits of accptable temperature differences of a local radiant source for clothed sedentary persons in thermally neutral environments. Fanger et al. [77] conducted an experimental study in order to determine the limits of overhead radiation to which man in thermal neutrality could be exposed without feeling discomfort. The experiments took place in the environmental chamber at the Laboratory of Heating and Air Conditioning, Technical University of Denmark. In the room, the supply air was uniformly distributed over the lighting troffers and the perforated floor, while was exhausted through along the periphery of the ceiling. For application in the present experiments, an electrically heated plastic foil (radiant ceiling) was placed underneath the suspended ceiling. Sixteen college-age persons (8 males and 8 females) were used as subjects, seated one by one under the center of the heated ceiling. During each half-hour period (one radiant condition) each subject was asked six times whether he/she felt warm or cool on any part of the body and whether he/she regarded this as uncomfortable. From the processing of results a curve was established, showing the percentage of people feeling discomfort (PPD) due to overhead radiation, as a function of the radiant temperature asymmetry, for sedentary people who felt thermally neutral for the body as a whole. Besides, it was recommended that a heated ceiling should not provide a radiant temperature asymmetry exceeding 4 K in spaces with high standards for the indoor climate. Less than 5% of the population were then predicted to feel uncomfortable due to

overhead radiation. Finally, increasing discomfort due to increasing overhead radiation with lowered air temperature, could be attributed to warmer head and colder feet. Fanger et al. [78] conducted an experimental study in order to determine the limits of asymmetric radiation to which man could be exposed without feeling discomfort. As in the previous research, the experiments took place in the environmental chamber at the Laboratory of Heating and Air Conditioning, Technical University of Denmark. In the room, the supply air was uniformly distributed over the perforated floor, while was exhausted through the lighting troffers and along the periphery of the ceiling. Two different experimental set up were investigated in the test room. To simulate the radiant asymmetry caused by a cool or warm wall, a vertical panel was placed in the chamber, consisted of four water-filled panel radiators. On the other hand, to simulate the radiant asymmetry caused by a cool ceiling, the same panel as described previously was situated horizontally above the subject. Thirty-two college-age persons (16 females and 16 males) were used as subjects in the cool wall experiments, while sixteen college-age persons (8 females and 8 males) participated in the warm wall and the cool ceiling experiments. As in the previous research, during each half-hour period (one radiant condition) each subject was asked six times whether he/she felt warm or cool on any part of the body and whether he/she regarded this as uncomfortable. For cool walls, warm walls and cool ceilings, different curves were established showing the percentage of dissatisfied subjects (PPD) as a function of the radiant temperature asymmetry. These results revealed that radiant asymmetry at a warm wall caused less discomfort than at a cool wall, while a cool ceiling caused less discomfort than a warm ceiling. Accepting that 5% of subjects might feel uncomfortable, a radiant temperature asymmetry of 10 °C was found permissible at a cool wall, 23 °C at a warm wall and 14 °C under a cool ceiling. Finally, radiant asymmetry had no significant impact on the operative temperature preferred by the subjects and no significant differences were observed between the responses of men and women. Satish et al. [79] conducted an experimental analysis in order to

investigate detrimental effects of higher concentrations of CO_2, within the range found in buildings and without changes in ventilation rate, on occupants' decision making performance. Experimental sessions were conducted in a controlled environmental chamber outfitted like an office at LBNL (Lawrence Berkeley National Laboratory). A small heating, ventilating, and air-conditioning system served the chamber with thermally conditioned air filtered with an efficient particle filter (ventilation rate and temperature were constant). Twenty-two participants were exposed to three different environmental conditions, with CO_2 concentrations of approximately 600, 1,000, and 2,500 ppm. During each exposure condition (2.5 hours), participants completed a computer-based test of decision-making performance. Furthermore, before and after each test of decision-making performance, occupants also completed computer based questionnaires on perceived indoor air quality and health symptoms. Obtained results showed that increases in indoor CO_2 concentrations, with all other factors held constant, were associated with statistically significant and meaningful reductions in decision-making performance. In fact, at 1,000 ppm CO_2, compared with 600 ppm, performance was significantly diminished on six of nine metrics of decision-making performance. At 2,500 ppm CO_2, compared with 600 ppm, performance was significantly reduced in seven of nine metrics of performance, with percentile ranks for some performance metrics decreasing to levels associated with marginal or dysfunctional performance. Therefore, the direct impacts of CO_2 on human performance might be economically important and might limit energy-saving reductions in outdoor air ventilation per person in buildings. Tian and Love [80] conducted a field study in order to examine thermal comfort conditions in a building with radiant slab cooling. The main objectives of this research were to assess predicted mean votes (PMV) in determining occupant-reported thermal sensation votes and to analyze the main factors affecting occupant thermal comfort, including both overall and secondary comfort factors. The field study was carried out in the Information and Communication Technology (ICT) Building at the University of Calgary (a seven-storey teaching and research

facility) designed to house the Departments of Computer Science and Electrical Engineering. The radiant slabs provided cooling over most of the floor plates on levels 2–7, by circulating water at 16–22 °C in polyethylene pipes that were embedded in the concrete slabs. There was no insulation layer in the slabs, so the system acted as both a chilled ceiling and a chilled floor. The thermal comfort investigation combined field measurements and occupant questionnaires. 82 participants (professors, support staff and students - 58 in summer and 58 in winter, with some individuals participating in both seasons) were involved in the two rounds of the survey. The occupant questionnaire included two parts: thermal comfort (thermal sensations, air movement acceptability, and general comfort) and background. The analysis of results revealed that occupant whole-body thermal sensations with radiant cooling were consistent with the PMV model. The main advantage of radiant cooling for thermal comfort was found to be reduced local thermal discomfort with reduced vertical air temperature difference as well as reduced draft rate. Moreover, survey results showed that 14–22% of participants in the study reported local cold discomfort in the arm–hand and the leg–foot regions. These results indicated that there might be lower limits on air speeds acceptable to occupants. Finally, statistical analysis indicated that occupant thermal votes were free of significant correlation with personal, contextual and psychological factors. Maerefat et al. [60] (*section 1.5.1.3*). Leung and Ge [62] (*section 1.5.1.3*).

1.5.1.5. Occupant-based surveys

We found 25 studies that were fully or partially based on subjective surveys. Karmann et al. [81] conducted a critical literature review on thermal comfort for radiant and all-air buildings. The goal of this study was to compare IEQ as reported by the occupants within a large set of buildings using radiant and all-air systems. The used method to perform data collection was the online Occupant Indoor Environmental Quality Survey administered by the Center for the Built Environment (CBE), University of California, Berkeley. The web-based survey asked a set of basic questions about indoor environmental quality, including thermal

comfort, air quality, acoustics, lighting, cleanliness/maintenance, spatial layout, office furnishing, and general building and workspace satisfaction, using a 7-point Likert scale with answers ranging from 'very satisfied' to 'very dissatisfied'. 3892 respondents in 60 office buildings located in North America participated in the survey; 34 of which used all-air systems and 26 of which used radiant systems as the primary conditioning system. The analysis of results showed that radiant and all-air buildings had equal indoor environmental quality, including acoustic satisfaction, with a tendency towards improved temperature satisfaction in radiant buildings. Besides, acoustic satisfaction showed the lowest scores from all the categories surveyed. This result highlighted acoustical quality to be the most challenging aspect in regard to occupant satisfaction in buildings. Neto et al. [82] conducted a study to assess the people's thermal comfort without using any kind of measurement, just by interviewing them. This proposal included the creation of a ratio scale, ranging from -10 (very cold) to +10 (very hot), and a set of statistical procedures to treat the data gathered from this scale. This procedure was used to evaluate the influence of fans in the thermal comfort feeling of the occupants of a small office by three students, two males and one female, during two normal workdays. On the first day of the experiment, there were no fans operating in the office. During the second day, a fan operated full time at the maximum speed. From obtained results, the proposed method proved to be useful and robust for thermal comfort assessment. Nkurikiyeyezu et al. [64] (*section 1.5.1.4*). Pfafferott et al. [83] (*section 1.5.1.2*). Kolarik et al. [38] (*section 1.5.1.2*). Schellen et al. [65] (*section 1.5.1.4*). Schellen et al. [66] (*section 1.5.1.4*). Imanari et al. [67] (*section 1.5.1.4*). Zagreus et al. [84] conducted an analysis of the Indoor Environmental Quality Occupant Survey developed by Center for the Built Environment, University of California, Berkeley. The core questions assessed occupant satisfaction with different IEQ areas as office layout, office furnishings, thermal comfort, indoor air quality, lighting, acoustics, and building cleanliness and maintenance. This survey could be used to assess the performance of a building, identify

areas needing improvement, and provide useful feedback to designers and operators about specific aspects of building design features and operating strategies. The survey was used to evaluate the performance of over 70 buildings in the USA, Canada and Europe, including office buildings, laboratories, banks and courthouses. Furthermore, three case studies were presented in this paper, in order to demonstrate different applications of the survey: a pre/post analysis of occupants moving to a new building, a survey used in conjunction with physical measurements to determine how environmental factors affect occupants' perceived comfort and productivity levels, and a benchmarking example of using the survey to establish how new buildings are meeting a client's design objectives. Results showed that the occupant IEQ survey was as usefull tool that helped assess how well a building was performing from the viewpoint of its occupants. Lin et al. [68] (*section 1.5.1.4*). Akimoto et al. [69] (*section 1.5.1.4*). Kim et al. [85] conducted a research activity in order to better understand how desk-sharing environments could affect the office workforce, in relation to their satisfaction with various IEQ factors. In particular, the goals of this study were to address side effects of the non-territorial working policy, and examine the influence of this type of workplace on occupants' perceived productivity and health. The empirical analysis was based on an occupant survey database from BOSSA (Building Occupant Survey System Australia), collected in 20 office buildings located in capital cities in Australia between 2012 and 2014. All the buildings in the current dataset were serviced by centralised HVAC systems. The online-survey was composed by seven-point rating scale (from 1 to 7) and typically took 6/7 minutes for a participant to complete. A total of 3974 individual responses were obtained. The analysis of results indicated a fall in occupant self-assessed productivity as spatial factors (such as the office layout allowing easiness of interaction with colleagues, the ability to adjust/personalise workspace, and the amount of storage space provided) performed below occupant expectations. Moreover, it showed that the association of spatial factors with occupants' self-assessed productivity was more pronounced among those in non-territorial

workplaces, compared to those who were assigned with a pre-allocated desk. Therefore, these spatial factors, rather than the desk ownership itself, played a more significant role in the non-territorial work arrangement, affecting occupant attitude towards their building. Wong et al. [49] conducted a field survey in order to evaluate the indoor environmental quality (IEQ) in offices from the prospect of an occupant's acceptance in four aspects: thermal comfort, indoor air quality, noise level and illumination level. In particular, empirical expressions were proposed to approximate an overall IEQ acceptance of an office environment at certain operative temperature, carbon dioxide concentration, equivalent noise level and illumination level. Subjective evaluations made by 293 occupants of indoor environmental conditions in typical air-conditioned office (central or free-standing) in Hong Kong were studied with a dichotomous assessment scale (Acceptable - Unacceptable). The correlation between subjective response to each parameter and the overall IEQ acceptance was evaluated by a statistic χ^2-test. The processing of results showed that the operative temperature, carbon dioxide concentration, equivalent noise level and illumination level all had important effects on the overall IEQ acceptance. A range of acceptance in typical office environmental conditions and its dependence on the four parameters stated above were determined for typical design conditions. The relative significance of them, ranking from the most important to the least, was the indoor thermal environment, the air quality, the noise level and the illumination level. Therefore, the proposed overall IEQ acceptance could be used as a quantitative assessment criterion for an office environment. Kawamura et al. [50] (*section 1.5.1.4*). Boerstra et al. [70] (*section 1.5.1.4*). Shan et al. [71] (*section 1.5.1.4*). Lan et al. [72] (*section 1.5.1.4*). Lan et al. [73] (*section 1.5.1.4*). Lan et al. [13] (*section 1.5.1.4*). Lan and Lian [74] (*section 1.5.1.4*). Hodder et al. [75] (*section 1.5.1.4*). Fanger et al. [77] (*section 1.5.1.4*). Fanger et al. [78] (*section 1.5.1.4*). Satish et al. [79] (*section 1.5.1.4*). Tian and Love [80] (*section 1.5.1.4*).

1.5.2. Evaluated parameters classification

In Fig. 5, results of the evaluated parameters classification are summarized.

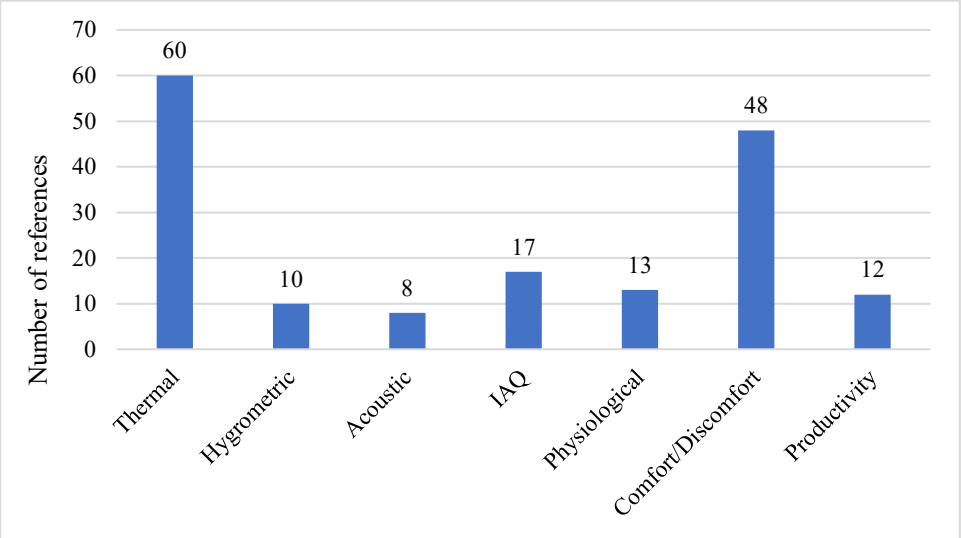

Fig. 5. *Evaluated parameters classification*

As we can see, the most analyzed are thermal parameters (60 references), while the least taken into consideration are acoustic ones (8 references). Moreover, the remaining five subjects show different results. Comfort/Discomfort parameters attest to the first with numerous references, while the others attest to the last with few references. The main reasons for this disparity are certainly attributable to the fact that thermal comfort is the most commonly considered aspect regarding the satisfaction of occupants with the environment, while the remaining ones are often considered less important and therefore negligible. However, we have to remember that for a global assessment of indoor environment quality, the analysis of hygrometric, acoustic and air quality parameters is also fundamental, as they are linked to the well-being and health

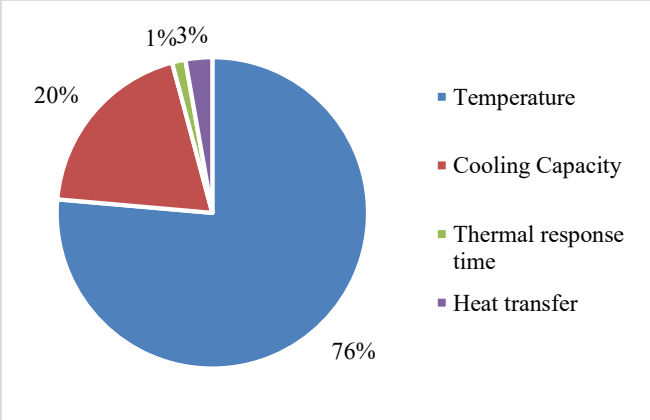

Fig. 6. *Thermal parameters*

problems of people (e. g. Sick Building Syndrome). The parameters evaluated are described in previous *sections 1.4.1 and 1.4.2*. In particular, a more in-depth analysis of the two most considered aspects was carried out. In the first one, thermal parameters have been investigated. As we can see in Fig. 6, the common way to quantify thermal comfort is consider temperature parameters (55 references), through the measure of dry-bulb air temperature, globe temperature, mean radiant temperature (MRT) (derived from the globe temperature), and operative temperature (calculated using dry-bulb air temperature and MRT). However, sometimes more specific parameters are considered, such as cooling capacity (14 references), thermal response time (1 reference) and heat transfer (2 references). On the contrary, results obtained from comfort/discomfort analysis reveal a substantial balance between all the parameters investigated (apart for the aspect of lighting), with a number of references above twenty. The following values represented in Fig. 7 were found: Vertical ΔT - 26; Draft Risk - 24; Radiant Asymmetry - 24; PMV/TSV/TCV - 22; Lighting - 5.

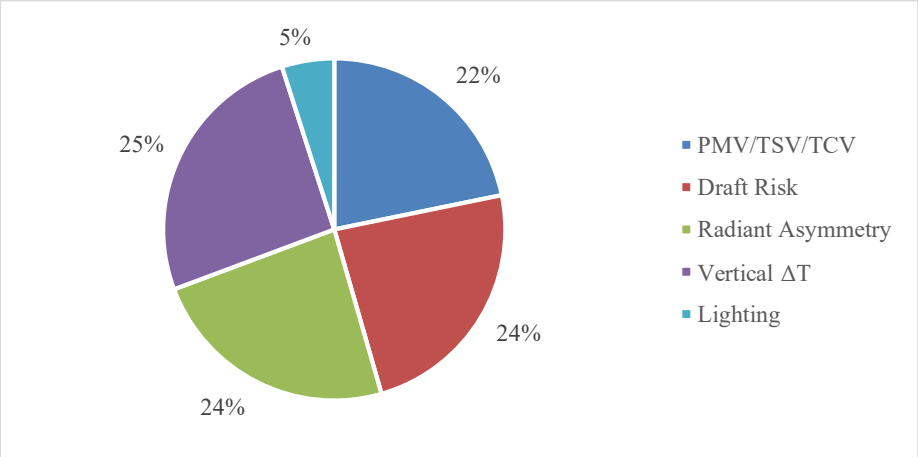

Fig. 7. *Comfort/Discomfort parameters*

1.6. Analysis of climate chambers

In this section we introduce the results of the climate chambers research carried out during our review. In the papers analyzed, we found informations about 36 test rooms, of which 29 physically built and 7 only simulated. Sometimes it was not possible to include some chambers due to the lack of details or incomplete

descriptions. The objective of this investigation is to compare the characteristic dimensions of our reference test room (CORE-CARE) with the others described in the analyzed articles and then to select those geometrically similar in order to determine possible comparison terms with the results that will be obtained in the future.

In the following table (Tab. 1) are summarized respectively some informations of the test chambers considered, floor area (*A floor*), volume (*V*) and characteristic ratios (*A/A** and *V/V**), useful for the comparison with the reference test room (*A**, *V**).

Tab. 1. *Informations of the test chambers, floor area (A floor), volume (V) and characteristic ratios (A/A* and V/V*)*

Informations	A floor [m^2]	Volume [m^3]	A/A*	V/V*
Test facility located at the Technical University of Denmark (DTU) [41,39,14]	21,60	77,76	1,22	1,58
Office at the Laboratory of Heating & Air Conditioning (DTU) [15,57]	11,52	31,10	0,65	0,63
Highly-Insulated Full Scale Test Room of the Building Technology and Structural Engineering Department at Aalborg University (DK) [46]	15,12	37,80	0,86	0,77
Office/Meeting room (Mustakallio et al. – Finland) [19,30]	17,30	50,01	0,98	1,02
Laboratory of the unit Building Physics and Services of the department of the Built Environment at the Eindhoven University of Technology [66,65]	19,44	52,49	1,10	1,07
Meeting room (Imanari et al. – Japan) [67]	33,00	89,10	1,87	1,81
Facility for Low Energy eXperiments (FLEXLAB) at the Lawrence Berkeley National Laboratory (LBNL) [20]	55,66	243,25	3,15	4,94
Certified controlled climatic chamberat the Price Industries in Winnipeg, Manitoba (Canada) [17,18,21,25]	18,23	54,70	1,03	1,11
Certified reverberant chamber at the Armstrong World Industries in Lancaster, PA [21]	50,82	265,27	2,88	5,39
Controlled environment chamber in Zhuhai (China) [22]	4,32	8,21	0,24	0,17
Office rooms in the Architecture Building of Tsinghua University (Beijing, China) [68]	18,99	51,28	1,08	1,04
Tutorial rooms at the Nanyang Technological University, Singapore [71]	64,00	176,00	3,63	3,57
Ordinary but low-polluting office (Lan et al. – China) [72,13,74]	24,00	120,00	1,36	2,44

Normal office (Lan et al. – China) [73]	18,00	57,60	1,02	1,17
Test room (Hodder et al. – United Kingdom) [75]	16,20	45,36	0,92	0,92
Environmental chamber at the Laboratory of Heating and Air Conditioning (DTU) [76]	12,60	35,28	0,71	0,72
Environmental chamber at the Laboratory of Heating and Air Conditioning (DTU) [77,78]	28,20	67,68	1,60	1,37
T5 experimental house, built in Rennes, France [26]	14,00	37,80	0,79	0,77
Office/Residential building (Causone et al. – Italy) 27]	11,61	29,72	0,66	0,60
Test chamber (Rahimi et al. – Iran) 28]	5,76	13,82	0,33	0,28
Laboratory (Casale et al. – Italy) 31]	45,40	126,21	2,57	2,56
Field Environmental Chamber (FEC) at National University of Singapore (NUS) [32]	85,80	223,08	4,86	4,53
Chamber facility at LBNL (Lawrence Berkeley National Laboratory) [79]	21,16	50,78	1,20	1,03
Test chamber (Rees and Haves – United Kingdom) [34]	16,72	46,49	0,95	0,94
Simulation of an office at the National Taiwan University of Science and Technology (NTUST), Taipei, Taiwan [56]	77,06	223,49	4,37	4,54
Test chamber (Behne – USA) 35]	45,50	136,50	2,58	2,77
Simulation of PASSYS test cell [61]	13,80	37,95	0,78	0,77
Office at the ground floor of a six-storey reinforced concrete building Shibuya Ward, Tokyo, Japan 36]	37,50	78,75	2,12	1,60
Test bed of low exergy ventilation technologies (BubbleZERO) in Singapore, near the campus of NUS 37]	27,80	67,83	1,57	1,38
Simulation of an office (Salvalai et al. – Italy) [45]	20,28	60,84	1,15	1,24
Simulation of an office (Jin et al. – United Kingdom) [48]	13,50	40,50	0,76	0,82
Simulation of an open plane office (Wang et al. – USA) [51]	64,00	179,20	3,63	3,64
Simulation of a test chamber (Feng et al. – USA) [24]	48,00	129,60	2,72	2,63
Simulation of a test chamber (Atmaca et al. – Turkey) [53]	8,70	20,89	0,49	0,42
Simulation of a residential building (Moslehi et al. – Iran) [54]	48,00	134,40	2,72	2,73
Simulation of a room (Niu and Kooi – Netherlands) [58]	18,36	48,47	1,04	0,98

Reference test room – CORE-CARE (A*, V*)	17,65	49,24

(Black: Existing test chambers; Blue: Simulated test chambers; Red: Reference test room)

Moreover, values of characteristic ratios are represented in the following graphs (Fig. 8 and Fig. 9).

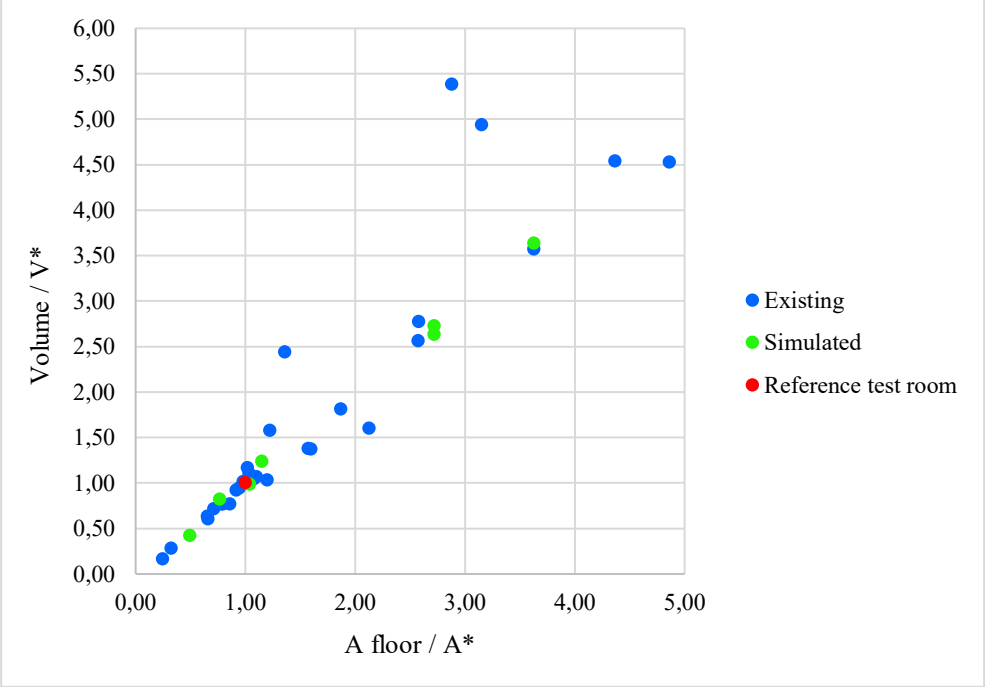

Fig. 8. *Characteristic ratios (geometrical relationship)*

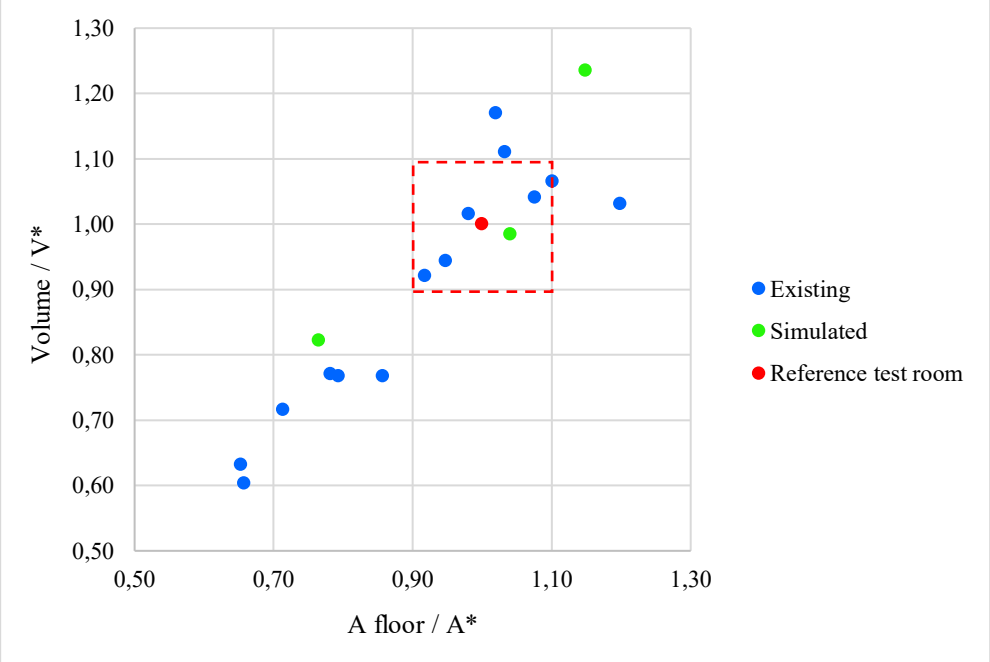

Fig. 9. *Test chambers geometrically similar to the reference room*

Considering as selection term a percentage variation of characteristic ratios equal to 10% (red rectangle in Fig. 9), we can observe that there are five test chambers geometrically similar to the reference room, four existing and one simulated.

These chambers are summarized in the following table (Tab. 2):

Tab. 2. *Five test chambers geometrically similar to the reference room*

Informations	A floor [m^2]	Volume [m^3]	A/A*	V/V*
Office/Meeting room (Mustakallio et al. – Finland) [19,30]	17,30	50,01	0,98	1,02
Simulation of a room (Niu and Kooi – Netherlands) [58]	18,36	48,47	1,04	0,98
Test chamber (Rees and Haves – United Kingdom) [34]	16,72	46,49	0,95	0,94
Office rooms in the Architecture Building of Tsinghua University (Beijing, China) [68]	18,99	51,28	1,08	1,04
Test room (Hodder et al. – United Kingdom) [75]	16,20	45,36	0,92	0,92

The most similar test room was used by Mustakallio et al. [19, 30] in two laboratory experiments. In the first one [19], the climate chamber (4.12 m x 4.20 m x 2.89 m, L x W x H) was modeled as a 2-person office and as a 6-person meeting room, with an entire glazed facade (width), in order to compare the performance of four systems based on radiant and convective cooling. These cooling variants tested were: chilled beam (CB), chilled beam with radiant panel (CBR), radiant ceiling panels with ceiling installed mixing ventilation (CCMV) and four desk partition-mounted local radiant cooling panels with ceiling installed mixing ventilation (MVRC). Measurements were performed under steady state conditions at 26 °C design room air temperature and two cooling conditions were simulated respectively for the office and the meeting room. The operating principle and measurements result of the four cooling systems are schematically described in *Appendix A* (Fig. A1, Tab. A1). In the second one [30], the climate chamber was modeled as a 6-person meeting room with an entire glazed facade (width), in order to analyze the differences in thermal conditions between radiant ceiling (integrated into the false ceiling tiles) with mixing ventilation, chilled beam and chilled beam with integrated radiant panels. As in the previous research, measurements were performed under steady state conditions at 26 °C design room air temperature and two levels of heat load were simulated. The operating principle and average values of measurements results of different cooling systems are schematically described in *Appendix A* (Fig. A2, Tab. A2). The only simulated test chamber geometrically

similar to the reference room was modeled by Niu and Kooi [58]. The room investigated had dimensions of 5.1 m x 3.6 m x 2.64 m (L x W x H), with 35% glazing area in the facade, equipped with three typical cooling strategies: a conventional displacement ventilation system, a cooled water-ceiling with a displacement ventilation system, and an air-ceiling with a ceiling diffuser system. The advantages and disadvantages of the different systems in terms of thermal comfort and indoor contaminant distributions was analyzed by comparison. It was supposed that the operative temperature in the room wass maintained at 23°C. Schematic representation of the room and simulated operation parameters of the three cooling systems are described in *Appendix A* (Fig. A3, Tab. A3). Another similar test room was used by Rees and Haves [63] for a series of experiments regarding displacement ventilation with and without chilled ceiling panel systems in order to analyze air mixing condition and distribution in the room. The test chamber, representative of a two-person office, had internal dimensions of 5.43 m x 3.08 m x 2.78 m (L x W x H), without any glazed surface. The displacement ventilation system air supply was via a semicylindrical diffuser, while the panels occupied 88% of the total ceiling area. The configuration of the environmental test chamber is described in *Appendix A* (Fig. A4). The fourth test room that we have selected was used by Lin et al. [68], in order to compare the thermal comfort performance of radiant heating system with convective heating system through objective measurements and subjective survey. The experiment was performed in three individual but consecutive office rooms (5.35 x 3.55 x 2.7 m, L x W x H) located in the northeast part of the Architecture Building of Tsinghua University (Beijing, China). These three rooms had the same dimensions but were heated by different heating facilities: Room 1 by Air Source Heat Pump (ASHP), Room 2 by radiator and Room 3 by Floor Heating (FH). The ASHP was installed 2.4 m above the ground and the radiator was installed under the north window. Up to 4 occupants were allowed to work or stay in each room simultaneously. The layout of the experiment chambers and a summary of heating facilities are described in *Appendix A* (Fig. A5, Tab. A4). Finally, the last similar test chamber was used by Hodder et al. [75], in order to determine the effect of ceiling temperatures on the vertical radiant temperature asymmetry within a chilled ceiling/displacement ventilation office environment and its effect on the thermal comfort of sedentary office workers. A typical chilled ceiling/displacement ventilation office was created

within a laboratory test room (5.4 m x 3.0 m x 2.8 m, L x W x H), in which the ceiling temperature could be varied over a range of typical operating values. The chilled ceiling had a 90% active area, consisting of six individual circuits connected in parallel. Besides, the room was equipped with a window to overlook the external environment. However, the window consisted of seven layers of glass, providing insulation from the external environment, and thus minimising temperature differences between wall and glass surface. The plan of the experimental room is described in Appendix A (Fig. A6).

For other details about results, please refer to the *sections 1.5.1.1, 1.5.1.3 and 1.5.1.4*.

Chapter 2

TEST ROOM AND TECHNICAL ROOM

2.1. Introduction

In a world increasingly connected and oriented to the construction of organized proposals according to a multidisciplinary approach, we are witnessing a growing formulation of projects that can be placed within the horizons proposed by what is commonly called "*social innovation".* Within this framework, there was the proposal to develop a significant collaboration between the Departments of Engineering and Psychology of Padua. Therefore, in the summer of 2016 the "Unified Indoor Climate Group" was founded, with the aim of studying, setting up and measuring thermal and interactive indices of a "test room", destined to be a working environment (office). These sectors, although very different, confirm what is typical of social innovation, allowing a study to be launched into the liveability of an interactive space based on work activities, starting from how the environment is inhabited and used.

The purpose of this project was to create a controlled environment from the point of view of the main thermophysical parameters of the building for Indoor Environmental Quality (IEQ) analysis in 2 rooms on the 3rd floor of the Technical Physics building in the University of Padua.

The first room was modified by installing radiant systems on each surface (ceiling, floor, walls), so as to be able to control surface temperatures and therefore thermal comfort, increasing at the same time the acoustic insulation of building structures. Each wall can be supplied with hot or cold water so as to simulate different climatic conditions and room types.

In the second one, all the systems to generate and control the fluid vectors were installed, as well as a machine for air ventilation able to heat or cool and dehumidify the test room, in order to control humidity and ventilation flow rate.

In future, the laboratory will be used to test the comfort and quality of the environment perceived by occupants and will not be used for tests to verify the energy performance of the systems installed.

Therefore, this project represents the beginning of an activity aimed at recognizing the effects of environmental parameters on the productivity of people and their perception of the working environment according to different room parameters (furniture, natural and artificial lighting, climate devices, etc.). To this end, conditions of a workplace will be reproduced considering the engineering aspects (structures, climate, indoor air quality, etc.), accompanied by statistical and psychological analysis.

It is important to underline that is a 360° project that aims at the quality of the internal environment in a completely innovative way. The proposed project intends to fill a gap in the literature linked to the specificity of the research carried out so far, as demonstrated in the previous review. In fact, the proposed multidisciplinary approach has no similar in other universities. Moreover, it is also emphasized that this laboratory has no similar examples in Italian and European universities, due to the multidisciplinary nature of the aspects dealt with simultaneously.

In the following sections we present a detailed description of the laboratory and the technical room, analysing the geometry and the systems with which they are equipped.

2.2. Initial conditions

In this section are described rooms 52 (*test room*) and 53 (*technical room*) before the beginning of works with their original dimensions and characteristics. Located at the 3rd floor of the Technical Physics building, the two rooms were originally used for different functions: the big one was used as a seminar room, instead the small one was a meeting room, used by professors and PhD students. In Fig. 10 we can observe the plan of rooms 52 and 53 before the beginning of works. Moreover, in the following table (Tab. 3), are listed the original dimensions of room 52 surfaces (in brackets are indicated the adjacent spaces to the different surfaces).

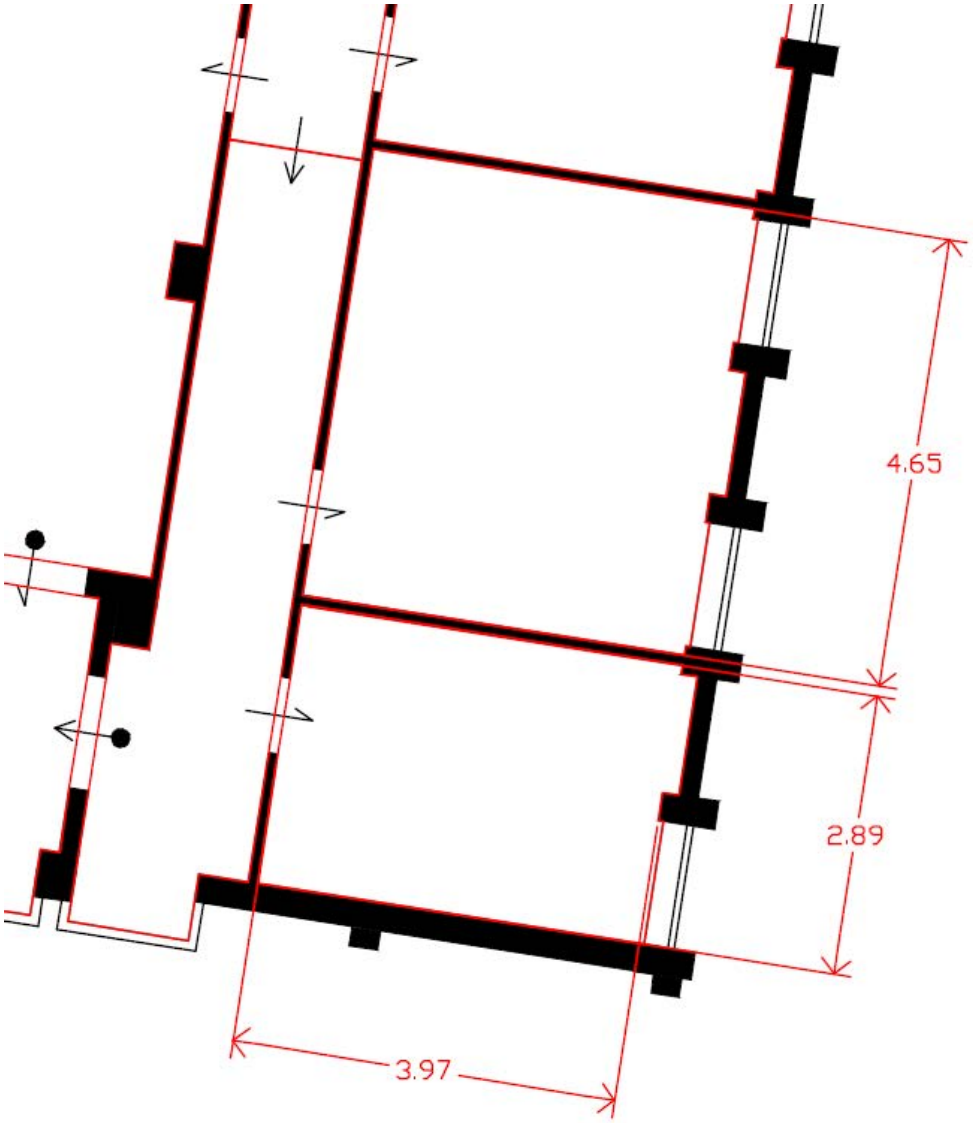

Fig. 10. *Plan of rooms 52 and 53 before the beginning of works*

Tab. 3. *Dimensions of room 52 surfaces before the beginning of works*

Surface	Dimensions [m]	A gross [m^2]	A net [m^2]
Floor	4,65 x 3,97	18,46	18,46
Ceiling	4,65 x 3,97	18,46	18,46
North wall (offices)	3,97 x 3,03	12,03	12,03
East wall (external)	4,65 x 3,03	14,09	10,02
South wall (technical room)	3,97 x 3,03	12,03	12,03
West wall (corridor)	4,65 x 3,03	14,09	11,99

As we can see in Fig. 10, the building is not perfectly aligned with the four cardinal points, presenting a slight inclination angle towards the east of 9 degrees.

Furthermore, the rooms are characterized respectively by two windows for the first and one for the second, facing east/south-east. In both cases, the original windows are equipped with double-glazing (*4-8-4 mm*) and a metal frame. It's important to highlight that these glazed surfaces were not replaced by new ones but were maintained as external windows in order to increase insulation.

The characteristic properties of original windows are presented in Tab. 4.

Tab. 4. *Properties of original external windows*

Dimensions	4-8-4	[mm]
Ug	3,1	[W/(m^2 K)]
Uf	5,9	[W/(m^2 K)]
Ag	1.404	[m^2]
Af	0,631	[m^2]

Values of the thermal transmittance (*U-value*) for glass and frame were assumed by BS EN ISO 10077-1:2006 [86], considering an uncoated glass (normal glass) with normal emissivity of 0.89 and filled with air, and a metal frame without thermal break.

Regarding heating and cooling system, the two rooms were equipped respectively by two fan coils for the seminar room and one for the meeting room, installed inside the niches generated by the supporting pillars below the windows. In the first one, these devices were removed and the niches subsequently closed by a false wall, while in the second one it is maintained as the only heating and cooling system in the room.

In Fig. 11 and Fig. 12 are represented rooms 52 and 53 before the beginning of works. In the first picture we can notice the niches due to the presence of the pillars, the external windows and the position of original fan coils, that we can see in the next photo.

***Fig. 11**. Picture of the room 52 before the beginning of works*

***Fig. 12**. Picture of the room 53 before the beginning of works*

2.3. Current conditions

In this section are described the climate chamber and the technical room at present, after the installation of radiant surfaces and ventilation equipment, and the connection of various systems. As stated previously, the spaces available were 2 rooms side by side. The floor, the ceiling and the walls (except for the windows) of the largest room (52) were suitably insulated and covered with radiant panels, in order to control the temperature. It will thus be possible to reproduce an environment with one or more dispersing walls and eventually the dispersing floor. Moreover, the supply circuits of the 6 surfaces of the room guarantee the possibility of simultaneous operation of some surfaces in heating mode and others in cooling mode, in addition to the possibility of independently controlling the supply temperature of each individual surface. Dry systems were used for all surfaces. In the case of the 3 internal walls, the insulating

package plus the radiant module were installed directly in contact with the existing surfaces, while in the case of the external one a false wall was built, in order to close the niches due to the presence of the pillars. Free areas have been left in the ceiling for lighting and in the walls for electrical boxes and internet connection. On the other hand, the smaller room was used as a technical space for all the systems. The following components were installed: a tank with a volume of 200 litres with an electric heater of 2,5 kW for hot water; a tank with a volume of 150 litres for chilled water; hydronic systems for managing flow rates and supply temperatures; an air handling unit for the renewal of the ambient air with high efficiency heat recovery and for the summer dehumidification treatment.

It's important to underline that all the components present in the two rooms were designed, provided and installed by more than 20 companies from northern Italy.

All the drawings showed in the following pages were made using the software AUTOCAD®, after having personally carried out measurements inside the two rooms.

In Fig. 13 is showed the exploded view drawing of the test room in order to give a general overview of how the chamber looks at present. As we can see, the position of different equipment is represented:

- Red: Electrical boxes;
- Blue: Supply/Extraction grille;
- Yellow: Lighting supports;
- Green: Fire protection device.

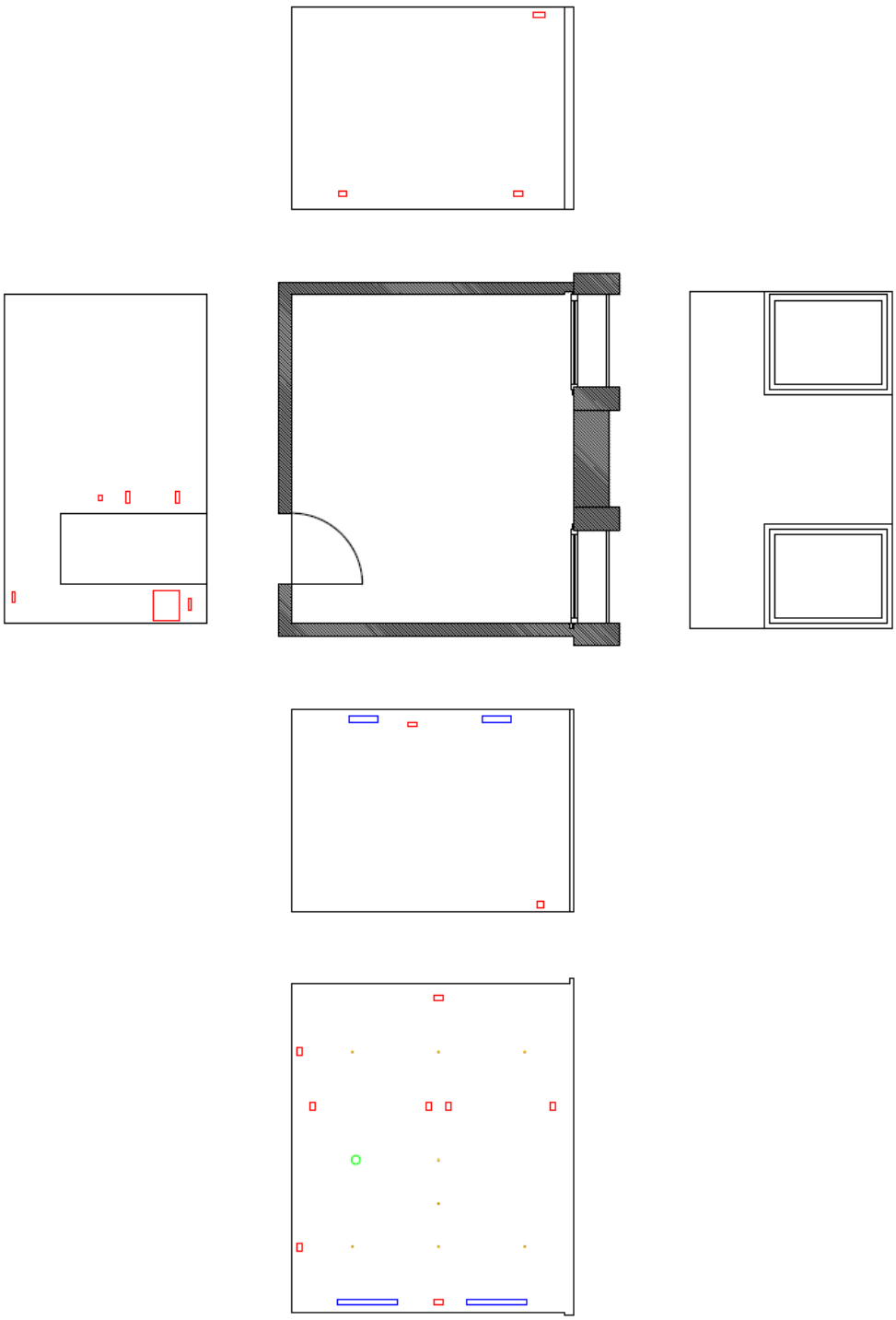

Fig. 13. *Exploded view drawing of the test room (Red: Electrical boxes; Blue: Supply/Extraction grille; Yellow: Lighting supports; Green: Fire protection device)*

2.3.1. Dimensions of the test room

In this section we present in detail the current dimensions of the climatic chamber. Surveys were carried out personally several times, using a measuring tape (resolution: *1 mm*; range: *5 m*), in order to guarantee an accurate truthfulness of the results.

The room has the following main dimensions:

- *Length: 4,54 m;*
- *Width: 3,89 m;*
- *Height: 2,79 m;*
- *Floor area: 17,65 m^2;*
- *Volume: 49,24 m^3.*

In Tab. 5 are listed the new dimensions of room surfaces (in brackets are indicated the adjacent spaces to the different surfaces).

Tab. 5. *New dimensions of room surfaces*

Surface	Dimensions [m]	A gross [m^2]	A net [m^2]
Floor	4,54 x 3,89	17,65	17,65
Ceiling	4,54 x 3,89	17,65	17,65
North wall (offices)	3,89 x 2,79	10,85	10,85
East wall (external)	4,54 x 2,79	12,67	8,61
South wall (technical room)	3,89 x 2,79	10,85	10,85
West wall (corridor)	4,54 x 2,79	12,67	10,69

As we can see from the comparison of the above-mentioned values with the respective ones reported in Tab 3, the dimensions of surfaces have been reduced due to the installation of the radiant panels on them.

In the following table (Tab. 6) are showed the percentage variations of these surfaces and the overall variation of volume of the room.

Tab. 6. *Percentage variations of room surfaces and overall variation of the volume*

Surface	**ΔA gross [%]**	**ΔA net [%]**
Floor	4,4	4,4
Ceiling	4,4	4,4
North wall (offices)	9,8	9,8
East wall (external)	10,1	14,1
South wall (technical room)	9,8	9,8
West wall (corridor)	10,1	10,8

ΔVolume [%]	13,1

In the following pages are included the drawings of these surfaces made using the software AUTOCAD®. All dimensions are represented in centimetres. Moreover, in every representation the exact position in which the radiant panels have been installed is showed in green, demonstrating the effective active surface.

For detailed information regarding the different radiant systems, please refer to the following *section 2.3.2*.

In Fig. 14 is represented the floor of the test room. From a comparison with the original plan described in Fig. 10, it is possible to notice the evolution that the chamber has undergone due to works. The thickness of the internal walls is considerably increased due to the installation of the radiant panels. Regarding the external wall instead, it is possible to notice how the niches have been closed by a counter wall on which panels have been positioned and filled inside with insulating material (rock wool). Furthermore, it is possible to observe how the niches of the original windows were closed by other internal windows (details in *section 2.3.4*), determining a double window configuration with an internal air space for high thermal and acoustic insulation. Finally, we can see that there are two small recesses in the north and south walls at the intersection with the external one. These precautions were necessary in order to guarantee a correct opening of the windows, being arranged on the border with the walls.

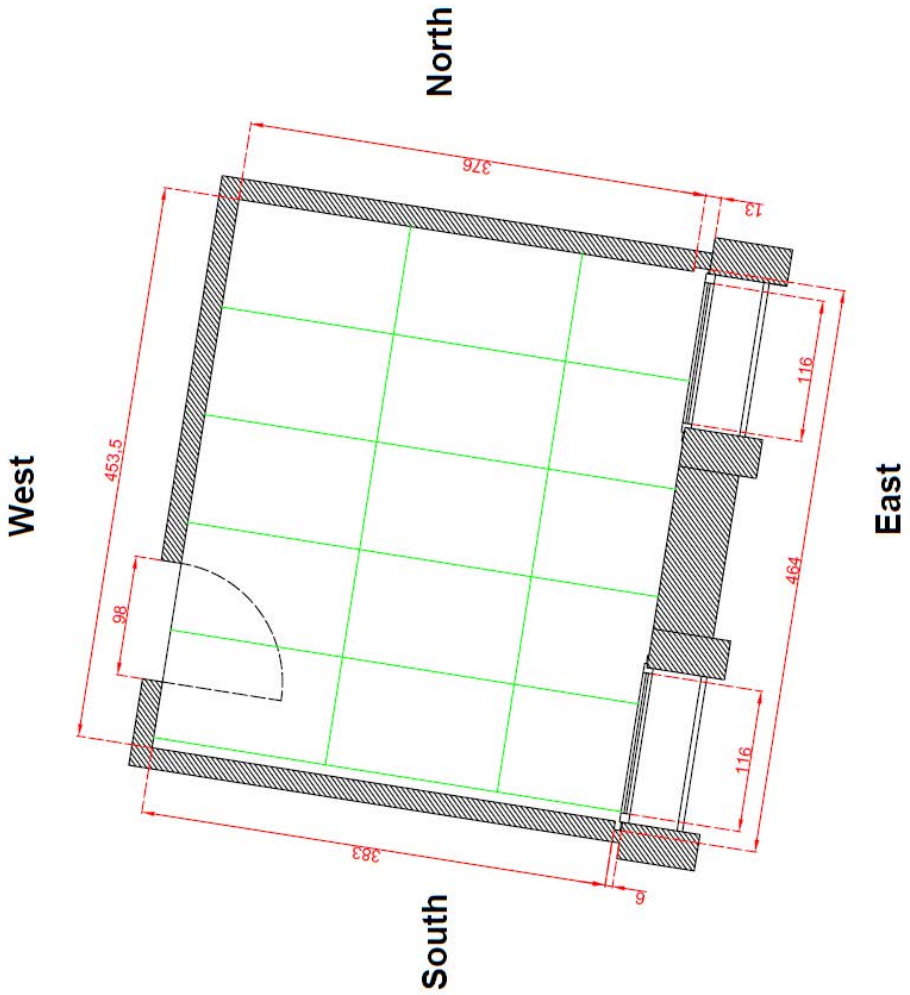

Fig. 14. *Floor of the test room (Green: Active surface)*

In Fig. 15 is represented the ceiling of the test room seen from above, as if it were projected on the floor. We can observe the position and dimensions of the supply grids of the ventilation system, as well as the 5 zones in which the panels of the radiant system have been positioned (the fifth is actually half of the module). Furthermore, the small recesses described above are even more evident and their quotations are reported.

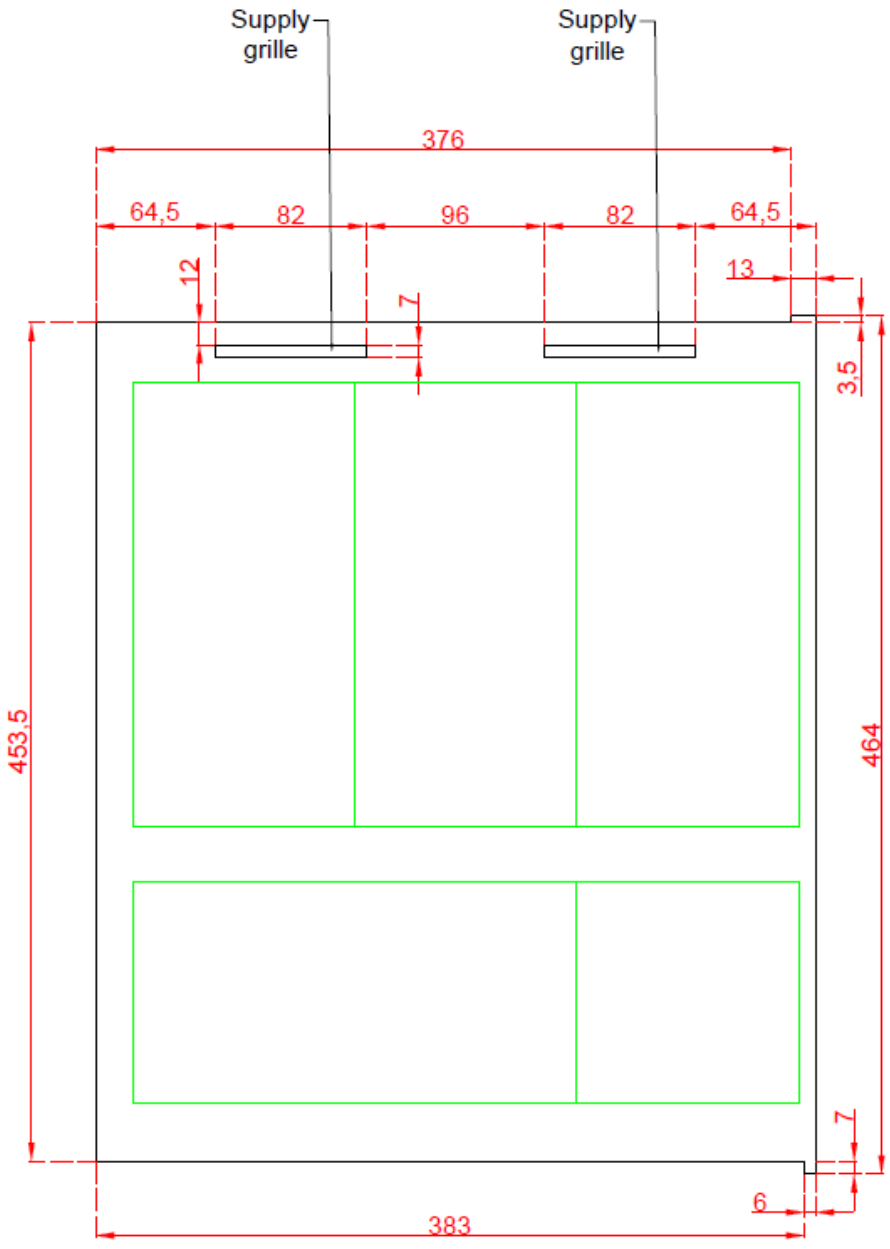

Fig. 15. *Ceiling (Green: Active surface)*

In Fig. 16 is represented the north wall of the test room, bordering the building area where the professors' offices are located, in which three radiant panels have been placed.

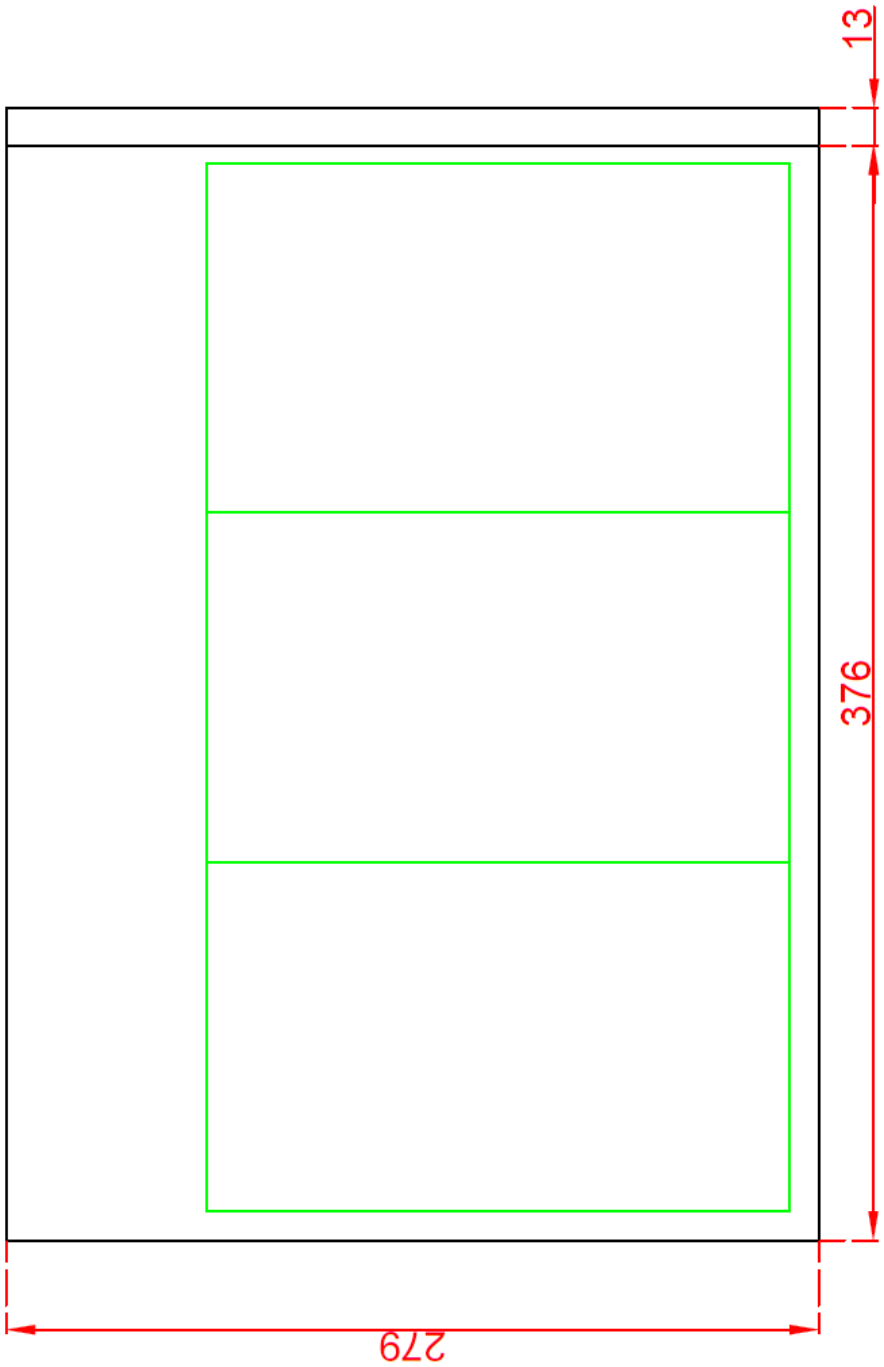

Fig. 16. *North wall – Offices (Green: Active surface)*

In Fig. 17 is represented the east wall of the test room, the only one bordering on the external environment. As we can see in the drawing, there are two windows of equal size, of which the glass surfaces, the internal frame and the decorative frame are respectively represented. In the left window the decorative frame has been reduced due to lack of space in the recess. Finally, it is possible to observe the different shapes of the radiant panels that have been installed (two under the windows, three in the previous central niche), in order to make the most of the available opaque surface.

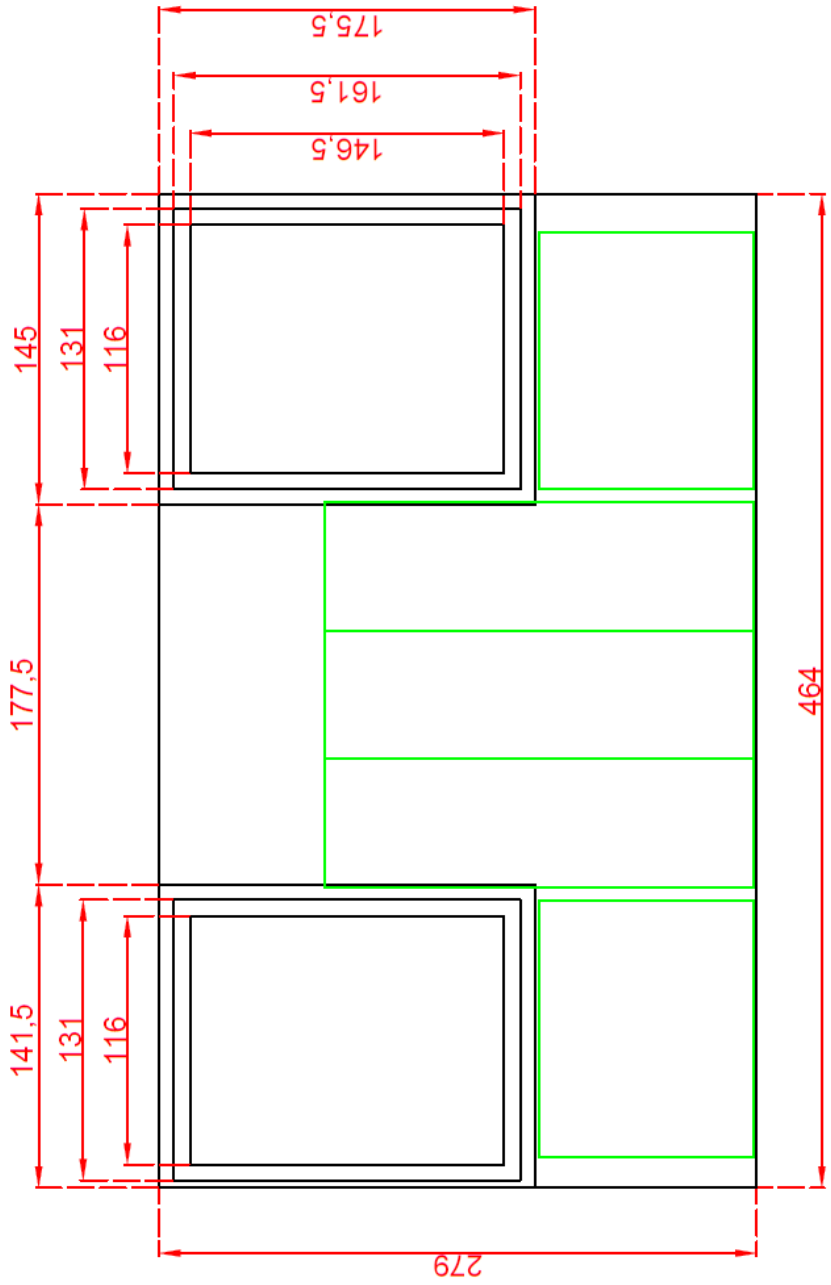

Fig. 17. *East wall – External (Green: Active surface)*

In Fig. 18 is represented the south wall of the test room, bordering the technical room. We can observe the position and dimensions of the extraction grids, as well as the 6 radiant panels which have been raised because of the presence of these components of the ventilation system.

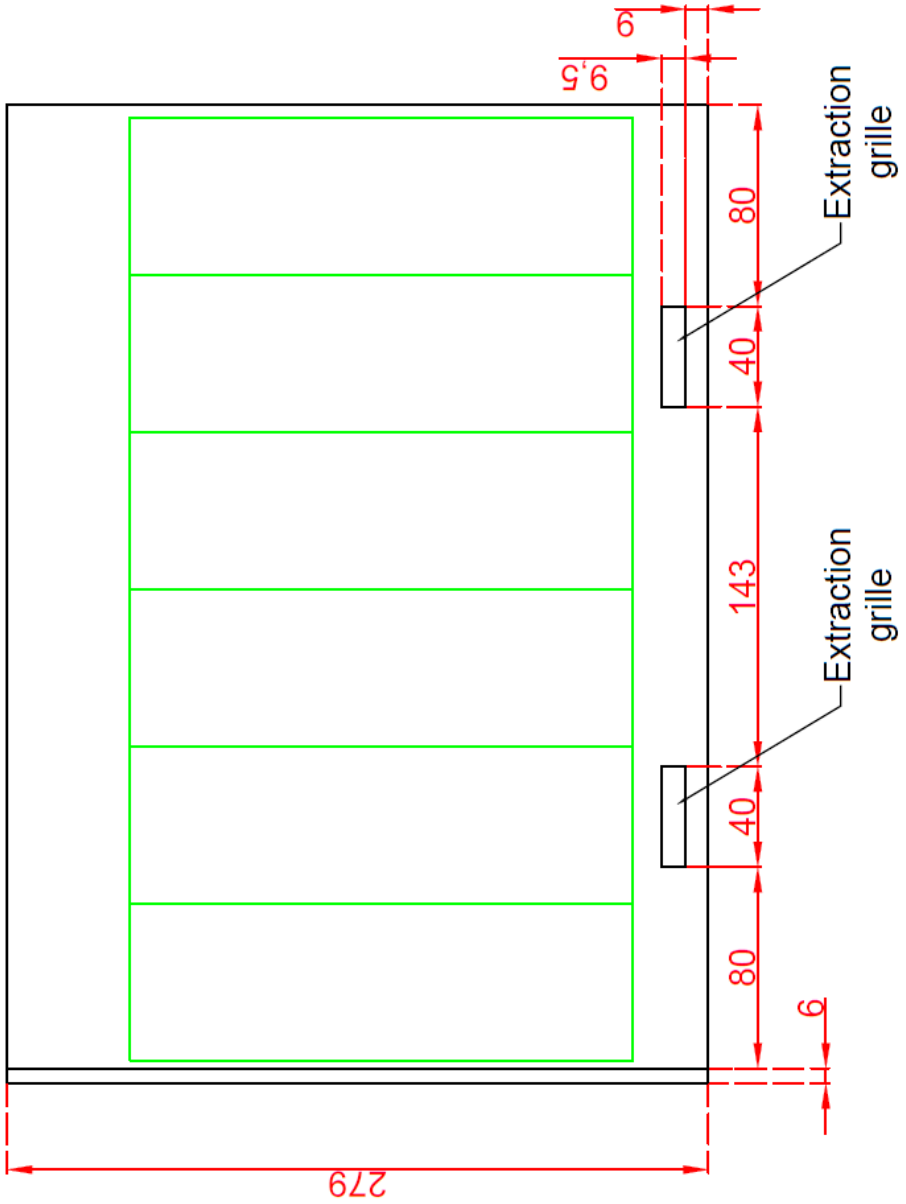

Fig. 18. *South wall – Technical room (Green: Active surface)*

In Fig. 19 is represented the south wall of the test room, bordering the corridor leading to the the professors' offices. As we can see, the actual dimensions of the hole in which the test chamber entrance door will be installed are showed, as well as the four radiant panels installed on this surface.

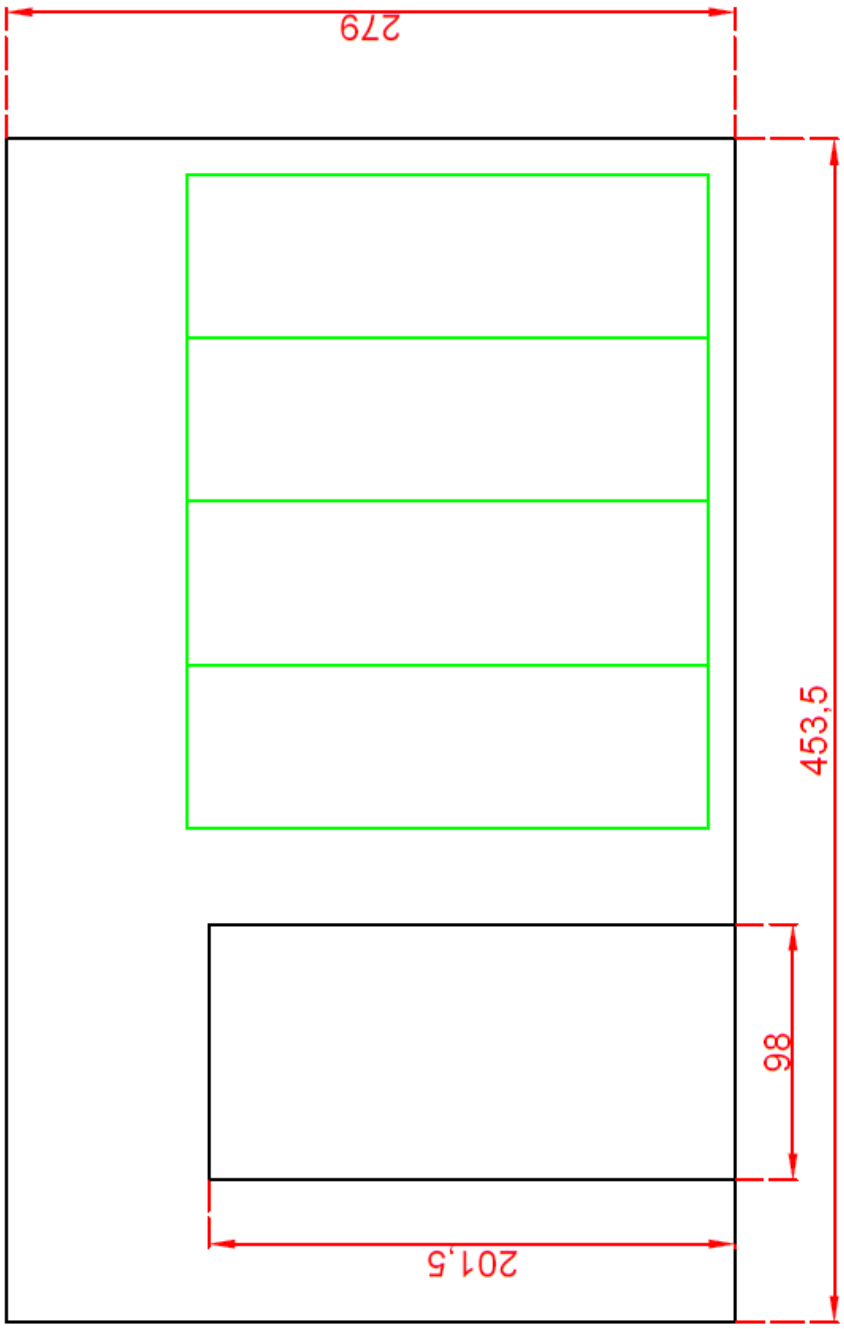

Fig. 19. *West wall – Corridor (Green: Active surface)*

2.3.2. Radiant systems

In this section, we give an introduction to the types of radiant systems provided in this research and a description of their thermal characteristics. As stated previously, the floor, the ceiling and the walls (except for the windows) of the test room were suitably insulated and covered with radiant panels. By definition, radiant systems provide at least 50% of the total sensible heat flux for space conditioning by thermal radiation. Current design standards, as the international standard ISO 11855 [87], the European standard EN 15377 [88], the ASHRAE Handbook on HVAC Systems and Equipment (chapter 6) [89] and the REHVA guidebook [90], categorize radiant systems as a function of their structure and geometry. Based on these standards and guidelines, we identified three main types of radiant systems:

- *Radiant Ceiling Panels* (RCP), where the pipes are attached to metal panels which are fixed to the construction by means of hangers [89,90];

- *Embedded Surface Systems* (ESS) where the pipes are embedded in the surface of the slab/wall, but are insulated from the structure (EN 15377/ISO 11855, Type A, B, C, D, G);

- *Thermally Activated Building Systems* (TABS), where the pipes are embedded in a massive concrete slab/mass (within the structure) (EN 15377/ISO 11855, type E, F).

According to the position of the embedded pipes, ESS is sub-classified as Type A, Type B, Type C, Type D, and Type G. As shown in Fig. 20, Type A is the system with pipes embedded in the screed (or topping slab); Type B contains pipes embedded outside of the screed; Type C contains pipes embedded in the screed below the separating layer; Type D contains capillary mats in a thin (e.g., gypsum) layer with insulation separating it from the building structure; Type G contains pipes embedded in the subfloor of a wooden construction. TABS are sub-classified as Type E and Type F. Type E is the system with pipes embedded in massive concrete slab, and

Type F is the system with capillary pipes embedded in a thin layer that can be thermally connected to a massive slab.

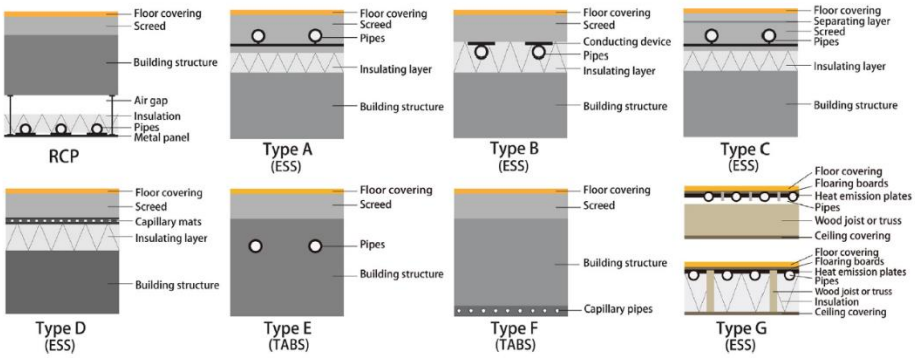

Fig. 20. *Schematic drawing of radiant systems*

For our test room were used two types of configurations: Radiant Ceiling Panels and Type A of Embedded Surface Systems for the floor and walls.

As stated at the beginning of this chapter, all the components present in the two rooms were designed, provided and installed by more than 20 companies from northern Italy. In the following table (Tab. 7) are listed the main companies that provided radiant systems.

Tab. 7. *Companies that provided radiant systems (* RESIN provided screed and resin coating)*

Surface	**Company**
Floor	SEPPELFRICKE*
Ceiling	LOEX
North	EUROTHERM
East	EMMETI
South	UPONOR
West	REHAU

In Tab. 8 are showed the main technical data and features of systems installed in the test chamber.

Tab. 8. *Main technical data and features of systems installed.*

Features	**SEPPELFR.**	**LOEX**		**EUROTH.**	**EMMETI**		**UPONOR**	**REHAU**
Number of modules	15 (1)	3	1,5	3	1,5	2	6	4
Dimensions [cm]	142 x 89 (2)	240 x 120		120 x 200	120 x 200	120 x 100	62,5 x 200	62,5 x 200
Number of circuits	5	6	3	6	3	2	6	4
Active Surface [m^2]	17,65	12,96		7,2	6		7,5	5
Insulating layer [mm]	11	40		30 (3)	30		50	50
Module thickness [mm]	/	52,5 (4)		25	15		15	15
Total thickness [mm]	30	100 (5)		55	45		65	65
Pipes [mm]	10,5 x 1,25	8 x 1		10 x 1,3	8 x 1		9,9 x 1,1	10,1 x 1,1
Internal diameter [mm]	8	6		7,4	6		7,7	7,9
Circuit length [m]	40	19		23	20		16,1	20
Pipe spacing [cm]	9	7,4		6,5	5		5	4,5

(1) Laying panels;

(2) Useful dimensions;

(3) Hollow space (not insulated);

(4) Plasterboard (12,5 mm) + Insulation (40 mm);

(5) Minimum total thickness (module thickness + minimum height of false ceiling hollow space).

Standard EN 1264 [91, 92] provides methods for the determination of the thermal output using calculation and test methods for water-based surface embedded heating and cooling systems. Considering heating conditions, the specific thermal output q is proportional to the temperature difference

between the average water temperature (supply and return) and the air temperature of the room ($\Delta\vartheta_h$). The constant of proportionality given before the temperature difference $\Delta\vartheta_h$ is called the equivalent heat transmission coefficient for heating K_h, which leads to the following abbreviated form of the expression:

$$q = K_h * \Delta\theta_h \quad [^W/_{m^2}] \qquad (1)$$

This equation can also be used in cooling conditions; in this case it is defined the equivalent heat transmission coefficient for cooling K_c.

The characteristic curves of radiant systems are calculated from the previous equation. Thanks to diagrams of thermal yield in heating and cooling conditions provided in the technical data sheets of the radiant systems installed in the test room, it was possible to determine the equivalent heat transmission coefficients represented by the gradient of characteristic curves. These parameters were calculated in order to determine the thermal resistance of panels to be included in the detailed thermal balance of the room described in *chapter 3.2*.

2.3.2.1. Seppelfricke

The radiant floor system was provided by Seppelfricke, a company based in the province of Brescia. Composed by a number of 15 laying panels (useful dimensions: 142 x 89 cm – Fig. 21), the system has a 100% active area, consisting of 5 individual circuits connected in parallel and placed on these modules. Pipes, made of high temperature resistant polyethylene, are characterized by an external diameter of 10,5 mm and an internal diameter of 8 mm. Each circuit is characterized by a length of

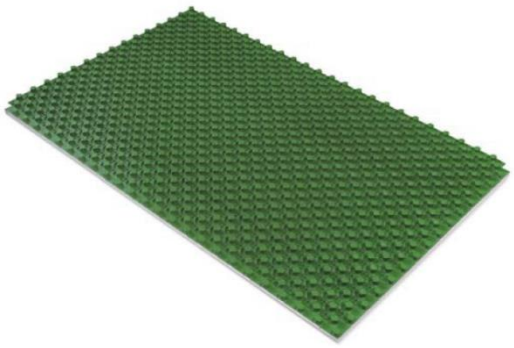

Fig. 21. *Laying panel*

about 40 meters (40 m the shortest, 46 m the longest), with a constant pipe spacing of 9 cm. The total thickness of the radiant floor structure is only 30 mm, consisting of 11 mm of insulating layer (27 mm of total height with clues and pipe clamps) and 3 mm of resinated quartzite as screed. Since diagrams of thermal yield in heating and cooling conditions were not provided, the equivalent heat transmission coefficients (K_h and K_c) were determined thanks to the following pre-design values determined by the company (Tab. 9 and Tab. 10).

Tab. 9. *Technical data – Heating (Seppelfricke)*

Technical data - *Heating*		
External temperature	-5	[°C]
Internal temperature	20	[°C]
Supply temperature	35	[°C]
Return temperature	30	[°C]
Power produced	2156	[W]
Flow rate	232	[l/h]

Tab. 10. *Technical data – Cooling (Seppelfricke)*

Technical data - *Cooling*		
External temperature	35	[°C]
Internal temperature	26	[°C]
Supply temperature	10	[°C]
Return temperature	18	[°C]
Power produced	572	[W]
Flow rate	62	[l/h]

Resulting values of equivalent heat transmission coefficients are:

- $K_h = 9,8\ W/(m^2\ K)$;
- $K_c = 2,7\ W/(m^2\ K)$.

In the following pictures, some characteristic moments in the realization of the radiant floor system were captured, including the laying of circuits (Fig. 22) and the realization of the superficial resin coating (Fig. 23 and Fig. 24). As we can see, this was the first work carried out in the room.

Fig. 22. *Laying of panels and circuits*

Fig. 23. *Surface resin coating (screed)*

Fig. 24. *Surface coating drying*

2.3.2.2. Loex

The radiant ceiling system was provided by Loex, a company based in the province of Bolzano. Composed by 4 and a half panels (dimensions: 240 x 120 cm), with an active area of 73,4%, the radiant ceiling consists of 9 autonomous circuits connected in parallel and incorporated on these modules. This innovative system consists of a new active panel with a sandwich structure (Fig. 25) that incorporates the polystyrene insulation panel and the molded aluminum diffusers with hydraulic circuit in PE-Xa (high density polyethylene) piping (external diameter of 8 mm and internal diameter of 6 mm). The plasterboard slab completes the ceiling system. The convenience of these systems is that they are available in different typologies, with different number and layout of the circuits, so that they can be cut along the special silk-

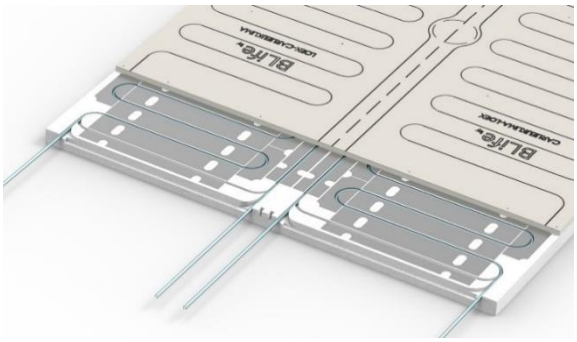

Fig. 25. *Ceiling panel structure*

screened lines to obtain smaller sized panels that help to better cover the available surface by increasing the active elements. Thanks to this

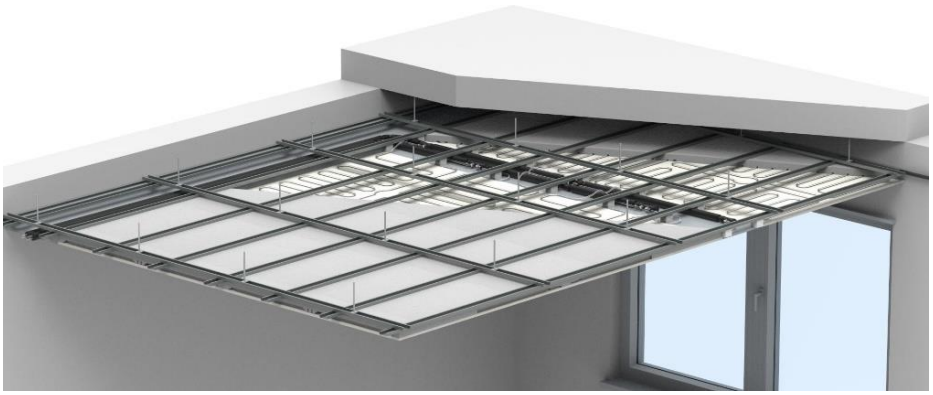

Fig. 26. *Thickness of the ceiling structure*

availability, in our test room were installed 3 active panels *Type 1* and 1 and a half panel *Type 2* (a panel was cut in order to obtain a smaller one with a size of 120 x 120 cm). For more detailed information, please refer to *Appendix B* (Fig. B1 - picture taken from technical data sheet). Each circuit (two for each panel) is characterized by a length of 19 meters, with a constant pipe spacing of 7,4 cm. The minimun total thickness of the ceiling structure (Fig. 26) is 100 mm, because it is composed by a panel thickness of 52,5 mm (12,5 mm of plasterboard + 40 mm of insulation) and a minimum height of false ceiling hollow space of 47,5 mm. In our case the total thickness of the structure is 240 mm, with an hollow space of 187,5 mm, insulated (rock wool) and in which hydraulic connections and ventilation ducts were placed (Fig. 27 and Fig. 28). The equivalent heat transmission coefficients were determined from diagrams of thermal yield in heating and cooling conditions provided by the company (Appendix B **-** Fig. B2 and Fig. B3).

Resulting values of equivalent heat transmission coefficients are:

- $K_h = 4,1\ W/(m^2\ K)$;
- $K_c = 5,7\ W/(m^2\ K)$.

In the following pictures are represented some details of the installation of the radiant ceiling panels after the mounting of the metal substructure and the insulation of the hollow space (Fig. 27 and Fig. 28).

Fig. 27. *Active panels Type 1*

Fig. 28. *Active panel Type 2*

2.3.2.3. Eurotherm

The radiant system for the north wall was provided by Eurotherm, a company based in the province of Bolzano. Composed by 3 panels (dimensions: 120 x 200 cm), with an active area of 66,4%, the radiant wall consists of 6 individual circuits connected in parallel and incorporated in these plates. This system is composed by modular plasterboard panels with MidiX piping (polyethylene with increased thermal resistance) already inserted and arranged in a spiral pattern in order to maximize the exchange surfaces between pipe and plasterboard.

As the previous system, also this can be cut in order to obtain smaller sized panels, but that's not our circumstance. Pipes are characterized by an external diameter of 10 mm and an internal diameter of 7,4 mm. Each circuit is characterized by a length of about 23 meters, with a constant pipe spacing of 6,5 cm. The total thickness of the radiant structure is 55 mm, consisting of 25 mm of plasterboard and 30 mm of hollow space (not insulated). Since diagrams of thermal yield in heating and cooling conditions were not provided, the equivalent heat transmission coefficients were determined thanks to the following pre-design values determined by the company (Tab. 11 and Tab. 12).

Tab. 11. *Technical data – Heating (Eurotherm)*

Technical data - *Heating*		
Internal temperature	20	[°C]
Supply temperature	50	[°C]
Temperature difference	5,0	[°C]
Mean water temperature	47,5	[°C]
Specific power	146	[W/m^2]
Flow rate (circuit)	30,2	[l/h]

Tab. 12. *Technical data – Cooling (Eurotherm)*

Technical data - *Cooling*		
Internal temperature	26	[°C]
Supply temperature	7	[°C]
Temperature difference	3	[°C]
Mean water temperature	8,5	[°C]
Specific power	115	[W/m^2]
Flow rate (circuit)	38,5	[l/h]

Resulting values of equivalent heat transmission coefficients are:

- $K_h = 5,3\ W/(m^2\ K)$;
- $K_c = 6,6\ W/(m^2\ K)$.

In the following pictures are represented the three panels after the wall installation (Fig. 29) and during the hydraulic and electrical connection (Fig. 30).

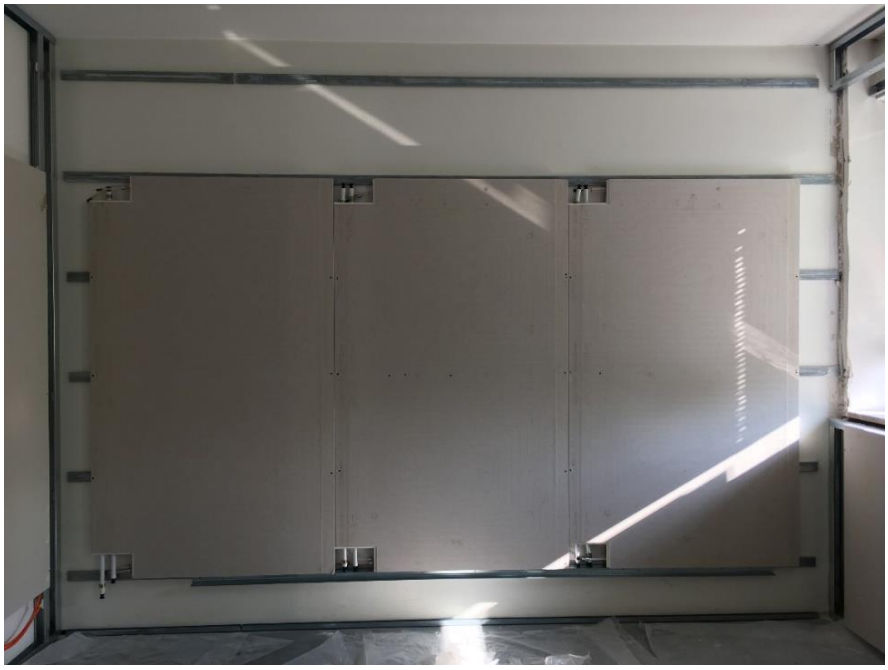

Fig. 29. *North panels after the installation*

Fig. 30. *North panels during the hydraulic and electrical connection*

2.3.2.4. Emmeti

The radiant system for the east wall was provided by Emmeti, a company based in the province of Pordenone. The radiant wall is composed by 3 and a half panels with different dimensions, in order to better cover the available surface between and below windows:

- 1 panel composed by 2 autonomous circuits (dimensions: 120 x 200 cm - Fig. 31);
- 1 panel composed by 1 autonomous circuit (dimensions: 60 x 200 cm - half of the previous one);
- 2 panels composed by 2 autonomous circuits (dimensions: 120 x 100 cm - Fig. 32).

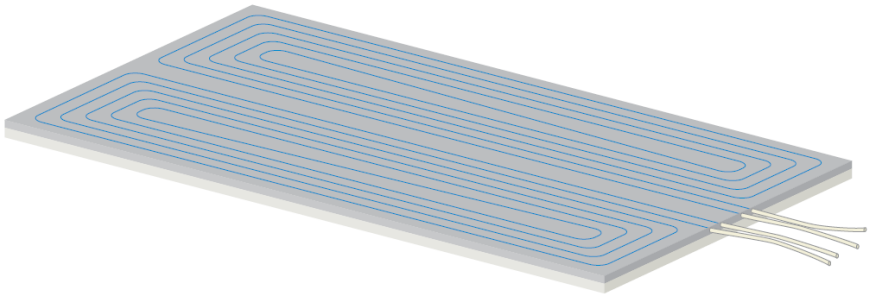

Fig. 31. *Central panel between windows (120 x 200 cm)*

With an active area of 69,7%, all the circuits are connected in parallel and incorporated on the modules. This system consists of a prefabricated plasterboard panel (thickness of 15 mm) that integrates one or two PE-MDXc (medium density polyethylene) pipe circuits (external diameter of 8 mm and internal diameter of 6 mm), coupled with an EPS 250 insulating slab (thickness of 30 mm), which guarantees an adequate rigidity of the panels being installed for an optimum flatness of the surface. The traces of the spiral circuits are screen-printed on the surface of the panel. Each circuit is characterized by a length of about 20 meters (20,8 m for the first two panels, 21,5 m for the last one), with a constant pipe spacing of 5 cm. The total thickness of the radiant structure is only 45 mm. The equivalent heat transmission coefficients were determined from diagrams of thermal yield in heating and cooling conditions provided by the company (Appendix B - Fig. B4 and Fig. B5).

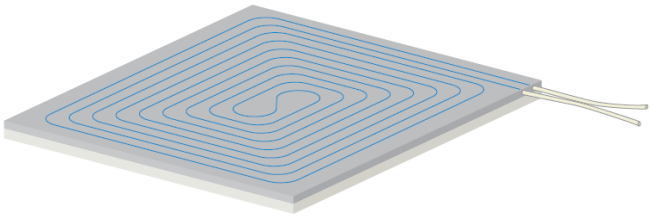

Fig. 32. *Side panels below windows (120 x 100 cm)*

Resulting values of equivalent heat transmission coefficients are:

- $K_h = 4,6\ W/(m^2\ K)$;
- $K_c = 4,6\ W/(m^2\ K)$.

In the following pictures, some characteristic moments in the realization of the east radiant wall were captured, including the mounting of the metal profiles necessary to close the existing niches (Fig. 33), the laying of the insulating material (rock wool) inside them (Fig. 34) and panels after the installation (Fig. 35).

Fig. 33. *Metal substructure necessary to close the existing niches*

Fig. 34. *Insulating material (rock wool) inside niches*

Fig. 35. *East panels after the installation*

2.3.2.5. Uponor

The radiant system for the south wall was provided by Uponor, a company based in the province of Monza-Brianza. Composed by 6 panels (dimensions: 62,5 x 200 cm - Fig. 36), with an active area of 69,1%, the radiant wall consists of 6 individual circuits connected in parallel and incorporated in these plates. This system is composed by a plaster panel (thickness of 15 mm) that encloses inside a PE-Xa (high density polyethylene) piping (external diameter of 9,9 mm and internal diameter of 7,7 mm). No additional plasterboard is needed. Each circuit is characterized by a length of about 16 meters, with a constant pipe spacing of 5 cm, a heating flow rate of 136 l/h and a cooling flow rate of 130 l/h. The total thickness of the radiant structure is 65 mm, consisting of 15 mm of the active panel and 50 mm of hollow space due to the mounting metal frame (insulated with rock wool panel). The equivalent heat transmission coefficients were determined from diagrams of thermal yield in heating and cooling conditions provided by the company (Appendix B - Fig. B6).

Fig. 36. *Active plaster panel*

Resulting values of equivalent heat transmission coefficients are:

- $K_h = 6,5\ W/(m^2\ K)$;
- $K_c = 6,5\ W/(m^2\ K)$.

In the following pictures are represented the six panels after the wall installation (Fig. 37) and during the hydraulic connection and the insulation of hollow space (Fig. 38).

Fig. 37. *South panels after the installation*

Fig. 38. *South panels during the hydraulic connection and the insulation of hollow space*

2.3.2.6. Rehau

The radiant system for the west wall was provided by Rehau, a German company with some branches in Italy (Treviso, Milano, etc.). Composed by 4 panels (dimensions: 62,5 x 200 cm), with an active area of 46,8 %, the radiant wall consists of 4 autonomous circuits connected in parallel and incorporated in these modules. This system is composed by grooved plaster panels (thickness of 15 mm - Fig. 39) that integrate RAUTHERM S tubes (PE-Xa, high density polyethylene - Fig. 40), individually packaged, with an external diameter of 10,1 mm and an internal diameter of 7,9 mm. These panels are characterized by a fiber reinforcement, impregnated inside the plaster, which makes them extremely resistant to impact and bending. Each circuit is characterized by a length of 20 meters, with a constant pipe spacing of 4,5 cm (double serpentine laying). The total thickness of the radiant structure is 65 mm, consisting of 15 mm of the active panel and 50 mm of hollow space due to the substructure with metal frame (insulated with rock wool panel). The equivalent heat transmission coefficients were determined from diagrams of thermal yield in heating and cooling conditions provided by the company (Appendix B - Fig. B7 and Fig. B8).

Fig. 39. *Grooved plaster panels*

Fig. 40. *RAUTHERM S tubes integrated in panels*

Resulting values of equivalent heat transmission coefficients are:

- $K_h = 4,8\ W/(m^2\ K)$;
- $K_c = 4,2\ W/(m^2\ K)$.

In the following pictures are represented the four panels after the wall installation (Fig. 41) and during the hydraulic connection and the insulation of hollow space (Fig. 42).

Fig. 41. *West panels after the installation*

Fig. 42. *West panels during the hydraulic connection and the insulation of hollow space*

2.3.3. Mechanical ventilation system

In this section, we give a brief introduction to the type of ventilation system provided in this research and a description of its main characteristics. Mixing ventilation (MV) is a traditional air distribution method to regulate the indoor environment, which supplies fresh air from ceiling level with high velocity to achieve an even distribution of temperature and pollutant in the whole space. This kind of system is the most widely used ventilation principle, because it can be used for both heating and cooling and it can cope with higher heat loads compared to displacement ventilation. The air movement is produced by the introduction into the environment of one or more jets of air (primary air) with enough kinetic energy to move the surrounding ambient air (secondary air), create a high turbulence and obtain a good mix. The use of MV has been well defined in various international standards regarding thermal comfort and indoor air quality [6, 7, 93]. Recently, one practical guidebook, which introduces comprehensively the various application of mixing ventilation, was published by REHVA [94]. Moreover, methods of testing for room air diffusion and the performance of air outlets and air inlets has been developed and standardized [95, 96].

As we can see in the previous Fig. 15 and Fig. 18, the primary air jet is supplied through two inflow vents (L x W = 82 x 7 cm) located on the north side of the ceiling (2,79 m above the floor), symmetrically arranged (64.5 cm from the east and west walls), 12 cm before the north wall. On the other hand, the secondary air is extracted through two exhaust vents (L x W = 40 x 10 cm) located on the lower part of south wall, symmetrically arranged (80 cm from the east and west walls), 9 cm above the floor. Supply ventilation ducts were placed inside the hollow space above radiant ceiling panels, as we can see in Fig. 43.

Fig. 43. *Supply vents with plenums and ventilation ducts*

In Fig. 44 and Fig. 45 are represented respectively one of the extraction vents and its plenum, placed in the north wall of the technical room.

Fig. 44. *Extraction vent*

Fig. 45. *Plenum of an extraction grid*

All these components (ducts, plenums, vents, grids) were provided by Brofer, a company based in the province of Treviso.

Instead, the ventilation machine was provided by RDZ, a company based in the province of Pordenone. This air handling unit for the renewal of the ambient air with high efficiency heat recovery and for the summer dehumidification treatment (R134a refrigerant) is able to heat or cool and dehumidify the test room, in order to control humidity and ventilation flow rate. Operative with all external air and standard bypass supply for free-cooling (with NTC probe incorporated on the outdoor air intake channel). To facilitate installation and optimize the available space, the machine, equipped with G4 filters, consists of three separate modules: two ventilation units and a recovery / treatment unit, which can be installed close to each other or in distinct positions. Ventilation units consist of two double suction centrifugal fans directly coupled to its motor (inflow and exhaust fan), incorporated inside two silencers (Fig. 46). The heat recovery unit on the air expulsion in counter-current (cross-flow, Fig. 47) is at high efficiency (about 90%). The system foresees the connection with the air outside the ventilating section and the connection with the extract air from the rooms to the recovery / treatment unit.

From an acoustic point of view, the noise produced by the machine and by fans can be transmitted through the distribution line and transported to the various rooms. For this reason, it was provided a silencer near the outlet vent and rigid pipes for connection to it.

As stated previously in *section 2.3*, all the systems were installed in the technical room; the whole machine for air ventilation was located in the ceiling of the technical room, with an obstruction of 40 cm (Fig. 48).

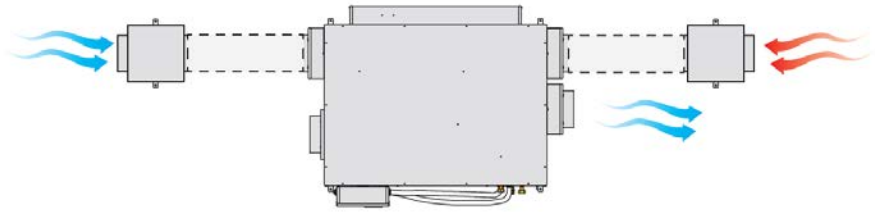

Fig. 46. *Machine for air ventilation (three separate modules: two ventilation units and a recovery/treatment unit). Red: Discharge; Light blue: Supply.*

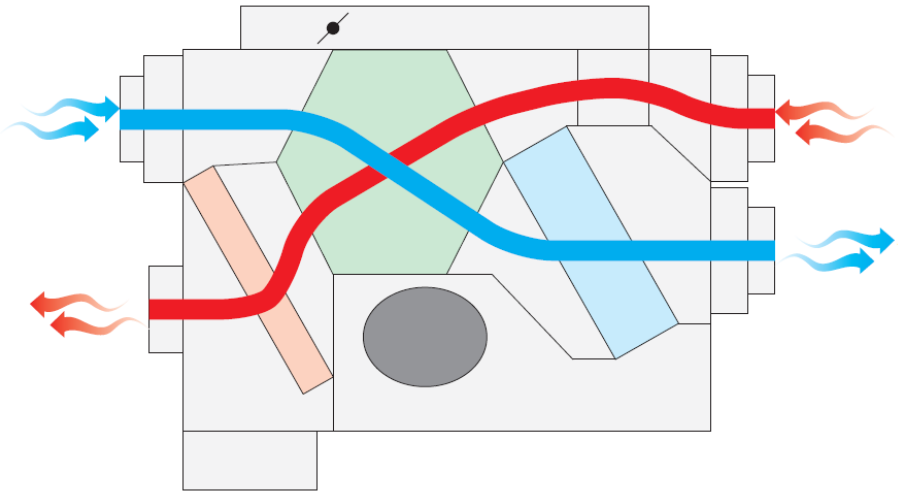

Fig. 47. *Heat recovery unit in counter-current (cross-flow). Red: Discharge; Light blue: Supply.*

In APPENDIX B are reported two tables obtained from the technical manual of the system, in which are listed technical characteristics (Tab. B1) and summer performances (Tab. B2). For further information regarding the recovery unit performance, please refer to the technical manual available on the web-site of the company (UAP 200-PDC, RDZ).

Fig. 48. *Ventilation machine and aeraulic ducts installed in the ceiling of the technical room*

2.3.4. Windows

As stated previously in *section 2.3.1*, the niches of the two original windows were closed by other internal windows, determining a double window configuration with an internal air space for high thermal and acoustic insulation (45 cm). Provided by Elledi, a company based in the province of Vicenza, the new windows are equipped with double-glazing (6-16-6 mm, with low emissive internal glass), filled with Argon, and a PVC frame (Fig. 49).

Fig. 49. *Profile of new internal windows*

The characteristic properties of new windows, some of these extracted from the technical data sheet, are listed in Tab. 13.

Tab. 13. *Properties of new internal windows*

Dimensions	6-16-6	[mm]
Gas	Argon	
Uw	1,17	[W/(m^2 K)]
Ag	1,699	[m^2]
Af	0,329	[m^2]
Profile depth	70	[mm]
Soundproofing power ($R_{w,p}$)	up to 45	dB
Security against break-ins	2*	Class of resistance

** Laminated safety glass on the inside*

In Fig. 50 is represented one of the two windows installed in the test room. We can observe the high glass surface, the internal frame and the decorative frame showed in the previous Fig. 17. Moreover, we can notice the double window configuration with the internal air space for high thermal and acoustic insulation. The original shutters have been removed and will be replaced in future by electrically controlled shutters.

Fig. 50. *One of the two windows installed in the test room*

Following are reported some panoramic pictures of the room carried out during the construction in order to give an overall view of the work done.

In Fig. 51 and Fig. 52 are represented the four walls after the installation of radiant panels.

In Fig. 53 and Fig. 54 are represented the four walls during the hydraulic and aeraulic connections and after the installation of windows and insulating material.

In Fig. 55 and Fig. 56 are represented three of the four walls during the finishing of plasterboard and the painting of room.

In Fig. 57 are represented the test chamber as it currently appears, after completing the electrical connections and the finishing work on surfaces.

Fig. 51. *North and east wall after the installation of radiant panels*

Fig. 52. *South and west wall after the installation of radiant panels*

Fig. 53. *North and east wall during the hydraulic and aeraulic connection and after the installation of windows and insulating material*

Fig. 54. *South and west wall during the hydraulic and aeraulic connection and after the installation of windows and insulating material*

Fig. 55. *North and east wall during the finishing of plasterboard and the painting of room*

Fig. 56. *East and south wall during the finishing of plasterboard and the painting of room*

Fig. 57. *Test chamber as it currently appears*

2.4. Obstructions of the technical room

In this section we present in detail the current dimensions of the technical room. As for the climate chamber, surveys were carried out personally several times, using a measuring tape (resolution: *1 mm*; range: *5 m*), in order to guarantee an accurate truthfulness of the results. Unlike what was done previously for the test chamber, the objective for the technical room was not to measure its actual dimensions (almost unchanged during works), but rather to determine the obstructions caused by systems installed in it. The determination of these sizes was fundamental to evaluate a correct and orderly arrangement of the systems within the room. Furthermore, it allowed to determine the empty spaces in order to place the future control station of the climate chamber (control and data acquisition computer) or any other system.

The following components were installed:

- A storage tank with a volume of 200 litres with an electric heater of 2,5 kW for hot water;
- A storage tank with a volume of 150 litres for chilled water;
- Hydronic systems for managing flow rates and supply temperatures (valves, pumps, pipes, manifolds);
- An air handling unit for the renewal of the ambient air with high efficiency heat recovery and for the summer dehumidification treatment.

In the following pages are included the drawings of the technical room made using the software AUTOCAD®. For the reason stated at the beginning of this section, the dimensions of measurements have not been reported. As we can see, the equipment is represented with different colours:

- Red: Dimensions of systems;
- Blue: Pipes;
- Yellow: Switchboards.

Furthermore, obstructions (continuous line) are differentiated from the actual dimensions of components (dotted line).

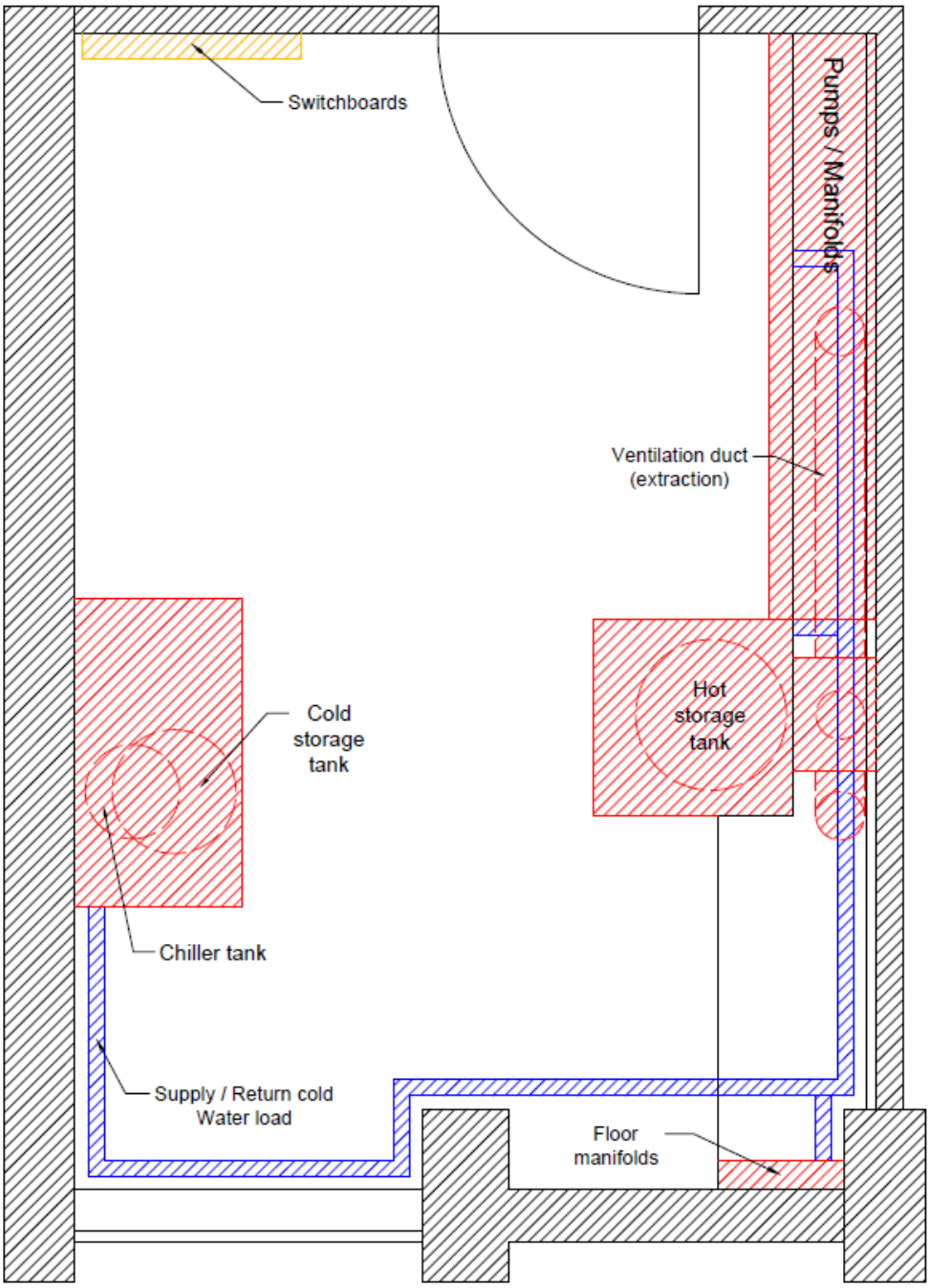

Fig. 58. *Obstructions technical room – floor (Red: Dimensions of systems; Blue: Pipes; Yellow: Switchboards)*

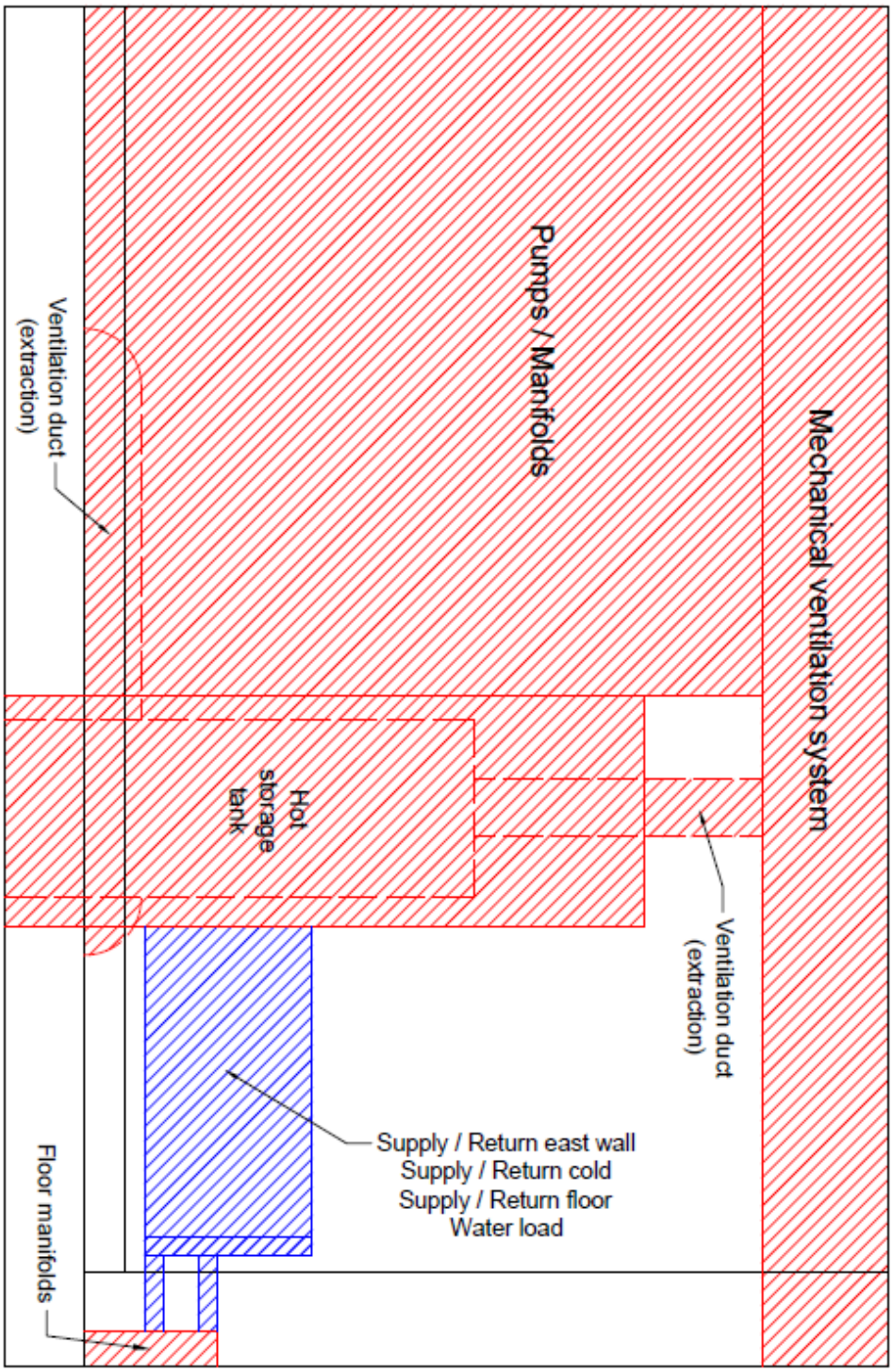

Fig. 59. *Obstructions technical room – North wall (Red: Dimensions of systems; Blue: Pipes)*

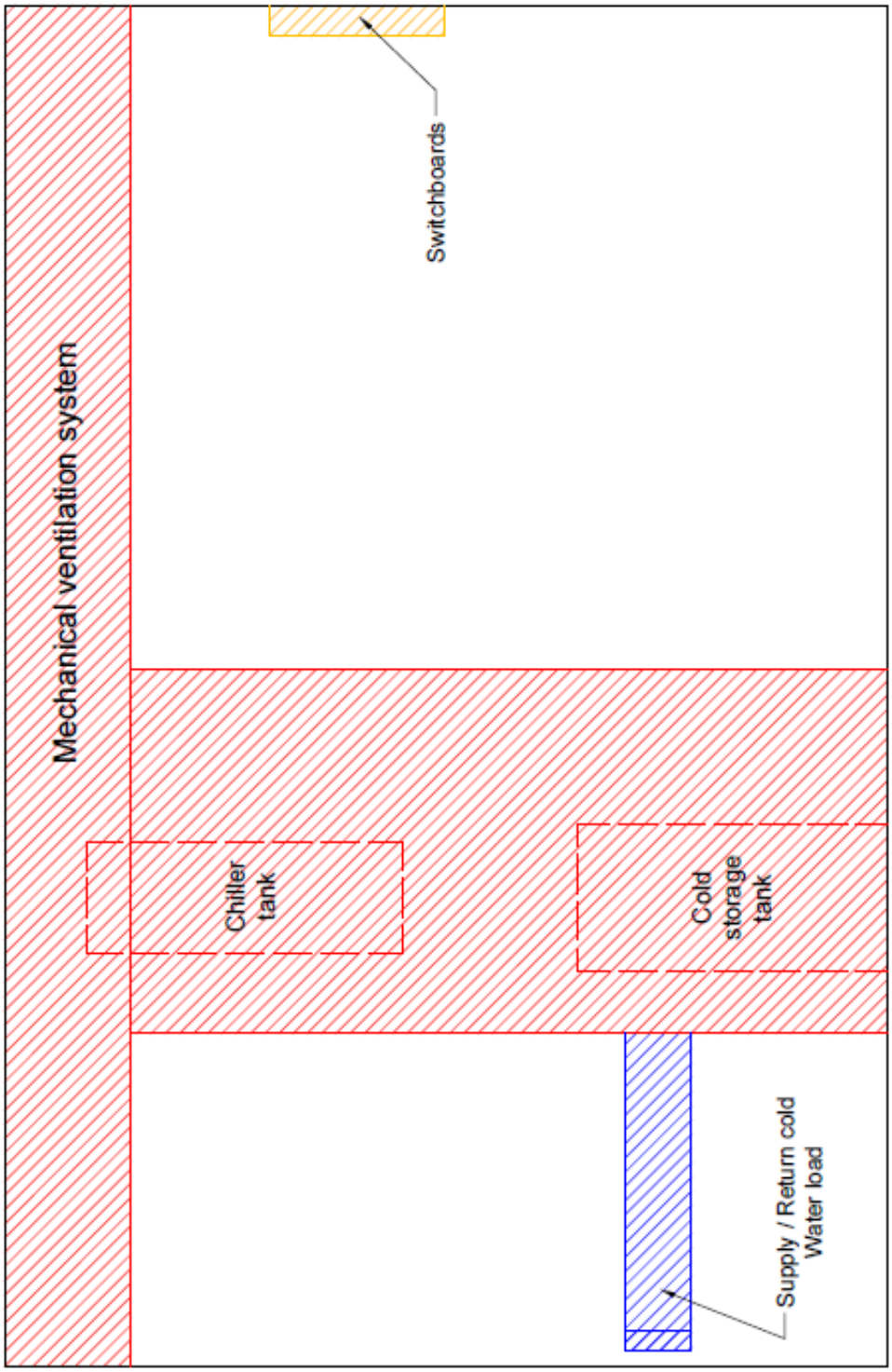

Fig. 60. *Obstructions technical room – South wall (Red: Dimensions of systems; Blue: Pipes; Yellow: Switchboards)*

In Fig. 58 is represented the floor of the technical room.

As we can see, on the north wall (Fig. 59), the hydronic systems of radiant panels (pumps, manifolds and pipes of ceiling and side walls), which occupy approximately half of the wall itself, the storage tank to produce hot water, the extraction ducts of the ventilation system and numerous pipes (supply and return of east wall/floor/cold storage tank and water load) have been placed. Moreover, it should be noted that in the lower part of the surface a plasterboard step was made, in order to hide the plenums of the extraction vents (Fig. 45) and the radiant floor pipes (Fig. 61), with the exception of manifolds.

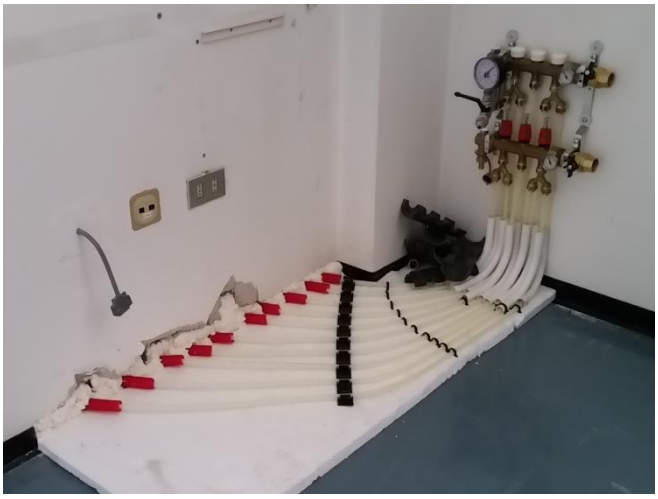

Fig. 61. *Radiant floor pipes and manifolds*

On the opposite side, on the south wall (Fig. 60), the storage tank for chilled water, the chiller tank and some pipes (supply and return of cold storage tank/water load) have been placed. Again, it should be noted that the area near the switchboards has been completely left free, having been identified as the site in which to place the control station, when the climate chamber will be operational.

Finally, the ceiling of the technical room is completely occupied by the mechanical ventilation system, as already stated in *section 2.3.3* and evident in the previous Fig. 48.

Following are reported some pictures of the systems installed in the technical room (Fig. 62, Fig. 63 and Fig. 64).

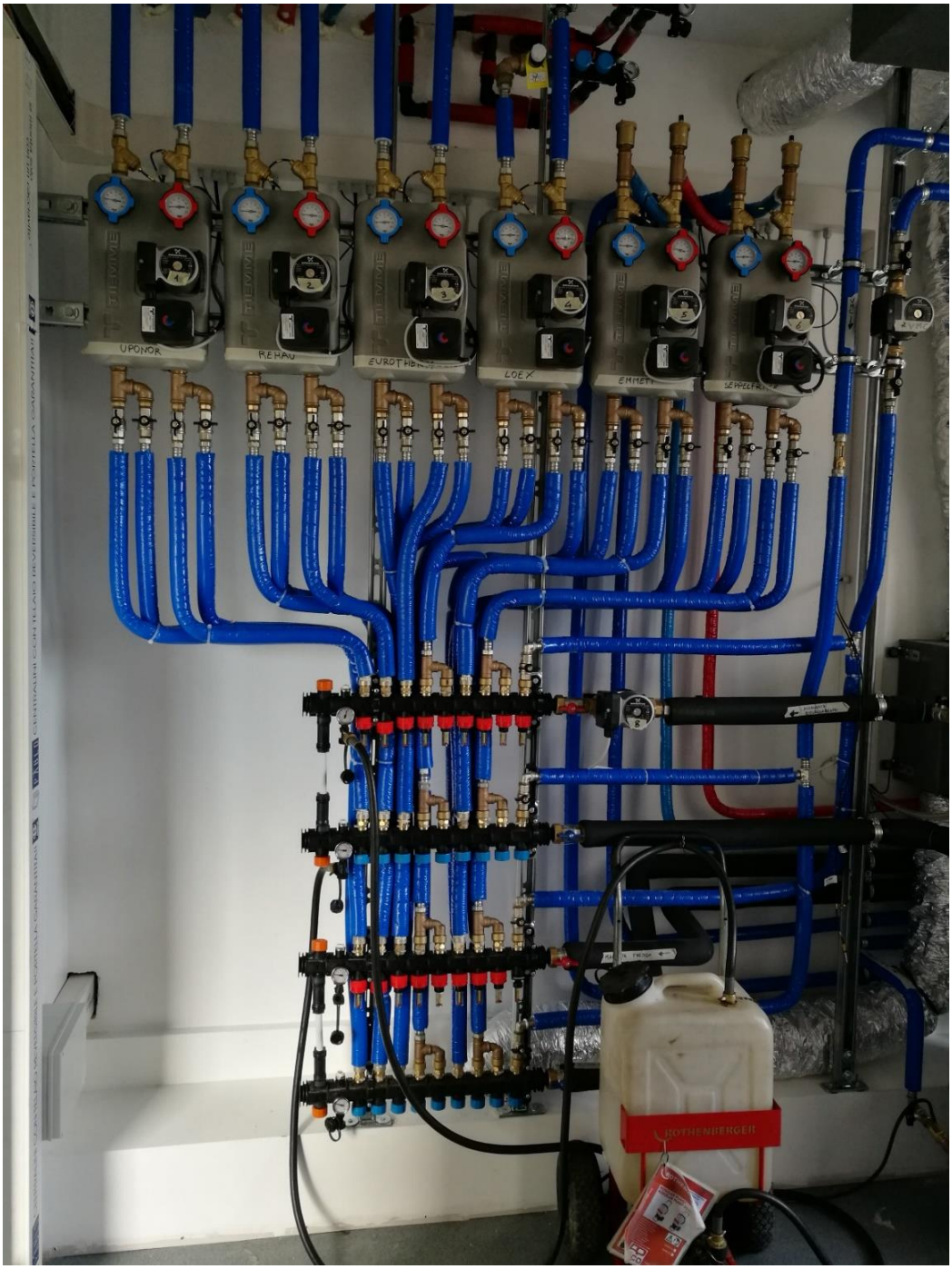

Fig. 62. *Hydronic systems (valves, pumps, pipes, manifolds)*

Fig. 63. *Storage tank for hot water. Besides, we can see the extraction ducts and the plasterboard step*

Fig. 64. *Below: storage tank for chilled water. Above: chiller tank*

Chapter 3

SIMULATION MODEL

3.1. Introduction

Heat transfer between indoor surfaces and room are very important, since it affects the resulting temperatures. This is a very important issue, since room simulation models are increasingly used. The problem is even more critical, since radiant systems are becoming more and more popular and there is the need to correctly predict their performance in different operating conditions. Heating and cooling capacity of surface systems (floor, ceiling and walls) have been recently debated in the European Standards EN 1264 [91, 92] and EN 15377 [88] as well as in the new draft of ISO standard on radiant systems.

Both convective and radiant heat transfer have to be considered in heat transfer analysis within an enclosed room. There are different ways to consider the heat exchange between a surface and its surroundings. One possibility is to look in detail at the heat flows between each surface and the other ones through radiation and between each surface and the air through convection. This problem is showed in Fig. 65.a for a simplified case where three surfaces (floor, ceiling and wall) are

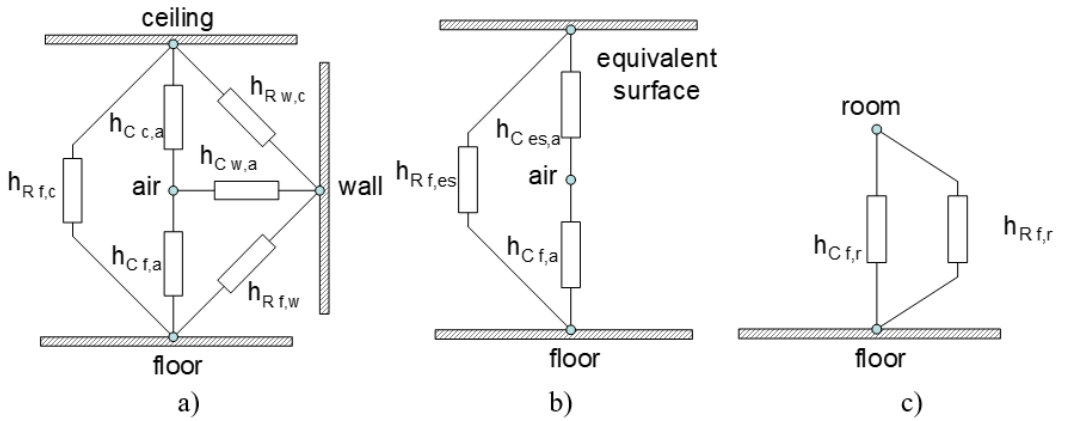

Fig. 65. *Example of heat exchange between floor and surrounding; a) overall balance (including heat flows to walls and ceiling), b) considering radiation with an equivalent surface and convection with the air, c) synthetic approach (heat flow with the room).*

considered. In the more comprehensive description of the problem, at least six surfaces appear. Another possibility is to deal with the problem considering the radiation between the examined surface and the other surfaces at an equivalent

temperature and the convection between the surface and the air. This case is reported in Figure 65.b for the case of the heat exchange between the floor and the surrounding environment. The third case represents the heat exchange between the surface and the room at a unique temperature, which is the operative temperature (T_{op}), as reported in Figure 65.c for the case of the heat exchange between the floor and the room.

Following the method of the detailed energy balance of a room (Fig. 65.a), the present work aims at creating a simulation model in steady-state conditions that allows to determine the internal surface temperatures of the climate chamber (floor, ceiling, walls and windows) and the internal air temperature (consequently the operative temperature – *section 3.4.1*) as a function of the external temperature, temperatures of the water into the six radiant systems and solar radiation (transmitted and absorbed). Furthermore, this model has been realized to carry out an analysis of the radiant asymmetry that occurs at different thermal conditions (hot/cold floor and hot/cold ceiling, according to the season considered). To do this, the hourly profile of the water temperature that flows inside floor or ceiling radiant systems was determined (depending on the thermal condition considered), respecting some conditions to be simulated, such as keeping constant the operative temperature inside the room, equal to the set-point value (26 °C in summer season, 20 °C in winter season).

The present work represents the first step of the research for evaluating the indoor environmental quality in our test room. Results obtained from the theoretical model will be verified by means of measurements as soon as the operation of the climate chamber is guaranteed. Moreover, they will be used to calibrate and set up the different radiant systems in order to perform experimental tests with human subject on radiant asymmetry and indoor environmental quality.

3.2. Detailed energy balance of a room

In this section, we give a detailed description of the method used in order to determine the energy balance of our test room.

3.2.1. Surfaces heat balance

The heart of the detailed energy balance of a room is the internal heat balance involving the inside faces of the zone surfaces. This heat balance is generally modelled with four coupled heat transfer components:

- Conduction through the building element;
- Convection to the air;
- Short wave radiation absorption and reflectance;
- Longwave radiant interchange.

The incident short wave radiation is from the solar radiation entering the zone through windows and emittance from internal sources such as lights. The longwave radiation interchange includes the absorption and emittance of low temperature radiation sources, such as all other zone surfaces, equipment, and people.

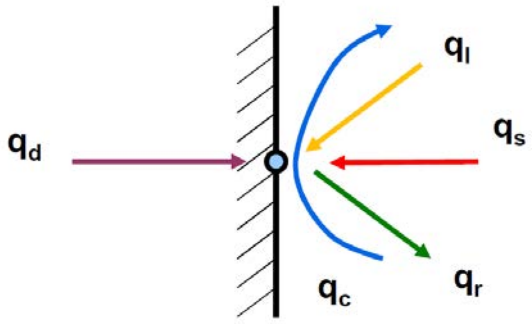

Fig. 66. *Schematic representation of the surface balance*

Considering each i-th internal surface, the heat balance can be written as follows (schematic representation in Fig. 66):

$$q_{d,i} + q_{c,i} + q_{r\,i,j} + q_{s,i} + q_{l,i} = 0 \qquad (2)$$

- q_d : conduction [W];
- q_c : convective heat exchange with the air [W];
- q_r : mutual infra-red radiation between internal surfaces [W];
- q_s : incoming radiation due to solar radiation [W];
- q_l : incoming radiation due to internal radiative gains [W].

Following are listed formulas used to determine the previous parameters in the balance.

Conduction

$$q_{d,i} = \frac{t_{s,i} - t_{w,i}}{R_i} * S_i \qquad (3)$$

- $t_{s,i}$: internal surface temperature [K];
- $t_{w,i}$: water temperature [K];
- R_i : conductive thermal resistance for heating (h) or cooling (c) [(m^2 K)/W];

$$R_i = \frac{1}{K_{(h,c),i}} - \frac{1}{h_{t,i}} \qquad (4)$$

- $K_{(h,c)}$: equivalent heat transmission coefficient for heating (h) or cooling (c) [W/(m^2 K)] *(1)*;
- $h_{t,i}$: total heat exchange coefficient (convection + radiation) between surface and space [W/(m^2 K)];

$$h_{t,i} = h_{c,i} + h_r \qquad (5)$$

- $h_{c,i}$: convective heat exchange coefficient (heating or cooling) [W/(m^2 K)];
- h_r : radiant heat exchange coefficient = 5,5 W/(m^2 K);
- S_i : active surface area [m^2].

Convective heat exchange with the air

$$q_{c,i} = S_i * h_{c,i} * (t_{s,i} - t_{air}) \qquad (6)$$

- S_i : active surface area [m^2];
- $h_{c,i}$: convective heat exchange coefficient (heating or cooling) [W/(m^2 K)];
- $t_{s,i}$: internal surface temperature [K];
- t_{air} : indoor air temperature [K].

Mutual infra-red radiation between internal surfaces

Considering the i-th and the j-th internal surface:

$$q_{r\,i,j} = F_{i-j} * S_i * h_r * (t_{s,i} - t_{s,j}) \qquad (7)$$

- F_{i-j} : view factor between surfaces;
- S_i : active surface area [m^2];
- h_r : radiant heat exchange coefficient = 5,5 W/(m^2 K);
- $t_{s,i}$, $t_{s,j}$: internal surface temperatures [K];

Incoming radiation due to solar radiation

Considering each k-th glazed surface:

$$q_{s,i} = \frac{S_i}{S_t - \sum_{k=1}^{f} S_k} * \sum_{k=1}^{f}(q_{s,k}) = f_{r,i} * \sum_{k=1}^{f}(q_{s,k}) \qquad (8)$$

- S_i : active surface area [m^2];
- S_t : total active surfaces area (opaque walls + windows) [m^2];
- S_k : glazed surface [m^2];
- $q_{s,k}$: transmitted solar radiation (beam + diffuse) [W];
- $f_{r,i}$: surface fraction.

Incoming radiation due to internal radiative gains

Considering each g-th internal load:

$$q_{l,i} = f_{r,RAD} * \frac{S_i}{S_t - \sum_{k=1}^{f} S_k} * \sum_{g=1}^{m}(q_{l,g}) = f_{r,RAD} * f_{r,i} * \sum_{g=1}^{m}(q_{l,g}) \qquad (9)$$

- $f_{r,RAD}$: radiant fraction of internal gains = 0,3;
- S_i : active surface area [m^2];
- S_t : total active surfaces area (opaque walls + windows) [m^2];
- S_k : glazed surface [m^2];
- $q_{l,g}$: internal load [W];
- $f_{r,i}$: surface fraction.

Thanks to the previous expressions, it was possible to write 7 equations, 6 for each surface (floor, ceiling and walls) plus 1 for the internal glazed surface of windows, in 9 variables, represented by the six internal surface temperatures, the internal and external glass surface temperature and the indoor air temperature.

In the equation for the internal glazed surface of the windows, the solar loads are not represented by the portion transmitted and spread on the different surfaces (as previously expressed), but by the half of the absorbed radiation by the glass itself, where:

- I_a : absorbed solar radiation (beam + diffuse) [W];

3.2.2. Air balance (thermal/sensible)

In order to continue with the definition of our model, it is necessary to take into account the air balance. It consists of two aspects:

- Thermal balance of the air (sensible);
- Mass balance for the air (latent).

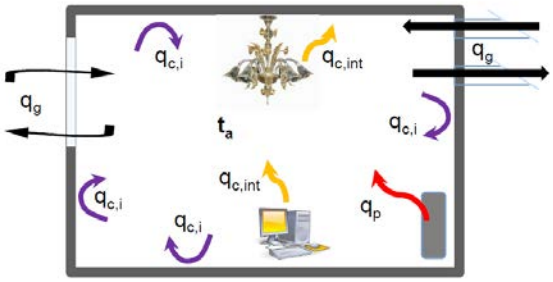

Fig. 67. *Schematic representation of the thermal balance of the air (example)*

Being interested only in the thermal aspect, the air balance in steady-state conditions can be written as follows (schematic representation in Fig. 67):

$$\sum_{i=1}^{n} q_{c,i} + q_{c,int} + q_g + q_p = 0 \qquad (10)$$

- $\sum_{i=1}^{n} q_{c,i}$: convective heat exchange with the n surfaces (floor, ceiling, walls and glazed surfaces) *(6)*;
- $q_{c,int}$: convective power of internal gains;
- q_g : ventilation power (infiltration, ventilation, AHU);
- q_p : thermal plant convective power.

Following are listed formulas used to determine the previous parameters in the balance.

Convective power of internal gains

Considering each g-th internal load:

$$q_{c,int} = f_{r,CONV} * \sum_{g=1}^{m} (q_{l,g}) \qquad (11)$$

- $f_{r,CONV}$: convective fraction of internal gains = 0,7;
- $q_{l,g}$: internal load [W];

Ventilation

$$q_g = G_a * c_{p,a} * (t_{air} - t_{imm,air}) \qquad (12)$$

- G_a : air mass flow rate [kg/s];
- $c_{p,a}$: specific heat of the air at constant pressure = 1005 J/(kg K);
- t_{air} : indoor air temperature [K];
- $t_{imm,air}$: supply air temperature [K];

Thanks to the previous expressions, it was possible to write another equation in two variables, the indoor air temperature and the thermal plant convective power. Therefore, there are two possibilities:

- if the air temperature is fixed, a convective heating or cooling system, (e.g. fan-coil units) can be simulated. The result is the heat flow required by the plant to maintain the set-point temperature;
- if the heat flow required by the plant is fixed (usually it is null, in case the plant is switched off), the resulting air temperature of the room can be calculated.

In our circumstance, the heat flow required by the plant is null, because the test room was not equipped with any system that generates this kind of convective power.

3.2.3. Windows heat balance

Finally, to conclude our simulation model, it is necessary to take into account the windows heat balance. Since the heat balance of the internal glazed surface of the windows has already been considered previously in *section 3.2.1*, in this case we focus on determining the influence of the external temperature on the internal glazed surface temperature. We consider:

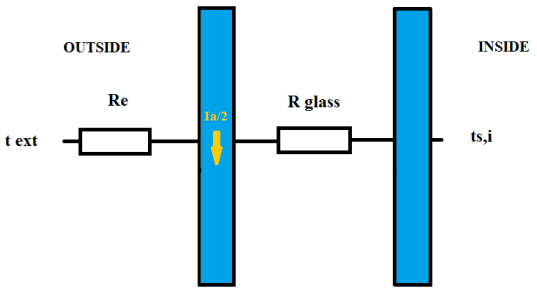

Fig. 68. *Schematic representation of the windows thermal balance (example)*

- convective heat exchange between the outside air and the external surface of the window;
- absorbed solar radiation (beam + diffuse);
- conduction through the glass layers.

In Fig. 68 is represented an example of the thermal balance considered in our model.

Following are listed formulas used to determine the previous parameters in the balance.

Conduction through the glass layers

As described previously in *chapter 2.3*, the test room is equipped with a double window configuration with an internal air space for high thermal and acoustic insulation (45 cm).

For this reason, the thermal resistance of our windows is calculated with the following expression:

$$R_{glass} = \frac{1}{U_{w1}} + \frac{1}{U_{w2}} - R_{si} - R_{se} + R_{cavity} \qquad (13)$$

- U_{w1} : thermal transmittance of the external window [W/(m^2 K)];

- U_{w2} : thermal transmittance of the internal window [W/(m^2 K)];

$$U_w = \frac{\sum A_g U_g + \sum A_f U_f}{\sum A_g + \sum A_f} \qquad (14)$$

- U_g : thermal transmittance of the glazing [W/(m^2 K)];
- U_f : thermal transmittance of the frame [W/(m^2 K)];
- A_g : glazed surface area [m^2];
- A_f : frame area [m^2];

In the calculation of the thermal transmittance of the windows *(14)*, linear thermal losses Ψ_g due to the combined thermal effects of the frame, glazing and spacer have been neglected.

- R_{si} : internal surface thermal resistance = 0,125 (m^2 K)/W;

$$R_{si} = {}^{1}/_{h_{si}} \qquad (15)$$

- h_{si} : internal liminal coefficient (convection + radiation) = 8 W/(m^2 K);
- R_{se} : external surface thermal resistance = 0,04 (m^2 K)/W;

$$R_{se} = {}^{1}/_{h_{se}} \qquad (16)$$

- h_{se} : external liminal coefficient (convection + radiation) = 25 W/(m^2 K);
- R_{cavity} : thermal resistance for coupled and double vertical windows [(m^2 K)/W].

Thanks to this last thermal balance, it was possible to write another equation in two variables, the internal and external glass surface temperature.

Once all the aspects of the detailed energy balance of a room have been analysed, it is now possible to write 9 equations in 9 variables, represented by:

- the six internal surface temperatures ($t_{s,i}$) ;
- the internal and external glass surface temperature ($t_{sG,i}$ and $t_{sG,e}$);
- the indoor air temperature (t_{air}) ;

The system resolution is represented in *Appendix C*, implemented and resolved using an Excel spreadsheet.

3.3. Description and assumption of the model parameters

In this section, we give a detailed description of the parameters used in our simulation model, explaining values and assumptions made in order to solve the energy balance.

3.3.1. Active surfaces areas

Thanks to the continuous monitoring of works and the information provided by the companies, it was possible to determine the exact dimensions of the surfaces of the radiant systems installed in the room (active surface) and the exact position in which they were placed. Furthermore, thanks to the measurements taken personally, it was also possible to determine the effective glazed surface.

In the following table (Tab. 14) are listed values of the active surfaces areas assumed in the model.

Tab. 14. *Active surfaces areas;*

Active surfaces		
S floor	17,65	[m^2]
S ceiling	12,96	[m^2]
S north	7,2	[m^2]
S east	6	[m^2]
S south	7,5	[m^2]
S west	5	[m^2]
S glass*	3,4	[m^2]

** active surface area of windows (sum of the two effective glazed surfaces)*

3.3.2. Heat exchange coefficients

Values of the heat exchange coefficients vary according to the surface and the season considered. Several expressions for calculating these coefficients

for heating and cooling conditions are available, but in our model they have been assumed constant and obtained from the standard 11855-2: 2015 [87].

In Tab. 15 are listed the heat exchange coefficients obtained from the standard.

Tab. 15. *Heat exchange coefficients (α) obtained from the standard 11855-2: 2015*

Case of application	α W/(m²·K)	ΔRα = 1/α - 1/10,8 m²·K/W
Floor heating	10,8	0,000 0
Floor cooling	6,5	0,061 3
Wall heating	8	0,032 4
Wall cooling	8	0,032 4
Ceiling heating	6,5	0,061 3
Ceiling cooling	10,8	0,000 0

It is necessary to point out that the above values represent the total heat exchange coefficient (convection + radiation) between surface and space ($h_{t,i}$). Therefore, knowing that the radiant heat exchange coefficient is constant and equal to 5,5 W/(m^2 K), it is possible to determine the convective heat exchange coefficients that enter the balance *(5)*.

In Tab. 16 are listed the convective heat exchange coefficients.

Tab. 16. *Convective heat exchange coefficients*

Case of application	$h_{c,i}$	
Floor heating	5,3	[W/(m^2 K)]
Floor cooling	1	[W/(m^2 K)]
Wall heating	2,5	[W/(m^2 K)]
Wall cooling	2,5	[W/(m^2 K)]
Ceiling heating	1	[W/(m^2 K)]
Ceiling cooling	5,3	[W/(m^2 K)]

3.3.3. View factors between surfaces

The heat transmission by radiation between two surfaces depends, in addition to the radiative properties and temperatures, on the relative orientation of the surfaces. To take into account the effect of orientation on

the heat transmission by radiation between two surfaces, a parameter called view factor is defined.

The view factor between an i-th surface and a j-th surface, F_{i-j}, is the fraction of radiation emitted by the i-th surface that directly affects the j-th surface. This quantity depends purely on the geometric properties of the two surfaces and depends neither on the radiative properties nor on the temperature of the two surfaces.

In Fig. 69 is represented an example of determination of the view factor between a k-th surface and a j-th surface, with the relative analytical formula for calculating it.

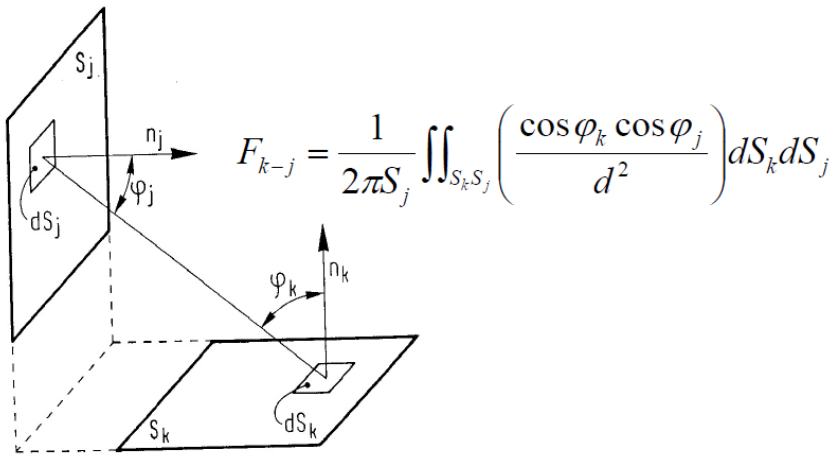

Fig. 69. *Example of determination of the view factor between a k-th surface and a j-th surface*

As we can see from the formula presented in Fig. 69, the analytical calculation of the view factors would be particularly elaborate. For this reason, the factors of sight, for particular geometries, are tabulated or represented in graphic form.

In our simulation, in order to obtain accurate values of the view factors between active surfaces, a specific program called *Trisfe* was used. This program allows you to determine the view factors by inserting a .DAT file containing the following parameters in series:

- Coordinates (x, y, z) of the point P from which we want to determine the view factors (the centre of the active surface considered);

- Characteristic dimensions of the room (Length x Width x Height);
- Base surface temperatures *(not relevant for the purpose of calculating the view factors)*;
- Subsurface temperatures entered *(not relevant for the purpose of calculating the view factors)*;
- The m and n coordinates (m_1,n_1,m_2,n_2), respectively of the nearest edge and the farthest edge from the origin of the room axes (predefined by the system), for the six surfaces of the room (north-west-south-east-ceiling-floor). The m and n coordinates can represent the respective coordinates x, y or z, depending on which axis the active surface is parallel to (exclude that coordinate).

Following is represented an example of a .DAT file to be included in the program to obtain the view factors. The surface analysed is the north wall.

- 0.001,1.9,1.1
- 4.54,3.89,2.79
- 293.15,293.15,293.15,285.15,304.01,293.15 *(random values)*
- 300,300,300,286.08,304.01,300 *(random values)*
- 1,1,1,1 (*values to be inserted by default for the view factor of the analysed surface with itself*)
- 0.14,0.1,2.64,2.1
- 0.05,0.3,3.8,2.3
- 0.1425,0.015,4.4625,1.18
- 0.325,0.2,4.225,3.8
- 0.001,0.001,4.45,3.89

In the following table (Tab. 17) are listed all the coordinates of the respective surfaces considered.

Tab. 17. *Coordinates of the respective surfaces considered*

Coord.	North	West	South	East	Glass	Ceiling	Floor
x	0	1,39	4,54	2,3025	2,3025	2,275	2,222
y	1,9	0	1,925	3,89	3,89	2	1,942
z	1,1	1,1	1,3	0,5975	1,9125	2,79	0
m_1	0,1	0,14	0,05	0,1425	1,1425	0,325	0
n_1	0,1	0,1	0,3	0,015	1,18	0,2	0
m_2	3,7	2,64	3,8	4,4625	3,4625	4,225	4,45
n_2	2,1	2,1	2,3	1,18	2,645	3,8	3,89

As we can see in Fig. 17, the glazed surface was also considered. For this reason, calculations for the east wall (eighth line of the .DAT file) have been duplicated, considering in one case the active surface of the installed radiant panels (East) and in the other the glazed surface (Glass).

Moreover, it is important to specify that simplifications were made in the geometry of some active surfaces:

- East : it was considered a single overall panel below the windows (neglected part of the central portion, Fig. 17);
- Glass : it was considered a single central window of size equal to the sum of the two separate windows;
- Ceiling : it was considered a single panel (not two detached as in Fig. 15).

A total of 14 .DAT file were made. Following (Tab. 18) are listed the view factors obtained with *Trisfe.*

Tab. 18. *View factors obtained with Trisfe*

Floor	F f-c	0,0992
	F f-n	0,0667
	F f-e	0,0619
	F f-s	0,0602
	F f-w	0,0536
	F f-g	0,0323

East	F e-f	0,3084
	F e-c	0,1052
	F e-n	0,0482
	F e-s	0,0506
	F e-w	0,0223
	F e-g	0

Glass	F g-f	0,1409
	F g-c	0,2192
	F g-n	0,0453
	F g-e	0
	F g-s	0,0515
	F g-w	0,0216

Ceiling	F c-f	0,1146
	F c-n	0,0497
	F c-e	0,0257
	F c-s	0,0567
	F c-w	0,0375
	F c-g	0,0606

South	F s-f	0,0922
	F s-c	0,077
	F s-n	0,0252
	F s-e	0,0357
	F s-w	0,0168
	F s-g	0,0233

North	F n-f	0,1645
	F n-c	0,1058
	F n-e	0,036
	F n-s	0,0261
	F n-w	0,0563
	F n-g	0,0386

West	F w-f	0,1558
	F w-c	0,0926
	F w-n	0,0854
	F w-e	0,0214
	F w-s	0,0365
	F w-g	0,0216

3.3.4. Ventilation

As stated previously in *section 2.3.3,* in the technical room was installed a machine for air ventilation, able to heat or cool and dehumidify the test room, in order to control humidity and ventilation flow rate. In our model, a constant volumetric flow rate has been assumed, both in heating and cooling conditions, equal to:

$$G_{vol} = 40 \quad {}^{l}/_{s}$$

To insert this parameter in the air balance equation, described in *section 3.2.2*, it is necessary to obtain the corresponding mass flow rate. To do this, it is necessary to determine the specific weight of the air, which however depends on the temperature.

Supply temperatures in heating and cooling conditions are assumed respectively:

- Heating : $T_{imm,air} = 9{,}7\ °C$ (this value derives from a preliminary balance of the cross-flow heat recovery, considering an efficiency of 80%);
- Cooling : $T_{imm,air} = 19\ °C$.

Therefore, the specific weight of the air is calculated with the following formula:

$$\gamma = \frac{p*MM}{R*T} \quad [{}^{g}/_{l}] \qquad (17)$$

- p : pressure = 1 [atm];
- MM : molecular mass = 28,96 g/mol;
- R : constant gas = 0,0821 (l*atm)/(mol*K);
- T : temperature [K].

Considering the supply air temperatures assumed previously and transforming the specific weight obtained from grams to kilograms, we can determine the mass flow rate with the following expression:

$$G_a = \gamma * G_{vol} \qquad (18)$$

The air mass flow rate corresponding to the assumed volumetric flow rate is almost identical in both heating and cooling seasons, equal to:

$$G_a = 0{,}05 \quad {}^{kg}/_{s}$$

3.3.5. Internal gains

In future, the laboratory will be used to test the comfort and the indoor environmental quality perceived by occupants. In fact, most likely, the test room will be used as a 4-person office.

For this reason, the following internal loads have been considered (Tab. 19):

Tab. 19. *Internal loads*

Occupants		
Number	4	
Human metabolism	70	[W/px]
Q int px	280	[W]

Computers		
Number	4	
Computer	55	[W/comp]
Q int comp	220	[W]

Therefore, the overall gains due to internal loads are:

$$\sum_{g=1}^{m} (q_{l,g}) = 500 \quad W$$

As we can see in *section 3.2.1* and *section 3.2.2*, thermal gains due to internal loads influence both the surfaces heat balance (radiant fraction $f_{r,RAD} = 0{,}3$) and the air balance (convective fraction $f_{r,CONV} = 0{,}7$). In particular, the radiation component is spread on the active surfaces of the room (except for the glazed surfaces) according to the surface fraction $f_{r,i}$, parameter previously defined as the ratio between the active surface area considered and the total active surfaces area minus the glazed surfaces *(9)*.

Values of this parameter are listed in the following Tab. 20.

Tab. 20. *Surface fractions*

$f_{r,i}$	
Floor	0,313
Ceiling	0,230
North	0,129
East	0,106
South	0,133
West	0,089

3.3.6. Conduction

Conductive heat exchange plays a fundamental role in our model. In fact, it appears in the thermal balance of opaque surfaces, linking the surface temperatures with the respective water temperatures inside the installed radiant systems, and in the thermal balance of windows, linking the surface temperature of the internal glass with that of the external glass.

When we talk about conduction, the characteristic parameters that describe the phenomenon are the conductive thermal resistances, defined respectively in equations *(4)* and *(13)*.

Conduction through the opaque surfaces

As we can see in expression *(4)*, the conductive thermal resistance for the case of opaque surfaces is defined by the difference of the inverse of two parameters:

- equivalent heat transmission coefficient for heating (h) or cooling (c) [W/(m^2 K)] *(1),* determined, for each radiant system installed in the room *section 2.3.2*, thanks to diagrams of thermal yield in heating and cooling conditions provided in the technical data sheets.
- total heat exchange coefficient (convection + radiation) between surface and space [W/(m^2 K)] *(5)*, whose values are shown in Tab.15.

In Tab. 21, values of equivalent heat transmission coefficients are summarized.

Tab. 21. *Equivalent heat transmission coefficient for heating or cooling*

Heating	K_h	
Floor	9,8	[W/(m^2 K)]
Ceiling	4,1	[W/(m^2 K)]
North	5,3	[W/(m^2 K)]
East	4,6	[W/(m^2 K)]
South	6,5	[W/(m^2 K)]
West	4,8	[W/(m^2 K)]

Cooling	K_c	
Floor	2,7	[W/(m^2 K)]
Ceiling	5,7	[W/(m^2 K)]
North	6,6	[W/(m^2 K)]
East	4,6	[W/(m^2 K)]
South	6,5	[W/(m^2 K)]
West	4,2	[W/(m^2 K)]

By replacing the above values in equation (4), we obtain the following conductive thermal resistances (Tab. 22):

Tab. 22. *Conductive thermal resistances for heating or cooling*

Heating	R_i	
Floor	0,0097	[(m^2 K)/W]
Ceiling	0,0890	[(m^2 K)/W]
North	0,0634	[(m^2 K)/W]
East	0,0938	[(m^2 K)/W]
South	0,0288	[(m^2 K)/W]
West	0,0833	[(m^2 K)/W]

Cooling	R_i	
Floor	0,2164	[(m^2 K)/W]
Ceiling	0,0824	[(m^2 K)/W]
North	0,0272	[(m^2 K)/W]
East	0,0924	[(m^2 K)/W]
South	0,0288	[(m^2 K)/W]
West	0,1150	[(m^2 K)/W]

Conduction through the glass layers

As we can see in expression *(13)*, the conductive thermal resistance of our windows is defined by the sum/difference of five parameters:

- internal *(15)* and external *(16)* surface thermal resistance [(m^2 K)/W];
- thermal resistance for coupled and double vertical windows:

$$R_{cavity} = 0{,}179 \text{ (m}^2\text{ K)/W}$$

This value was extracted from the BS EN ISO 10077-1: 2006 [86] standard, for unventilated air spaces (worst condition).

- inverse of thermal transmittance of the external and internal window [W/(m^2 K)];

As described previously in *chapter 2.3*, the test room is equipped with a double window configuration with an internal air space for high thermal and acoustic insulation (45 cm). Regarding the external windows, they are equipped with double-glazing (4-8-4 mm) and a metal frame. Values of the thermal transmittance for glass and frame were assumed by BS EN ISO 10077-1:2006 [86], considering an uncoated glass (normal glass) with normal emissivity of 0.89 and filled with air, and a metal frame without thermal break (Tab. 4, *chapter 2.2*). Through the application of equation (14), we obtain:

$$U_{w1} = 3{,}968 \ \mathrm{W/(m^2\ K)}$$

On the other hand, as described previously in *section 2.3.4*, the new windows are equipped with double-glazing (6-16-6 mm, with low emissive internal glass), filled with Argon, and a PVC frame. The value of the thermal transmittance of the internal window was extracted from the technical data sheet, equal to:

$$U_{w2} = 1{,}170 \ \mathrm{W/(m^2\ K)}$$

By replacing the above values in equation (13), we obtain the following thermal resistance of our windows:

$$R_{glass} = 0{,}179 \ \mathrm{(m^2\ K)/W}$$

3.3.7. Solar radiation

Last but not least is the analysis of thermal loads due to solar radiation. Indeed, this aspect has been the most thoroughly considered, due to its double effect:

- saving energy in heating season;
- heat loads in cooling season.

First, let's consider the properties of glazed element. Three characteristic coefficients are associated with each glazed surface:

- τ : transmission coefficient;
- α : absorption coefficient;
- ρ : reflection coefficient.

For glazed elements, these coefficients vary significantly according to the spectrum and the angle θ of the incident radiation. These parameters are fundamental, since they determine the amount of solar radiation that is respectively transmitted inside the room, absorbed by the glass surface and reflected outwards. Consequently, they influence the value of thermal loads.

In order to analyse and determine in detail the amount of thermal loads due to solar radiation, an Excel model was created that allowed us to evaluate the percentages of radiation transmitted, absorbed and reflected by the double window configuration installed in our test room. In particular, the focus was on determining the fraction of radiation transmitted and absorbed as a function of the angle of incidence of the sun. It’s important to underline that no radiation shielding elements (blinds, shutters, etc.) was considered in the simulation model.

Based on the type of glass of the external and internal windows, the following characteristic coefficient values were assumed as a function of the angle of incidence θ of the sun (Tab. 23). Values were extracted from the TRNSYS (dynamic simulation software) library.

Tab. 23. *Transmission, absorption and reflection coefficients as a function of the angle of incidence*

External window (4-8-4)			
Incidence Angle [deg]	**τ**	**α**	**ρ**
0	0,771	0,159	0,07
10	0,771	0,159	0,07
20	0,771	0,159	0,07
30	0,771	0,158	0,071
40	0,765	0,159	0,076
50	0,75	0,16	0,09
60	0,7	0,16	0,14
70	0,6	0,15	0,25
80	0,4	0,1	0,5
90	0	0	1

Internal window (6-16-6)			
Incidence Angle [deg]	**τ**	**α**	**ρ**
0	0,504	0,265	0,231
10	0,507	0,267	0,226
20	0,499	0,277	0,224
30	0,489	0,286	0,225
40	0,475	0,293	0,232
50	0,449	0,303	0,248
60	0,392	0,318	0,29
70	0,284	0,324	0,392
80	0,13	0,27	0,6
90	0	0	1

Thanks to these coefficients, it was possible to elaborate a simulation model of the solar radiation behaviour (characterized by a predefined angle of incidence) on the four glass that form the windows of our climate chamber. In particular, the portions of radiation transmitted inside the room and absorbed by the glass surface as a function of the angle of incidence were determined. In Fig. 70 is represented an example of this model, with an angle of incidence of 60 degrees (diffuse radiation).

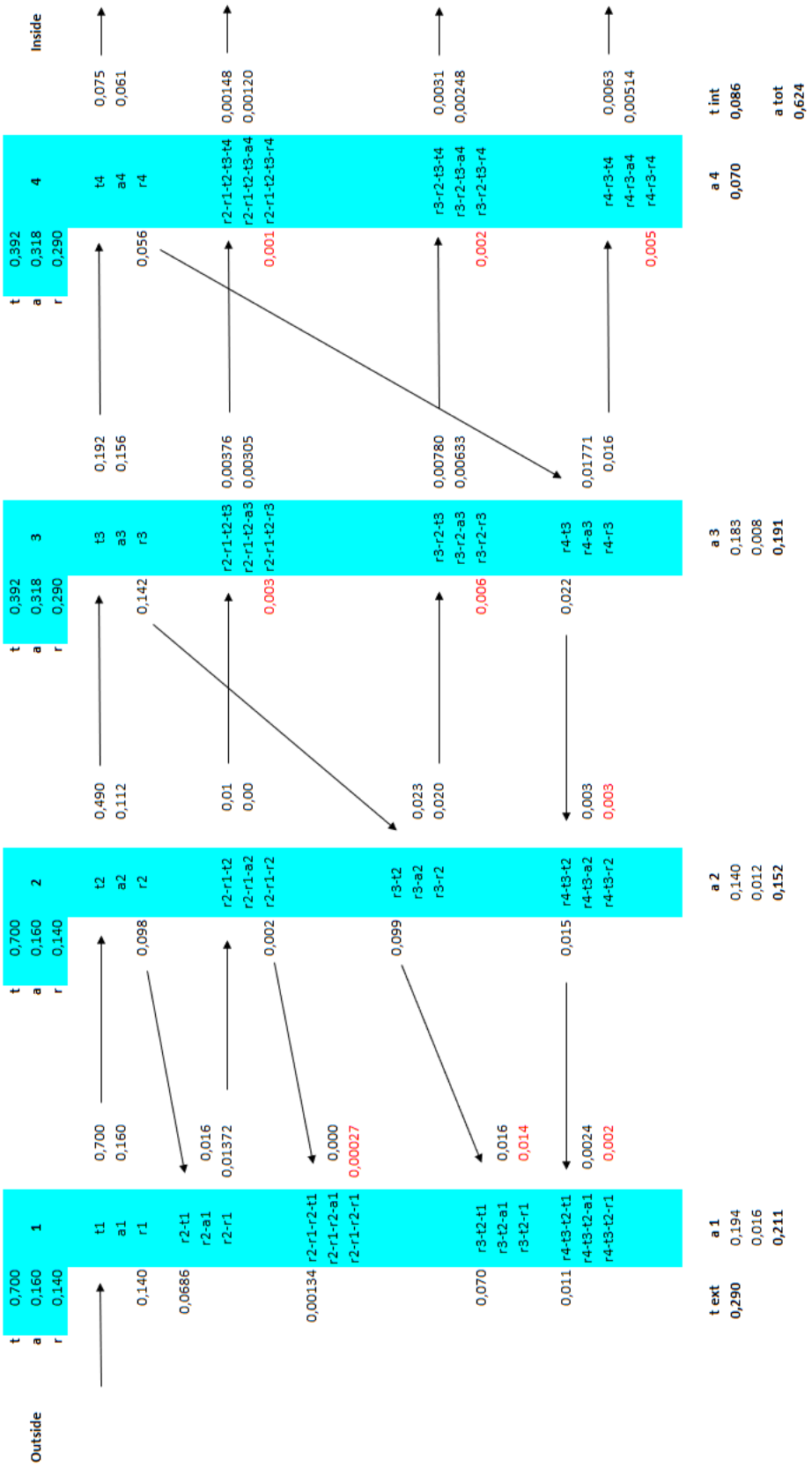

Fig. 70. *Example of the simulation model of the solar radiation behaviour on the four glass that form the windows of our climate chamber (θ=60°)*

As we can see in the previous figure, the black lines represent the behaviour of the solar radiation in contact with the glass surfaces: a portion is transmitted, one is absorbed and another is reflected. Moreover, some values are written in red. Being close to zero, and therefore having no sense to continue with the iteration, they were considered absorbed by the first three glass. Finally, we can observe in the lower part of the picture the fractions of solar radiation which are respectively reflected (t_{ext}), absorbed (a_1, a_2, a_3, a_4, a_{tot}) and transmitted (t_{int}).

By performing this simulation for each angle of incidence θ, it was possible to determine the trend of the transmission and absorption coefficients of the test room windows (Fig. 71 and Fig. 72).

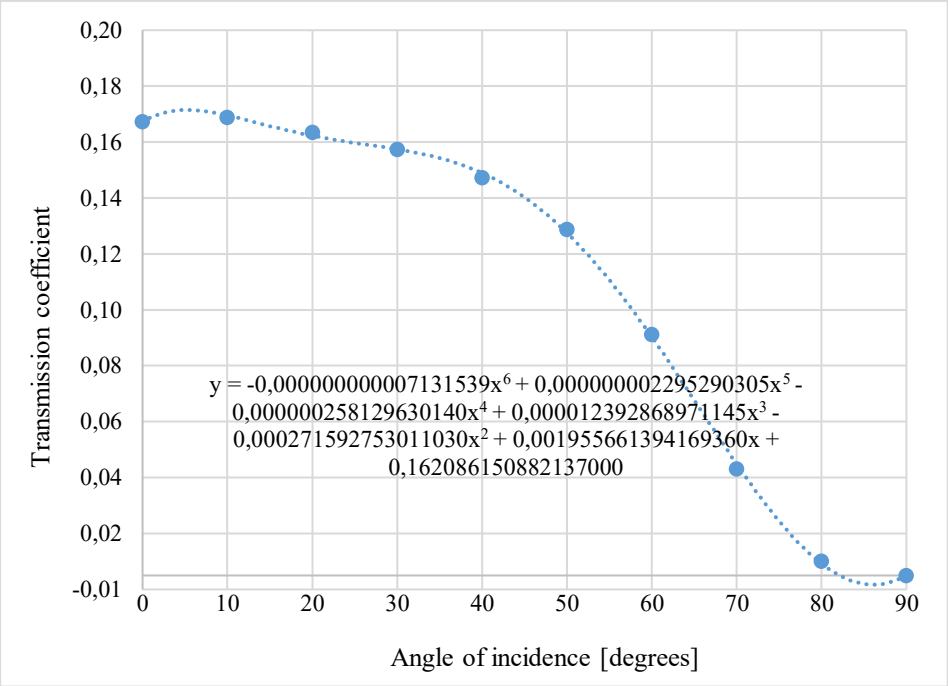

Fig. 71. *Trend of the transmission coefficient*

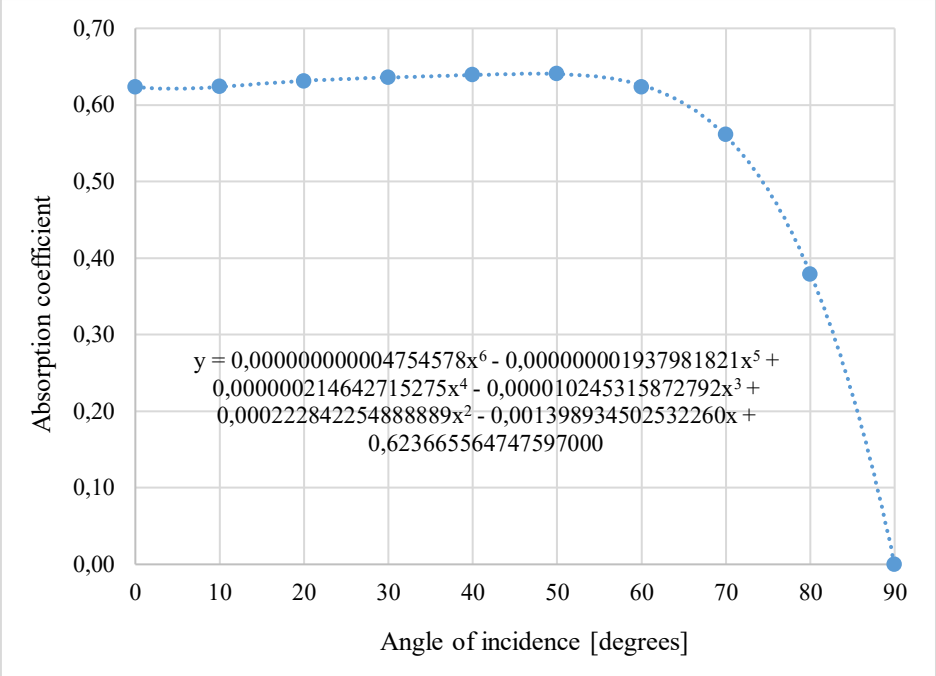

Fig. 72. *Trend of the absorption coefficient*

Moreover, as we can see in Fig. 71 and Fig. 72, thanks to the Excel trend line function, it was possible to determine the sixth-degree polynomial that interpolates the points obtained and analytically describes the variation of the two coefficients according to the angle of incidence. The expressions of these functions are showed on the previous diagrams. In the following table (Tab. 23), was made a comparison between the values of the transmission and absorption coefficients obtained from the previous simulation and the values determined by the sixth-degree polynomial that describes the trend. As we can see from the last column, the percentage error is almost zero for most of the considered incidence angles. The only conflicting data are found at high θ in the transmission coefficient, which however assumes very low values and therefore the error can be considered not particularly influential.

Tab. 23. *Comparison between the values of the transmission and absorption coefficients obtained from the previous simulation and the values determined by the sixth-degree polynomial that describes the trend.*

Transmission coefficient			
Angle	**t int**	**t int function**	**Error [%]**
0	0,1622	0,1621	0,092625
10	0,1638	0,1645	-0,45584
20	0,1585	0,1573	0,75491
30	0,1523	0,1524	-0,06238
40	0,1422	0,1439	-1,18371
50	0,1238	0,1225	1,042684
60	0,0862	0,0853	1,021591
70	0,0382	0,0399	-4,6053
80	0,0052	0,0042	18,25534
90	0,0000	0,0002	0

Absorption coefficient			
Angle	**a tot**	**a tot function**	**Error [%]**
0	0,6236	0,6237	-0,01239
10	0,6240	0,6237	0,056831
20	0,6308	0,6313	-0,07495
30	0,6357	0,6359	-0,02014
40	0,6396	0,6391	0,08999
50	0,6409	0,6403	0,078659
60	0,6236	0,6256	-0,32577
70	0,5613	0,5593	0,359012
80	0,3792	0,3801	-0,23591
90	0,0000	-0,0002	0

Once obtained functions describing the trend of the transmission and absorption coefficients, it is necessary to determine the effective solar radiation that affects our glazed surface. The solar radiation that reaches the earth surface is distinguished in:

- direct radiation, also called “beam radiation". It is used to describe solar radiation traveling on a straight line from the sun down to the surface of the earth, striking any surface with a single and well-defined angle of incidence.
- diffuse radiation. Describes the sunlight that has been scattered by molecules and particles in the atmosphere but that has still made it down to the surface of the earth. This radiation affects a surface with various angles of incidence. Despite this feature, for the calculation a constant angle of 60 degrees is assumed;
- reflected radiation. Given by the ground, by bodies of water or by other surfaces (e.g. walls of adjacent buildings), this contribution is called *albedo* and must be carefully evaluated. In our model it was neglected due to its evaluation complexity.

The proportions of direct, diffuse and reflected radiation received from a surface depend on:

- weather conditions. On a cloudy day the radiation is almost completely diffuse. On the other hand, on a clear day with a dry climate, the direct component predominates, which can reach up to 90% of the total radiation;
- inclination and orientation of the surface. A horizontal surface receives the maximum diffuse radiation and the minimum reflected. The reflected component increases as the inclination increases;
- presence of reflective elements. The greatest contribution to reflection is given by the light surfaces (e.g. presence of snow).

Neglecting the radiation reflected, the dynamic simulation software TRNSYS was used to determine the beam and diffuse radiation values for our model. The following input parameters were loaded:

- weather data of the Venezia-Tessera area [97], downloaded from EnergyPlus website;
- slope of surface: 90 degrees;
- azimuth of surface: -81 degrees (slight inclination angle towards the east of 9 degrees - *chapter 2.2*).

Considering an annual simulation duration, with a sampling interval of one hour, the following output parameters were determined (8760 values):

- Temperature [°C];
- Total radiation [kJ/(h m^2)];
- Beam radiation [kJ/(h m^2)];
- Diffuse radiation [kJ/(h m^2)];
- Incidence Angle [degrees];
- Day, month and hour of values.

Dividing by a constant of 3,6 we obtain the specific radiation in [W/m^2].

Obtained the beam and diffuse solar radiation values that affect our glass surface during the year, it was decided to select three days characterized by the following conditions in order to simulate the model:

- Summer day: 18th July (5.00-20.00). High temperatures and high solar radiation (Tab.24);
- Winter day: 15th February (7.00-19.00). Low temperatures and high solar radiation (Tab. 25);
- Winter day: 28th December (7.00-19.00). Low temperatures and low solar radiation (Tab. 26).

In the following tables are listed the values of the output parameters from the TRNSYS software for the three days selected.

Tab. 24. *Summer day: 18th July (5.00-20.00). High temperatures and high solar radiation*

Temper.	**Total radiation**	**Beam radiation**	**Diffuse radiation**	**Incidence Angle**	M	D	H
[°C]	[W/m^2]	[W/m^2]	[W/m^2]	[degrees]			
23,95	2,1808	1,5627	0,6181	38,6142	7	18	5
23,8	84,9127	37,8529	47,0598	32,7354	7	18	6
23,55	197,7220	110,7272	86,9948	27,6476	7	18	7
24	344,8403	194,1092	150,7310	29,9387	7	18	8
25,5	473,9167	261,6551	212,2615	37,9900	7	18	9
27,65	514,3542	284,6486	229,7056	49,3550	7	18	10
29,35	474,9176	244,1679	230,7496	62,1113	7	18	11
30	345,7858	143,5376	202,248	75,5443	7	18	12
30,2	164,3962	6,9611	157,4351	89,3216	7	18	13
30,4	151,6760	0	151,6760		7	18	14
30,75	142,4452	0	142,4452		7	18	15
31,05	122,1708	0	122,1708		7	18	16
31,1	95,12268	0	95,1226		7	18	17
30,75	66,02770	0	66,0277		7	18	18
30,1	35,85372	0	35,8537		7	18	19
29,45	8,721463	0	8,7214		7	18	20

Tab. 25. *Winter day: 15th February (7.00-19.00). Low temperatures and high solar radiation*

Temper.	**Total radiation**	**Beam radiation**	**Diffuse radiation**	**Incidence Angle**	M	D	H
[°C]	[W/m^2]	[W/m^2]	[W/m^2]	Degrees			
-4,85	0	0	0		2	15	7
-4,75	35,0560	22,3415	12,7145	13,7431	2	15	8
-3,45	187,4854	123,8266	63,6588	25,3319	2	15	9
-1,4	305,4899	209,8546	95,6352	39,7628	2	15	10
0,6	333,4025	230,8042	102,5982	54,3495	2	15	11
2,2	269,4326	172,6453	96,7873	68,9655	2	15	12
3,8	136,6294	56,9002	79,7292	83,5561	2	15	13
4,95	65,2423	0	65,2423		2	15	14
5,45	52,9341	0	52,9341		2	15	15
5,5	34,8833	0	34,8833		2	15	16
5,05	16,7535	0	16,7535		2	15	17
4,1	1,9119	0	1,9119		2	15	18
2,65	0	0	0		2	15	19

Tab. 26. *Winter day: 28th December (7.00-19.00). Low temperatures and low solar radiation*

Temper.	**Total radiation**	**Beam radiation**	**Diffuse radiation**	**Incidence Angle**	M	D	H
[°C]	[W/m^2]	[W/m^2]	[W/m^2]	Degrees			
0,3	0	0	0		12	28	7
0,2	0	0	0	25,7384	12	28	8
0,25	5,1319	0	5,1319	31,9414	12	28	9
0,35	14,4824	0	14,4824	44,7775	12	28	10
0,5	22,9084	0,5256	22,3827	58,2858	12	28	11
0,75	27,4239	1,2345	26,1893	72,0225	12	28	12
1,05	27,0166	0,2940	26,7225	85,7839	12	28	13
1,35	23,9997	0	23,9997		12	28	14
1,65	18,1476	0	18,1476		12	28	15
2	8,75466	0	8,7546		12	28	16
2,3	1,01716	0	1,0171		12	28	17
2,5	0	0	0		12	28	18
2,7	0	0	0		12	28	19

As we can see in the previous tables, when the angle of incidence exceeds 90 degrees, the value is not reported because the sun is beyond the glass surface (above the building) and therefore does not affect any direct

radiation. Multiplying by the active surface area of windows (Tab. 14), we obtain the radiation power [W]. At this point we are able to calculate the thermal loads transmitted into the environment ($q_{s,k}$) and absorbed by glazed surfaces (I_a). As stated previously, the beam radiation is characterized by a single and well-defined angle of incidence. On the other hand, the diffuse radiation affects a surface with various angles of incidence. Despite this feature, for the calculation a constant angle of 60 degrees is assumed.Therefore, thanks to the sixth-degree polynomials obtained from the previous graphs (Fig. 71 and Fig. 72), it is possible to calculate the transmission and absorption coefficients associated with the incidence angles of the three days selected for direct radiation, and the transmission and absorption coefficients for diffuse radiation associated with an incidence angle of 60 degrees.

In the following tables are listed the values of the beam and diffuse power radiation and the related transmission and absorption coefficients.

Tab. 27. *Beam and diffuse power radiation and the related transmission and absorption coefficients. Summer day: 18th July*

Hour	**Beam radiation**	**Incidence Angle**	**Diffuse radiation**	**τ**	**α**	**τ**	**α**
	[W]	[Degrees]	[W]	(Beam radiation)		(Diffuse radiation)	
5	5,3132	38,6142	2,1015	0,1457	0,6386	0,0862	0,6236
6	128,6999	32,7354	160,0033	0,1509	0,6368	0,0862	0,6236
7	376,4726	27,6476	295,7823	0,1535	0,6350	0,0862	0,6236
8	659,9715	29,9387	512,4856	0,1525	0,6358	0,0862	0,6236
9	889,6275	37,9900	721,6893	0,1464	0,6384	0,0862	0,6236
10	967,8054	49,3550	780,9990	0,1244	0,6405	0,0862	0,6236
11	830,1711	62,1113	784,5488	0,0759	0,6175	0,0862	0,6236
12	488,0280	75,5443	687,6438	0,0175	0,4789	0,0862	0,6236
13	23,6679	89,3216	535,2793	0,0009	0,0342	0,0862	0,6236
14			515,6985			0,0862	0,6236
15			484,3136			0,0862	0,6236
16			415,3808			0,0862	0,6236
17			323,4171			0,0862	0,6236
18			224,4941			0,0862	0,6236
19			121,9026			0,0862	0,6236
20			29,6529			0,0862	0,6236

Tab. 28. *Beam and diffuse power radiation and the related transmission and absorption coefficients. Winter day: 15th February*

Hour	Beam radiation	Incidence Angle	Diffuse radiation	τ	α	τ	α
	[W]	[Degrees]	[W]	(Beam radiation)		(Diffuse radiation)	
7			0				
8	0	13,7431	43,2295	0,1617	0,6267	0,0862	0,6236
9	75,9611	25,3319	216,4399	0,1546	0,6341	0,0862	0,6236
10	421,0106	39,7628	325,1598	0,1442	0,6390	0,0862	0,6236
11	713,5058	54,3495	348,8340	0,1081	0,6374	0,0862	0,6236
12	784,7345	68,9655	329,0770	0,0445	0,5701	0,0862	0,6236
13	586,9941	83,5561	271,0794	0,0019	0,2733	0,0862	0,6236
14	193,4608		221,8239			0,0862	0,6236
15			179,9761			0,0862	0,6236
16			118,6033			0,0862	0,6236
17			56,9621			0,0862	0,6236
18			6,5007			0,0862	0,6236
19			0				

Tab. 29. *Beam and diffuse power radiation and the related transmission and absorption coefficients. Winter day: 28th December*

Hour	Beam radiation	Incidence Angle	Diffuse radiation	τ	α	τ	α
	[W]	[Degrees]	[W]	(Beam radiation)		(Diffuse radiation)	
7	0		0				
8	0	25,7384	0				
9	0	31,9414	17,4487			0,0862	0,6236
10	0	44,7775	49,2402			0,0862	0,6236
11	1,7873	58,2858	76,1013	0,0926	0,6305	0,0862	0,6236
12	4,1975	72,0225	89,0434	0,0312	0,5346	0,0862	0,6236
13	0,9998	85,7839	90,8566	0,0033	0,1914	0,0862	0,6236
14			81,5993			0,0862	0,6236
15			61,7019			0,0862	0,6236
16			29,7658			0,0862	0,6236
17			3,4583			0,0862	0,6236
18			0				
19			0				

Thanks to the values listed in the previous tables, it is now possible to calculate the thermal loads transmitted into the environment ($q_{s,k}$) and absorbed by glazed surfaces (I_a), defined as follows:

$$q_{s,k} = q_{s,beam} * \tau_{beam} + q_{s,diffuse} * \tau_{diffuse} \quad [W] \qquad (19)$$

$$I_a = q_{s,beam} * \alpha_{beam} + q_{s,diffuse} * \alpha_{diffuse} \quad [W] \qquad (20)$$

Finally, it is necessary to remember that the radiation power transmitted inside the chamber has to be spread on the active surfaces of the room (except for the glazed surfaces) according to the surface fraction $f_{r,i}$, reported in Tab. 20.

3.4. Simulation results

In this section, we present a detailed analysis of the results obtained in our simulation model, describing them critically in order to provide a scientific and exhaustive explanation of the phenomena considered. We have to remember that these results obtained from the theoretical model will be verified by means of measurements as soon as the operation of the climate chamber is guaranteed. Moreover, they will be used to calibrate and set up the different radiant systems in order to perform experimental tests for evaluating the indoor environmental quality.

3.4.1. Calibration of floor and ceiling radiant systems - Water temperature profile

Once the detailed energy balance of the room was realized, the first objective we set ourselves was to determine the hourly profile of the temperature water that flows inside the floor and ceiling radiant systems, respecting the following conditions to be simulated:

- Two walls facing outwards (east and south walls);
- Two neutral walls (north and west);
- Four operating conditions depending on the season:
- Cold floor, neutral ceiling (summer season);
- Cold ceiling, neutral floor (summer season);
- Hot floor, neutral ceiling (winter season);
- Hot ceiling, neutral floor (winter season).
- Constant operative temperature inside the room.

Let's begin to describe in more detail the previous conditions to be respected in order to determine the required temperature profile. Remember that the set-point temperatures are respectively:

- 26 °C in cooling season;
- 20 °C in heating season.

Two walls facing outwards (east and south walls)

As we can see in *chapter 2.2*, the test room faces a single wall towards the outside (east wall). But, as stated previously in *chapter 2.3*, thanks to the presence of radiant systems installed it is possible to reproduce an environment with one or more dispersing walls. For this reason, it is possible to simulate a second dispersing surface towards the outside, chosen arbitrarily in the south wall.

Therefore, the purpose is to determine the water temperature inside the radiant panels of the east and south walls, taking into account that they are affected by external climatic conditions. To do this, a small balance of the walls was made, considering a thermal transmittance equal to:

$$U_{wall} = 0{,}6 \quad \mathrm{W/(m^2\,K)}$$

From this calculation we have obtained values that give us an idea of the water temperature inside the radiant panels of the east and south walls, as a function of the external temperature.

Neutral walls

When we talk about neutral walls (or floor / ceiling, depending on the operating condition), we refer to the fact that we assume the water temperature inside those walls constant and equal to the set-point temperature (heating or cooling season, values mentioned above).

Constant operative temperature inside the room

First of all, let's define the operative temperature. Mathematically operative temperature can be defined as follows [9]:

$$t_o = \frac{h_r * t_{mr} + h_c * t_{air}}{h_r + h_c} \quad [\text{K}] \qquad (21)$$

However, the operative temperature for conditions normally encountered in practice can be define as the simple arithmetic average between the mean radiant temperature and the air temperature [9]:

$$t_o = \frac{t_{mr} + t_{air}}{2} \quad [\text{K}] \qquad (22)$$

- t_{mr} : mean radiant temperature (MRT) [K];
- t_{air} : indoor air temperature [K].

For an enclosure, the calculation of the mean radiant temperature is based on the radiant heat exchange between all radiating surfaces and the point of interest (P). Thus, MRT can be defined with the following equation:

$$t_{mr}{}^4 = F_{p-1} * t_{s,1}{}^4 + F_{p-2} * t_{s,2}{}^4 + \ldots + F_{p-N} * t_{s,N}{}^4 \quad [\text{K}] \qquad (23)$$

- $t_{s,N}$: temperature of the N-th surface [K];
- F_{p-N} : view factor between the point of interest and the N-th surface.

As we can see from the above definition, to calculate the mean radiant temperature it is necessary to define the view factors between a point of interest (P) and the surfaces of the climate chamber.

The point P, in which we want to evaluate the mean radiant temperature, was considered in the centre of the room, at a height from the floor of 60 cm (height of the seat of an office worker). As previously described in *section 3.3.3*, the view factors were calculated using the specific program *Trisfe*.

In the following table (Tab. 30) are listed all the coordinates of the point of interest P and the values of the view factors obtained.

Tab. 30. *Coordinates of the point of interest P and view factors to calculate the mean radiant temperature*

Point - P	
x	2,2675
y	1,945
z	0,6

View factors							
North	West	South	East	Glass	Ceiling	Floor	Opaque
0,0771	0,0648	0,0755	0,0684	0,0371	0,1363	0,3708	0,17

As we can see, in the table above appears an eighth component (called "Opaque"). This term groups all those passive surface portions of the room where the radiant systems have not been installed. This value is fundamental for a correct calculation of the mean radiant temperature (sum of the view factors equal to 1). Furthermore, this portion of passive surface is considered neutral and therefore its temperature is equal to the seasonal set-point value.

Finally, it's important to state that the constancy of the operative temperature inside the room, equal to the seasonal set-point temperature (26 °C in cooling condition, 20 °C in heating condition), represents the "*condition to be satisfied*" in order to determine the exact water temperature that flows inside the floor and ceiling radiant systems.

Having defined the conditions which simulation have to comply, it is possible to describe the analytical procedure that led to determining the hourly profiles. The input parameters to be inserted in the Excel spreadsheet of the model are respectively:

- external temperature [K];
- water temperature of east and south walls [K];
- thermal loads transmitted into the environment [W];
- thermal loads absorbed by glazed surfaces [W].

Following are represented the input values to be inserted in the model for each hour of the three days selected for the simulation (Tab. 31, Tab. 32 and Tab. 33).

Tab. 31. *Input values. Summer day: 18th July*

Hour	T external	Tw east/south	q sol	I abs
	[°C]	[°C]	[W]	[W]
5	23,95	25,85	0,9552	4,7037
6	23,8	25,84	33,2051	181,7227
7	23,55	25,82	83,2840	423,5143
8	24	25,85	144,7702	739,2086
9	25,5	25,96	192,4348	1017,9815
10	27,65	26,12	187,6973	1106,8844
11	29,35	26,25	130,6135	1001,8905
12	30	26,30	67,7964	662,5234
13	30,2	26,32	46,1422	334,5910
14	30,4	26,33	44,4328	321,5723
15	30,75	26,36	41,7287	302,0018
16	31,05	26,38	35,7894	259,0176
17	31,1	26,38	27,8658	201,6721
18	30,75	26,36	19,3425	139,9871
19	30,1	26,31	10,5032	76,0144
20	29,45	26,26	2,5549	18,4906

Tab. 32. *Input values. Winter day: 15th February*

Hour	T external	Tw east/south	q sol	I abs
	[°C]	[°C]	[W]	[W]
7	-4,85	18,14	0	0
8	-4,75	18,14	16,0079	74,5594
9	-3,45	18,24	83,7209	401,9319
10	-1,4	18,40	130,9347	658,6830
11	0,6	18,55	114,8757	717,7359
12	2,2	18,67	54,4897	539,8637
13	3,8	18,79	23,7264	221,9039
14	4,95	18,87	19,1125	138,3220
15	5,45	18,91	15,5068	112,2271
16	5,5	18,91	10,2189	73,9570
17	5,05	18,88	4,9079	35,5197
18	4,1	18,81	0,5601	4,0537
19	2,65	18,70	0	0

Tab. 33. *Input values. Winter day: 28th December*

Hour	T external	Tw east/south	q sol	I abs
	[°C]	[°C]	[W]	[W]
7	0,3	18,52	0	0
8	0,2	18,52	0	0
9	0,25	18,52	1,5034	10,8804
10	0,35	18,53	4,2426	30,7046
11	0,5	18,54	6,7224	48,5812
12	0,75	18,56	7,8031	57,7688
13	1,05	18,58	7,8315	56,8465
14	1,35	18,60	7,0306	50,8826
15	1,65	18,62	5,3163	38,4753
16	2	18,65	2,5646	18,5610
17	2,3	18,67	0,2980	2,1565
18	2,5	18,69	0	0
19	2,7	18,70	0	0

The model simulations were carried out by systematically repeating the following operations:

- choice of one of the three days to be analysed (summer / winter) ;
- replacement of the input parameters listed in the previous tables according to the time slot considered;
- choice of one of the two floor / ceiling cases according to the season considered (cold / hot);
- variation of values of the water temperature inside the radiant system of the surface chosen in the previous point, until obtaining the operative temperature equal to the seasonal set-point value;
- repetition of the procedure described in the previous point for the second surface not considered in the third step;
- repetition of the entire process (except for the first step) in an iterative manner for all the hours of the day taken into consideration.

This process was repeated for all three days selected, obtaining the following water temperature values and the consequent hourly water temperature profiles:

Summer day: 18th July – COLD FLOOR

Tab. 34. *Water temperature values for the case of COLD FLOOR*

Hour	Tw floor	
5	24,9	[°C]
6	23	[°C]
7	20,4	[°C]
8	16,8	[°C]
9	13,4	[°C]
10	12,2	[°C]
11	13,5	[°C]
12	17,3	[°C]
13	20,6	[°C]
14	20,7	[°C]
15	20,9	[°C]
16	21,3	[°C]
17	21,9	[°C]
18	22,6	[°C]
19	23,3	[°C]
20	24	[°C]

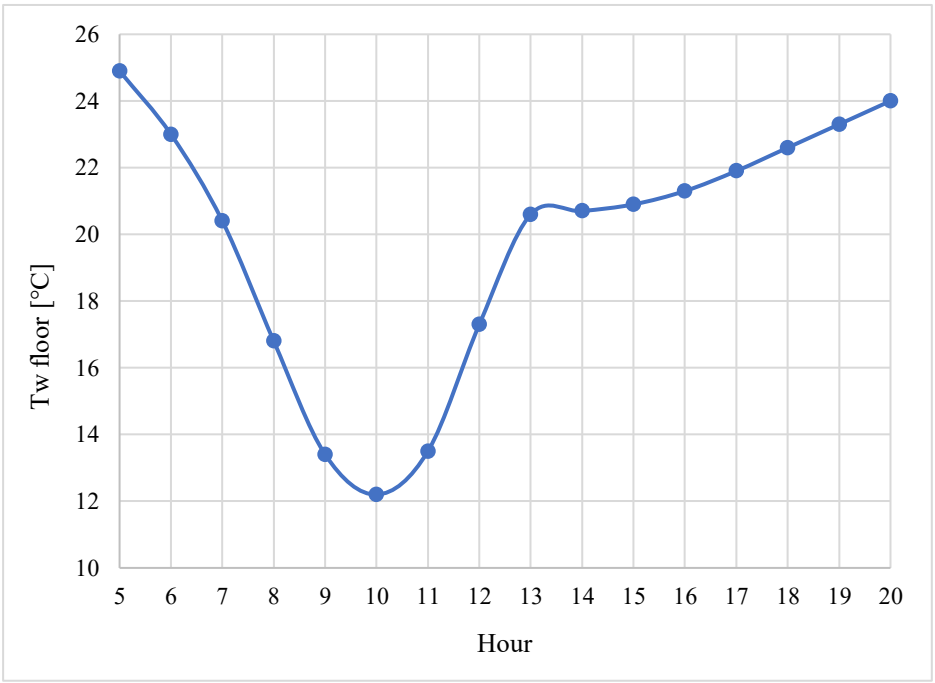

Fig. 73. *Calibration of the radiant floor system in the case of COLD FLOOR*

The minimum temperature of the water flowing inside the radiant floor system is showed in blue in Tab. 34. As we can see, the value is particularly low, but completely plausible since in the technical sheet provided by the

company (Seppelfricke, *section 2.3.2.1*) a preliminary sizing was reported in cooling conditions, with a supply water temperature of 10 °C.

Summer day: 18th July – COLD CEILING

Tab. 35. *Water temperature values for the case of COLD CEILING*

Hour	Tw ceiling	
5	25,1	[°C]
6	23,6	[°C]
7	21,5	[°C]
8	18,7	[°C]
9	16,1	[°C]
10	15,2	[°C]
11	16,2	[°C]
12	19,1	[°C]
13	21,7	[°C]
14	21,8	[°C]
15	21,9	[°C]
16	22,3	[°C]
17	22,7	[°C]
18	23,3	[°C]
19	23,9	[°C]
20	24,4	[°C]

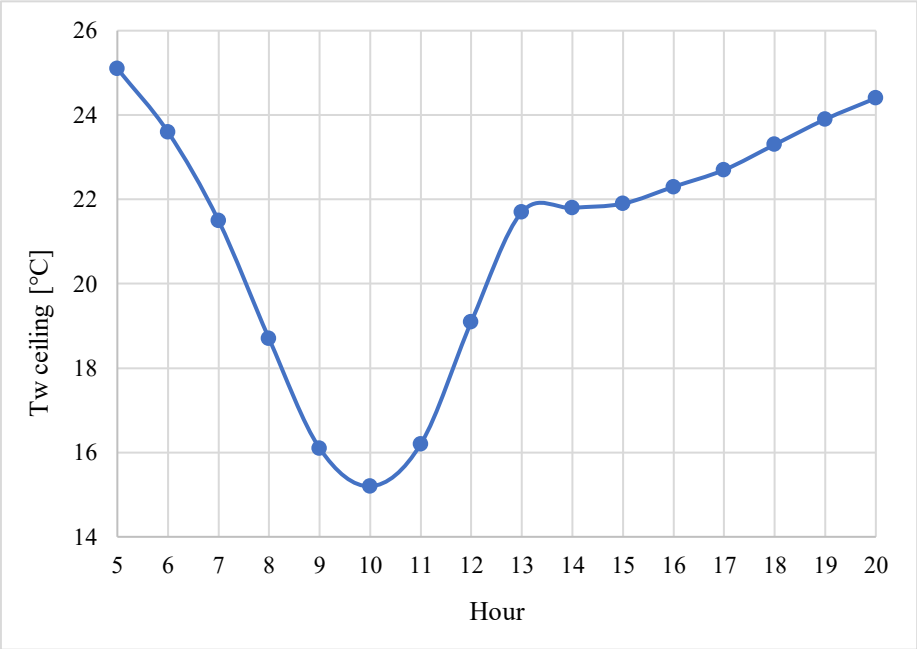

Fig. 74. *Calibration of the radiant ceiling panels in the case of COLD CEILING*

The minimum temperature of the water flowing inside radiant ceiling panels is showed in blue in Tab. 35. As we can see, the value is higher than the

previous one due to the marked difference in convective heat exchange coefficients between ceiling and floor in cooling conditions (Tab. 16). Despite this consideration that would lead to a cold ceiling solution (higher water temperature = lower energy to cool it = lower costs), it is not possible to compare the two applications in terms of the convenience of one or the other solution, since the analysis to be done is very wide and does not only involve thermal / energy issues but also constructive, applicative and sometimes normative.

Winter day: 15th February – HOT FLOOR

Tab. 36. *Water temperature values for the case of HOT FLOOR*

Hour	**Tw floor**	
7	21,7	[°C]
8	21,5	[°C]
9	20,4	[°C]
10	19,6	[°C]
11	19,3	[°C]
12	19,9	[°C]
13	20,7	[°C]
14	20,9	[°C]
15	21	[°C]
16	21,1	[°C]
17	21,2	[°C]
18	21,3	[°C]
19	21,4	[°C]

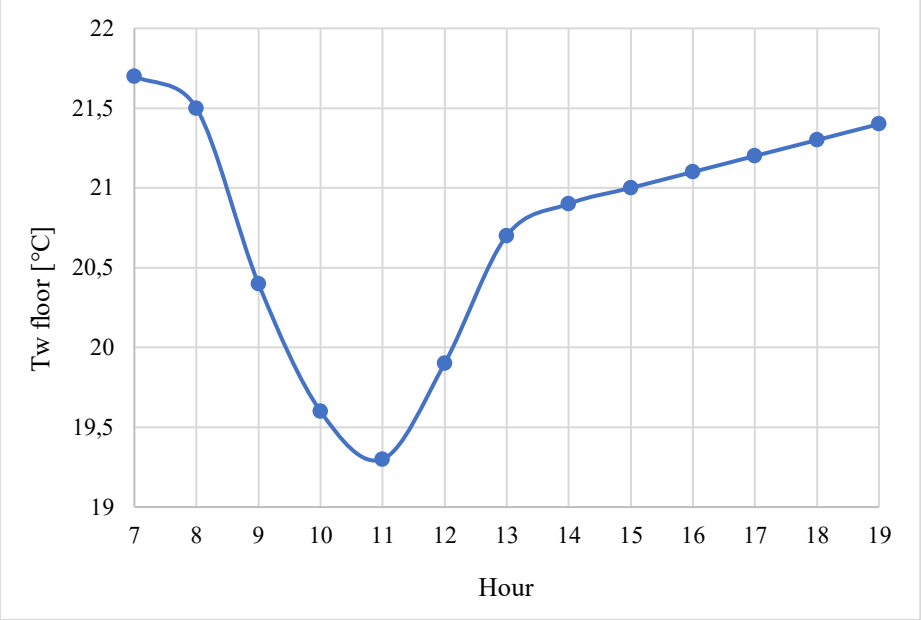

Fig. 75. *Calibration of the radiant floor system in the case of HOT FLOOR*

The maximum temperature of the water flowing inside the radiant floor system is showed in blue in Tab. 36. As we can see, there are three values highlighted in red. In the time period between 10.00 and 12.00 these temperatures fall below the neutrality condition of a surface (in heating conditions equal to 20 °C), and therefore the floor reverses its function, cooling the room instead to heat it up. This phenomenon is caused by the high thermal loads due to solar radiation on the selected day and, in particular, that no radiation shielding elements (blinds, shutters, etc.) was considered in the simulation model.

Winter day: 15th February – HOT CEILING

Tab. 37. *Water temperature values for the case of HOT CEILING*

Hour	Tw ceiling	
7	27,4	[°C]
8	26,4	[°C]
9	22	[°C]
10	18,1	[°C]
11	17,1	[°C]
12	19,4	[°C]
13	23,2	[°C]
14	24	[°C]
15	24,3	[°C]
16	24,7	[°C]
17	25,3	[°C]
18	25,9	[°C]
19	26,1	[°C]

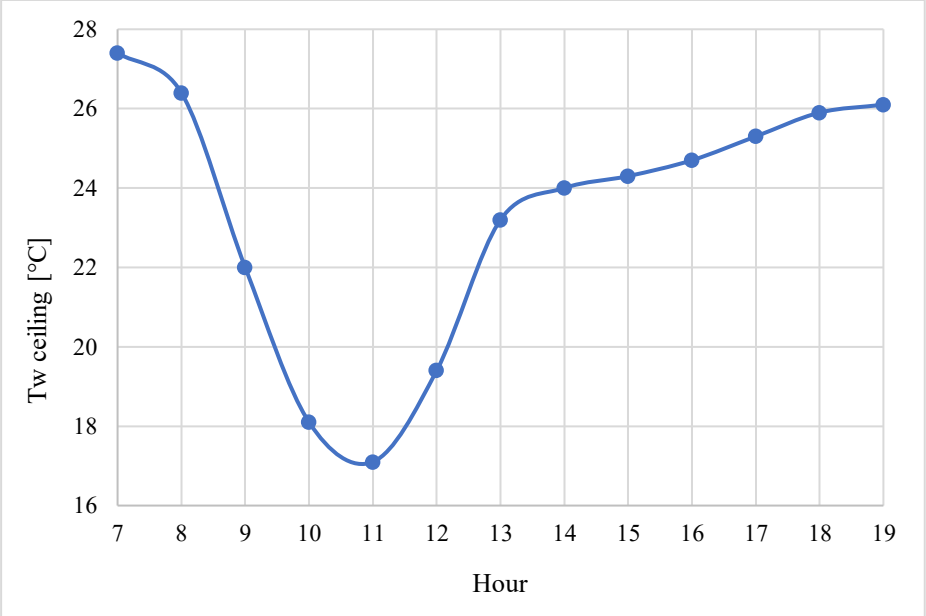

Fig. 76. *Calibration of the radiant ceiling panels in the case of HOT CEILING*

The maximum temperature of the water flowing inside radiant ceiling panels is showed in blue in Tab. 37. As in the previous case of a hot floor, the same phenomenon occurs in the time period between 10.00 and 12.00 for the hot ceiling. From a first comparison between the two applications, we can see that the phenomenon of temperature drop below the surface neutrality condition is more pronounced. Furthermore, the temperatures (in particular the maximum ones) are considerably higher. The reason for this difference

was already expressed previously for the summer simulation and is attributable to the difference in convective heat exchange coefficients between floor and ceiling in heating conditions (Tab. 16). However, it is not possible to compare the two applications in terms of the convenience of one or the other solution for the reasons previously stated.

Winter day: 28th December – HOT FLOOR

Tab. 38. *Water temperature values for the case of HOT FLOOR*

Hour	Tw floor	
7	21,5	[°C]
8	21,5	[°C]
9	21,5	[°C]
10	21,4	[°C]
11	21,4	[°C]
12	21,3	[°C]
13	21,3	[°C]
14	21,3	[°C]
15	21,3	[°C]
16	21,4	[°C]
17	21,4	[°C]
18	21,4	[°C]
19	21,4	[°C]

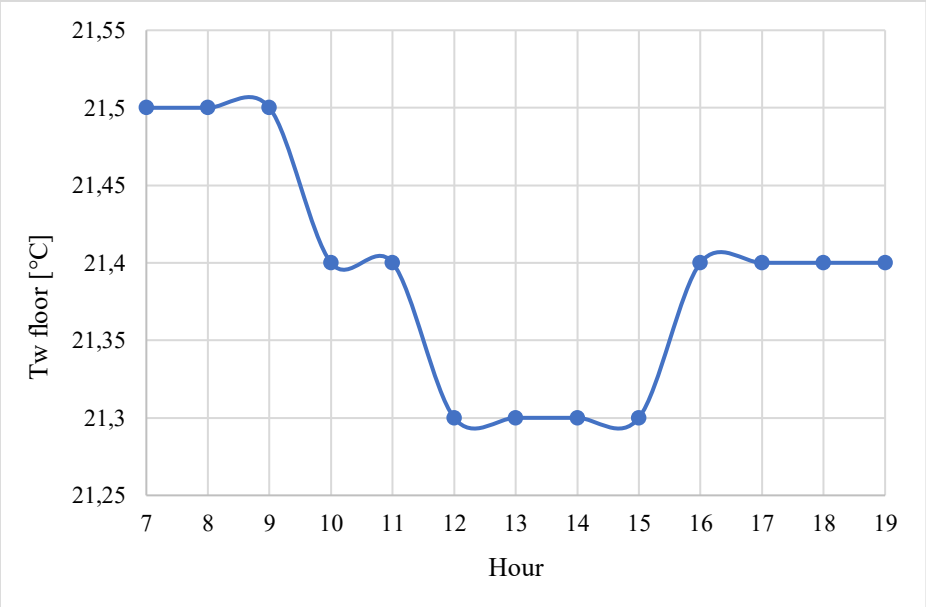

Fig. 77. *Calibration of the radiant floor system in the case of HOT FLOOR*

The maximum temperature of the water flowing inside the radiant floor system is showed in blue in Tab. 38. As we can see, the phenomenon of

temperature drop below the surface neutrality condition no longer appears because the thermal loads due to solar radiation are low. Moreover, the water temperature in the radiant floor system remains almost constant throughout the day.

Winter day: 28th December – HOT CEILING

Tab. 39. *Water temperature values for the case of HOT CEILING*

Hour	Tw ceiling	
7	26,5	[°C]
8	26,6	[°C]
9	26,4	[°C]
10	26,2	[°C]
11	25,9	[°C]
12	25,8	[°C]
13	25,7	[°C]
14	25,7	[°C]
15	25,8	[°C]
16	26	[°C]
17	26,2	[°C]
18	26,2	[°C]
19	26,1	[°C]

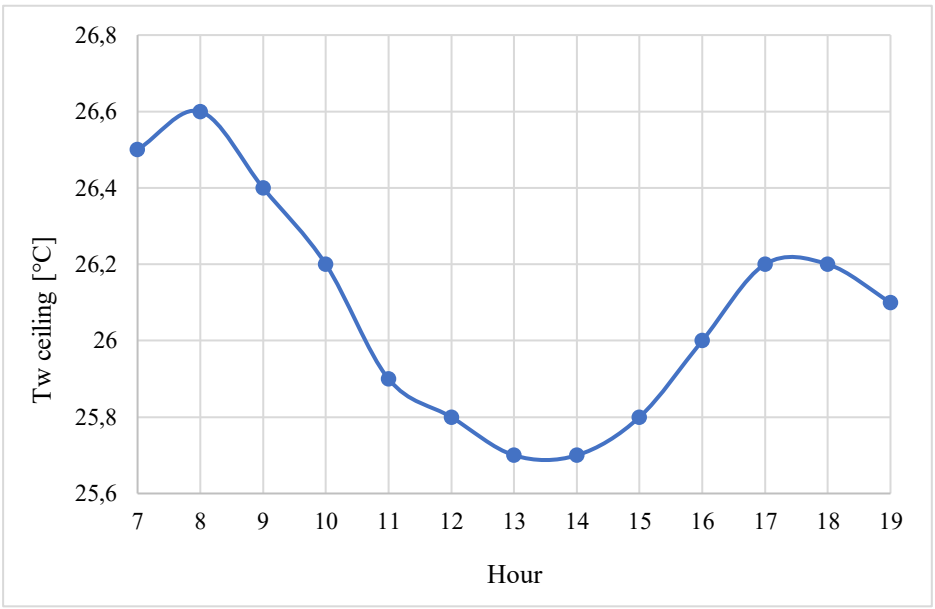

Fig. 78. *Calibration of the radiant ceiling panels in the case of HOT CEILING*

The maximum temperature of the water flowing inside the radiant floor system is showed in blue in Tab. 39. As in the previous case of a hot floor, the phenomenon of temperature drop below the surface neutrality condition

no longer appears and the water temperature in the radiant ceiling panels suffers a slight fluctuation during the day (about one degree). The only substantial difference between the two cases is that the temperatures are considerably higher for the reasons described previously.

Looking at all six diagrams representing the hourly water temperature profiles that flows inside the floor and ceiling radiant systems, we can see that the first four are very similar to each other (in terms of shape), while the last two deviate from them. The reason for this similarity is due to the high radiation that characterizes the first two days selected for the simulation, in particular, in the morning hours, since the glazed surfaces are exposed roughly to the east.

A comparison that can be made is between the hourly water temperature profiles of the two days selected in the winter season. From this comparative analysis it is possible to observe the fundamental role of solar radiation from the point of view of the energy saving in the heating season, as stated in *section 3.3.7*.

The following graphs (Fig. 79 and Fig. 80) show the comparisons between the two days selected in the winter season.

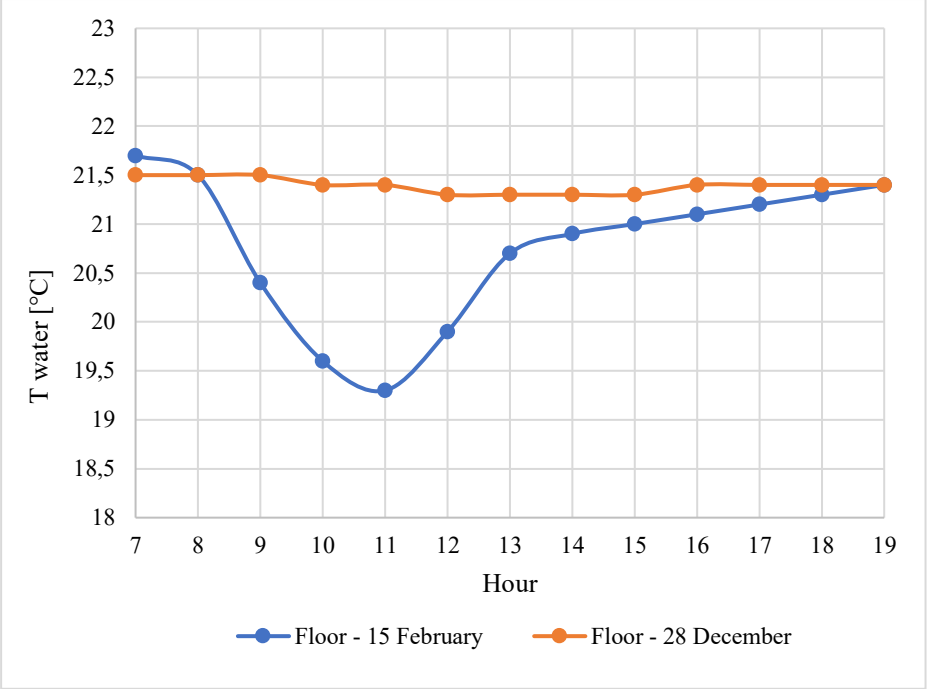

Fig. 79. *Floor: comparison 15th February – 28th December*

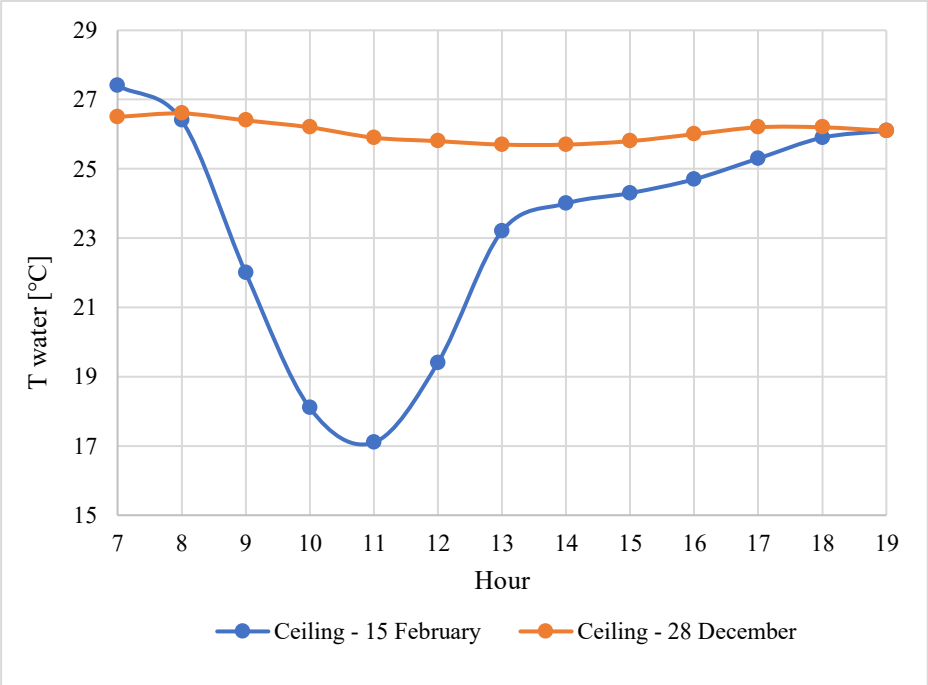

Fig. 80. *Ceiling: comparison 15th February – 28th December*

Thanks to the graphic representation of the comparisons in Fig. 79 and Fig. 80, it is possible to note the high influence that solar radiation has on the water temperature that flows inside the floor and ceiling radiant systems. As we can see, in the case of hot floor, the morning solar radiation causes a maximum lowering of the water temperature by about 2 °C. On the other

hand, in the case of hot ceiling, solar radiation causes a maximum lowering of the water temperature by about 9 °C. This lowering of temperature in some hours of the day translates into significant energy and cost savings.

3.4.2. Analysis of the radiant asymmetry

Radiant asymmetry is defined as the difference between the plane radiant temperature of the two opposite sides of a small plane element (*the plane radiant temperature is the temperature coming from the perpendicular direction to the measuring surface*). It is usually evaluated comparing temperatures of two opposing surfaces of a room. This kind of discomfort can derive from the presence of surfaces with a temperature different from the environmental one, as in the case of glazing, non-insulating walls, machinery, hot or cold radiant panels on walls, floors or ceilings. In particular, both EN ISO 7730 [6] and ASHRAE 55 [9] define limits of radiant asymmetry when using radiant walls, floors and ceilings based on percent dissatisfied curve.

In Fig. 81 are represented some example of radiant asymmetry and the percentage of people expressing discomfort due to asymmetric radiation.

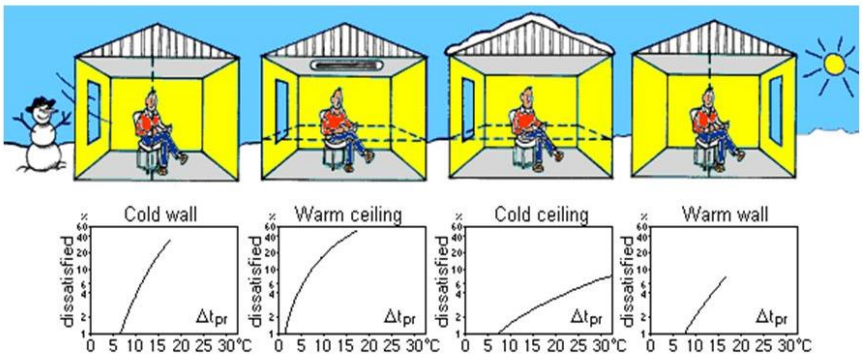

Fig. 81. *Example of radiant asymmetry*

Through experimental studies, conducted by subjecting people in thermal neutrality to increasing radiant asymmetries, a relationship between the percentage of dissatisfied (PD%) and radiant temperature asymmetry was derived by Fanger [98]. Studies have showed a different sensitivity to asymmetry caused by vertical or horizontal surfaces and by cold or hot

surfaces. In fact, from Fig. 82 we notice that, for the same values of radiant temperature asymmetry, a warm wall involves less discomfort than a cold one, while a warm ceiling determines more discomfort than a cold one.

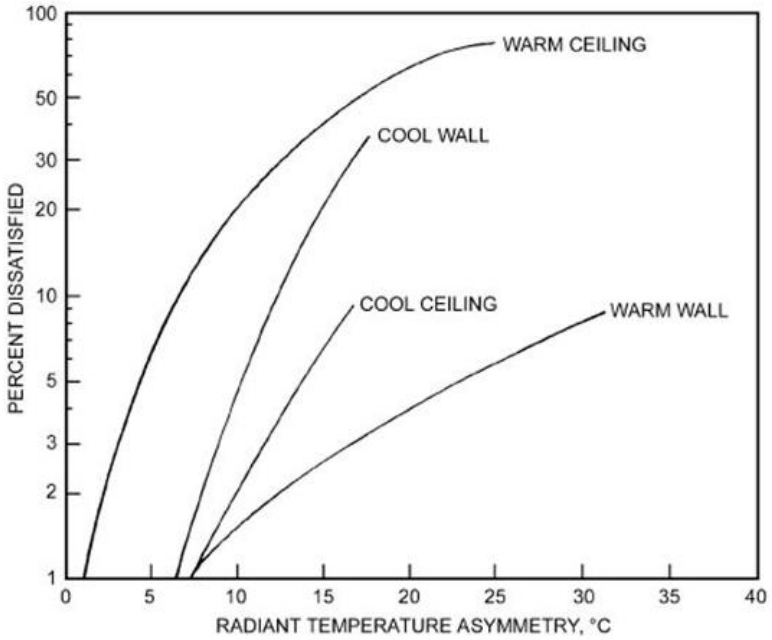

Fig. 82. *Percentage of people expressing discomfort due to asymmetric radiation*

As we can see from the previous graph, warm ceiling and cool walls (windows) causes greatest discomfort. This statement is also confirmed by the limits set in the EN ISO 7730 [6] standard and listed in Tab. 40.

Tab. 40. *Limits of radiant asymmetry*

Category (EN ISO 7730)	**Radiant temperature asymmetry [°C] ***			
	Warm ceiling	Cool wall	Cool ceiling	Warm wall
A - stringent thermo-hygrometric conditions (PPD=6%)	< 5	< 10	< 14	< 23
B - intermediate thermo-hygrometric conditions (PPD=10%)	< 5	< 10	< 14	< 23
C - higher PPD values are accepted (PPD=15%)	< 7	< 13	< 18	< 35

**Radiant temperature asymmetry in absolute value.*

The analysis of the radiant asymmetry that we performed through our model is closely linked to simulations performed previously. In fact, it was carried out once the temperature profiles for the calibration of the radiant systems

in the four cold / hot floor / ceiling configurations were determined, and the minimum value for the cooling season and the maximum value for the heating season were identified (highlighted in blue in the previous tables). The case of hot / cold wall has not been studied. On the other hand, the case of cold / hot floor has been study, even if not included in the standard. The objective we set ourselves was to verify whether in the simulations carried out previously arise temperature conditions such as to cause discomfort due to radiant asymmetry (Tab. 40).

The first step in determining the radiant temperature asymmetry was to perform simulations with a reverse procedure, i.e. replace the minimum / maximum water temperature value, according to the season considered, in order to obtain the surface temperatures of the six facades of the test room (floor, ceiling and walls) and the internal surface temperature of the glazed elements. After doing this, the climatic chamber was divided horizontally into two parts: the first constituted by the room volume below the point P (Tab. 30, *section 3.4.1*), the second constituted by the remaining portion above the same point. As stated previously, the assessment point was taken 60 cm from the floor since it represents the height of the seat of an office worker. In turn, as previously described in *section 3.3.3*, view factors were calculated from point P using the specific program *Trisfe*. In particular, unlike what was done for the calculation of the operative temperature, in this case two values of view factors were determined, respectively for the portions of surfaces above and below the virtual dividing line of the chamber. In the following table (Tab. 41) are listed the values of the view factors obtained.

Tab. 41. *View factors for the portions of surfaces above and below the virtual dividing line of the chamber*

View factors								
	North	West	South	East	Glass	Ceiling	Floor	Opaque
Up	0,0557	0,0464	0,0623	0,0341	0,0372	0,1364	0	0,1279
Down	0,0214	0,0184	0,0133	0,0343	0	0	0,371	0,0416
Up*	0,1114	0,0928	0,1246	0,0682	0,0744	0,2728	0	0,2558
Down*	0,0428	0,0368	0,0266	0,0686	0	0	0,742	0,0832

As we can see, also in the table above appears the eighth component (called "Opaque"). We remember that this term groups all those passive surface portions of the room where the radiant systems have not been installed. Besides, Tab. 41 shows two rows of view factors for each surface (with and without the asterisk). The first (without the asterisk) are the real values that are showed in output by the program, in which, however, the surfaces on which the point P lies are not counted (ceiling for the portion below, floor for the one above, with view factor equal to 0.5). For this reason, the values must be divided by 0.5 in order to obtain the normalized view factors (sum equal to 1) to be used for the analysis. Finally, once obtained the view factors, it has been possible to calculate the mean radiant temperatures for the sub-rooms below and above the point P, by means of equation *(23)*, and determine the radiant temperature asymmetry, conventionally defined as follows:

$$\Delta t_{pr} = t_{mr,up} - t_{mr,down} \quad [°C] \qquad (24)$$

Following are represented are represented the summary tables of the six simulations carried out, with the respective surface temperatures, the MRTs and the obtained value of radiant asymmetry.

Tab. 42. *Analysis of radiant asymmetry in the case of COLD FLOOR*

Summer	**Cold Floor**			
18-lug				
(10.00)	Tw floor	12,2	[°C]	
Ts floor	292,509441	[K]	19,36	[°C]
Ts ceiling	300,015982	[K]	26,87	[°C]
Ts north	299,36984	[K]	26,22	[°C]
Ts east	299,106259	[K]	25,96	[°C]
Ts south	299,498069	[K]	26,35	[°C]
Ts west	299,651277	[K]	26,50	[°C]
Ts glass int	327,250901	[K]	54,10	[°C]
MRT up	301,85	[K]	28,70	[°C]
MRT down	294,32	[K]	21,17	[°C]
Radiant asymmetry	7,53	[°C]		

Tab. 43. *Analysis of radiant asymmetry in the case of COLD CEILING*

Summer	**Cold Ceiling**			
18-lug				
(10.00)	Tw ceiling	15,2	[°C]	
Ts floor	300,0652207	[K]	26,92	[°C]
Ts ceiling	292,9870698	[K]	19,84	[°C]
Ts north	299,3260114	[K]	26,18	[°C]
Ts east	299,3749908	[K]	26,22	[°C]
Ts south	299,4053058	[K]	26,26	[°C]
Ts west	299,5341171	[K]	26,38	[°C]
Ts glass int	326,0835244	[K]	52,93	[°C]
MRT up	299,91	[K]	26,76	[°C]
MRT down	299,88	[K]	26,73	[°C]
Radiant asymmetry	0,03	[°C]		

Tab. 44. *Analysis of radiant asymmetry in the case of HOT FLOOR*

Winter	**Hot Floor**			
15-feb				
(7.00)	Tw floor	21,7	[°C]	
Ts floor	294,733116	[K]	21,58	[°C]
Ts ceiling	293,262101	[K]	20,11	[°C]
Ts north	293,258766	[K]	20,11	[°C]
Ts east	292,178228	[K]	19,03	[°C]
Ts south	291,533087	[K]	18,38	[°C]
Ts west	293,298008	[K]	20,15	[°C]
Ts glass int	289,604901	[K]	16,45	[°C]
MRT up	292,65	[K]	19,50	[°C]
MRT down	294,26	[K]	21,11	[°C]
Radiant asymmetry	-1,61	[°C]		

Tab. 45. *Analysis of radiant asymmetry in the case of HOT CEILING*

Winter	**Hot Ceiling**			
15-feb				
(7.00)	Tw ceiling	27,4	[°C]	
Ts floor	293,1645861	[K]	20,01	[°C]
Ts ceiling	299,0799763	[K]	25,93	[°C]
Ts north	293,3315448	[K]	20,18	[°C]
Ts east	292,18248	[K]	19,03	[°C]
Ts south	291,5621455	[K]	18,41	[°C]
Ts west	293,3629468	[K]	20,21	[°C]
Ts glass int	290,4658678	[K]	17,32	[°C]
MRT up	294,36	[K]	21,21	[°C]
MRT down	293,11	[K]	19,96	[°C]
Radiant asymmetry	1,26	[°C]		

Tab. 46. *Analysis of radiant asymmetry in the case of HOT FLOOR*

Winter	**Hot Floor**			
28-dic				
(8.00)	Tw floor	21,5	[°C]	
Ts floor	294,549361	[K]	21,40	[°C]
Ts ceiling	293,280666	[K]	20,13	[°C]
Ts north	293,262914	[K]	20,11	[°C]
Ts east	292,415783	[K]	19,27	[°C]
Ts south	291,873967	[K]	18,72	[°C]
Ts west	293,299647	[K]	20,15	[°C]
Ts glass int	290,32573	[K]	17,18	[°C]
MRT up	292,77	[K]	19,62	[°C]
MRT down	294,15	[K]	21,00	[°C]
Radiant asymmetry	-1,37	[°C]		

Tab. 47. *Analysis of radiant asymmetry in the case of HOT CEILING*

Winter	**Hot Ceiling**			
28-dic				
(8.00)	Tw ceiling	26,6	[°C]	
Ts floor	293,1659161	[K]	20,02	[°C]
Ts ceiling	298,4710147	[K]	25,32	[°C]
Ts north	293,3295301	[K]	20,18	[°C]
Ts east	292,4224265	[K]	19,27	[°C]
Ts south	291,900609	[K]	18,75	[°C]
Ts west	293,3595821	[K]	20,21	[°C]
Ts glass int	291,0990401	[K]	17,95	[°C]
MRT up	294,30	[K]	21,15	[°C]
MRT down	293,12	[K]	19,97	[°C]
Radiant asymmetry	1,17	[°C]		

From the previous simulations, the cases of hot / cold floor and hot / cold ceilings have been studied, according to the season considered, for the three selected days. The case of hot / cold wall has not been studied. On the other hand, the case of cold / hot floor has been study, even if not included in the standard. As we can see from the previous table, all the obtained values are within the limits established by the EN ISO 7730 [6] standard (Tab. 40), except for the case of cold floor. Once the test chamber is operational, it will certainly be interesting to verify this condition, which is not included in the standard because it is not considered to be a cause of discomfort. However, as already expressed above, warm ceiling is considered to be the cause of maximum discomfort (Fig. 82). Nevertheless, in our simulations, the radiant asymmetry for the hot ceiling case is abundantly within the limits set by the standard.

The next step will be to determine the maximum temperature difference that can be reached in the hot ceiling / cold floor condition, keeping the operative temperature constant at the set point value, in order to exceed the limit values set by the standard.

APPENDIX A

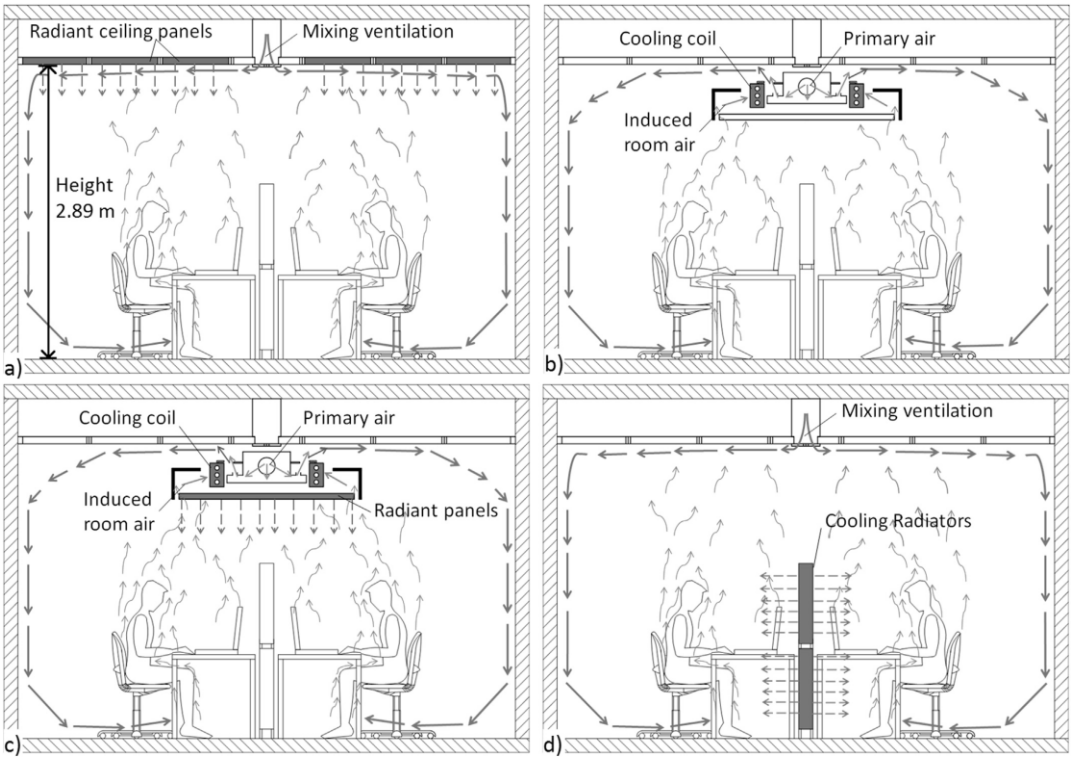

Fig. A1. *Operating principle of the four cooling systems that were studied: a) CCMV, b) CB, c) CBR and d) MVRC*

Tab. A1. *Summary of measurements result in the office room cases*

Office room	In design heat load (64 W/m^2) case				In usual heat load (38 W/m^2) case			
Measurement results in occupied zone at heights 0.1, 0.6, 1.1 and 1.7 m	CCMV	CB	CBR	MVRC	CCMV	CB	CBR	MVRC
Average air temperature [°C]	26.1	25.8	26.1	25.9	26.0	25.8	25.9	25.8
Min. air temperature [°C]	25.3	24.9	25.3	25.0	25.5	25.0	25.2	24.2
Max. air temperature [°C]	28.0	26.7	27.6	27.2	26.8	26.4	26.7	26.7
Std. dev. of air temperature [°C]	0.6	0.5	0.6	0.4	0.3	0.3	0.3	0.4
Average operative temperature [°C]	26.3	26.1	26.3	26.1	26.1	25.9	26.1	25.9
Min. operative temperature [°C]	25.3	25.1	25.4	25.4	25.5	25.1	25.2	24.5
Max. operative temperature [°C]	28.2	27.2	27.8	27.5	27.1	26.6	26.9	26.8
Std. dev. of operative temperature [°C]	0.7	0.6	0.6	0.5	0.3	0.4	0.4	0.4
Average operative-air temperature [°C]	0.1	0.3	0.2	0.1	0.1	0.1	0.0	0.1
Min. operative-air temperature [°C]	−0.2	−0.1	0.0	0.0	−0.1	−0.1	−0.3	−0.1
Max. operative-air temperature [°C]	0.6	0.7	0.5	0.6	0.5	0.4	0.3	0.3
Std. dev. of operative-air temperature [°C]	0.2	0.2	0.1	0.1	0.1	0.1	0.1	0.1
At height 1.1 m:								
Avrg. air temperature of window side [°C]	26.8	26.4	26.9	26.8	26.4	26.2	26.4	26.5
Avrg. air temperature of door side [°C]	25.7	25.4	25.7	25.9	25.7	25.6	25.7	25.9
Avrg. horizontal air temp. diff. [°C]	1.1	1.0	1.2	1.0	0.7	0.7	0.7	0.6
Avrg. oper. temp. of window side [°C]	27.4	27.1	27.4	27.3	26.8	26.6	26.7	26.7
Avrg. oper. temperature of door side [°C]	25.8	25.7	25.9	25.9	25.9	25.7	25.8	26.0
Avrg. horizontal oper. temp. diff. [°C]	1.6	1.4	1.5	1.3	0.8	0.9	0.9	0.8
Avrg. oper.-air temp. of window side [°C]	0.6	0.7	0.5	0.4	0.4	0.3	0.3	0.2
Avrg. oper.-air temp. of door side [°C]	0.1	0.2	0.2	0.1	0.2	0.1	0.0	0.0
At heights 0.1 m–1.7 m:								
Avrg. vertical air temperature diff. [°C]	0.0	0.3	0.2	0.6	0.3	0.4	0.2	0.8
Avrg. vertical oper. temperature diff. [°C]	−0.1	0.5	0.2	0.6	0.3	0.5	0.5	0.7
Max. radiant asymmetry (window–door) [°C]	5.0	4.0	4.2	3.3	2.3	3.2	2.5	2.3
Max. radiant asymmetry (side–side wall, except in MVRC radiator-side wall) [°C]	0.3	0.6	1.5	−3.4	0.7	0.7	0.8	−1.7
Max. radiant asymmetry (floor-ceiling, except in MVRC radiator-manikin) [°C]	4.1	0.8	1.7	−6.5	3.0	−0.8	0.3	−4.3
Average air velocity [m/s]	0.13	0.13	0.12	0.10	0.11	0.12	0.11	0.06
Average of 3 highest velocities [m/s]	0.23	0.27	0.24	0.20	0.21	0.26	0.25	0.13
Highest velocity [m/s]	0.24	0.29	0.25	0.21	0.23	0.27	0.26	0.14
Std. dev. of air velocity [m/s]	0.04	0.05	0.05	0.04	0.04	0.05	0.05	0.03
Average turbulence intensity [%]	39	45	45	47	40	42	48	46
Average of 3 highest turb. intensities [%]	76	74	77	78	71	72	84	100
Std. dev. of turbulence intensity [%]	14	13	12	15	12	15	16	58
Average draught rate [%]	7.9	9.5	8.1	6.1	5.7	7.8	6.9	2.0
Average of 3 highest draught rates [%]	14.7	19.8	18.0	14.1	12.3	18.2	16.6	7.2
Highest draught rate [%]	16.3	20.8	19.5	14.9	13.0	18.4	17.4	8.3
Std. dev. of draught rate [%]	3.3	4.6	4.2	3.7	2.8	4.6	4.2	2.1

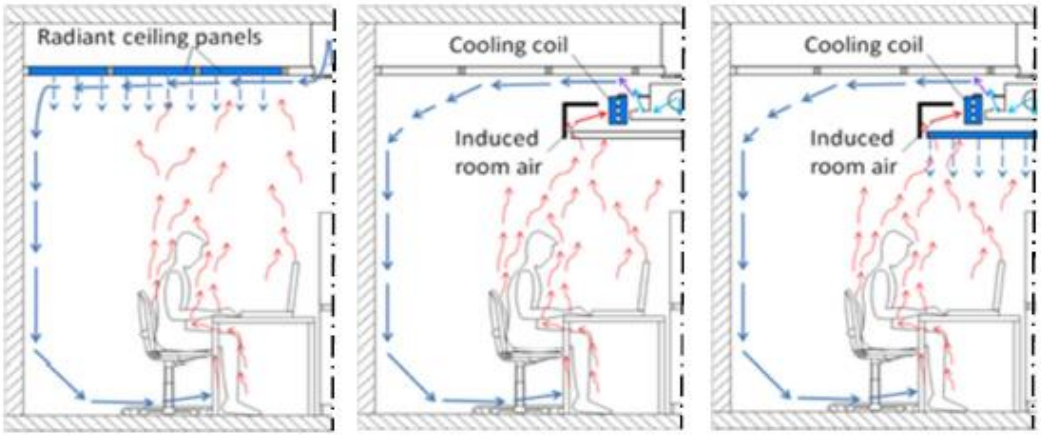

Fig. A2. *Operating principle of different cooling systems: Radiant ceiling (left side), Chilled beam (center) and Chilled beam integrated with radiant panels (right side). Note: Only half of the room shown with symmetry line on right side*

Tab. A2. *Average values of measurement results, in the first line of values in design conditions and in the second line in usual conditions for each variable*

MEETING ROOM IN DESIGN (WITH BOLD FONT) AND USUAL CONDITIONS (WITH NORMAL FONT)

Measurement results in occupied zone at heights 0.1 m - 1.7 m	Chilled ceiling with mixing vent.	Chilled beam	Chilled beam with radiant panels
Average air velocity [m/s]	**0.14**	**0.16**	**0.16**
	0.13	0.14	0.14
Average of 5 highest velocities	**0.27**	**0.31**	**0.31**
	0.24	0.31	0.31
Average air temperature [°C]	**25.9**	**25.6**	**25.9**
	25.9	25.9	25.9
Average temperature of window side	**26.5**	**26.2**	**26.3**
	26.3	26.5	26.3
Average temperature of door side	**25.4**	**24.8**	**25.2**
	25.6	25.5	25.3
Average horizontal temperature diff.	**1.1**	**1.3**	**1.1**
	0.7	1.0	1.0
Average vertical temperature diff.	**0.3**	**0.4**	**0.4**
	0.5	0.7	0.7
Horizontal operative temperature diff.	**1.4**	**1.6**	**1.4**
	0.9	1.1	1.2
Vertical operative temperature diff.	**0.1**	**0.5**	**0.4**
	0.4	0.7	0.7
Average operative-air temperature	**0.10**	**0.29**	**0.23**
	0.08	0.16	0.18
Average draft rate [%]	**8.8**	**11.2**	**11.0**
	7.5	8.6	8.6
Average of 5 highest draft rates	**17.7**	**23.9**	**23.8**
	16.1	21.8	21.5

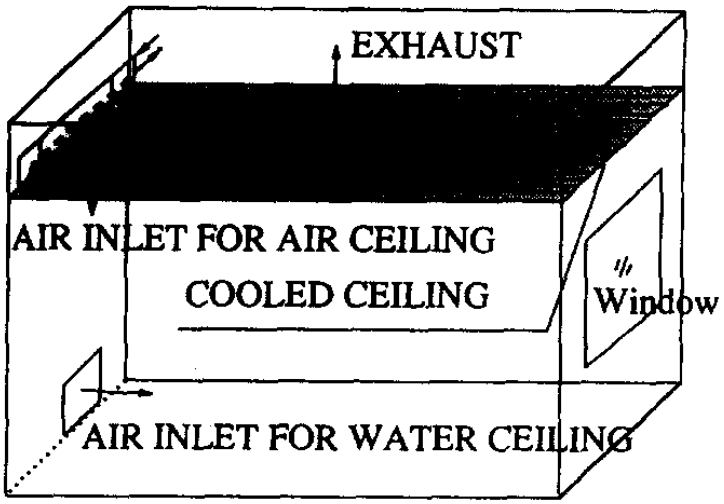

Fig. A3. *Schematic for constructions of cooled ceiling in a room*

Tab. A3. *Simulated operation parameters of the three cooling systems*

Case description	Cooling load					Vent air temp. (°C)	Total heat gains	
	Total(W)	Floor area (W/m^2)	By air (W)	By panel (W)			Int. (W)	Ext. (W)
				Total	Convection			
Displ. vent.	480	26	480	—	—	19	540	−60
Displ. vent. + water-ceiling*	875	48	415	460	273	20	800	75
Air-ceiling†	864	47	217	647	433	13/23	800	64

*60% of the ceiling area is installed with water panels, supplied water temperature is about 19°C, with a temperature rise of about 1.5°C over the panels; the consequent average panel surface temperature is about 20.2°C.

†70% of the ceiling area is installed with air panels; the ventilation air temperatures entering and leaving the panels are 13 and 23°C, respectively.

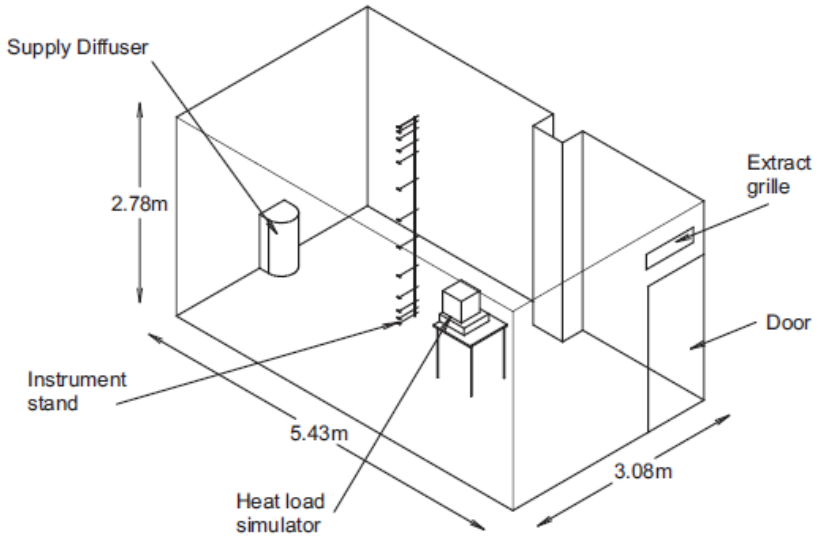

Fig. A4. *Configuration of the environmental test chamber*

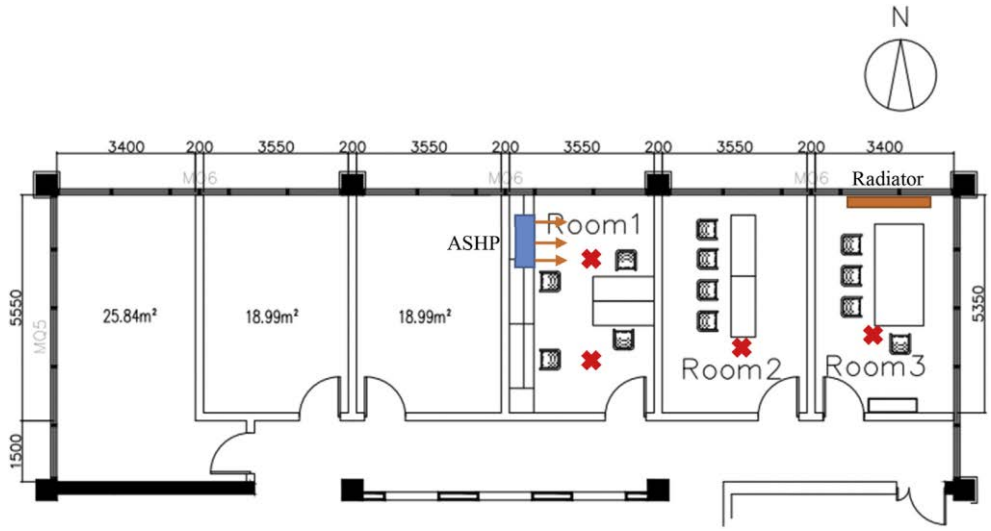

Fig. A5. *Layout of the experiment rooms (red cross indicate where the vertical air temperature difference is measured)*

Tab. A4. *Summary of heating facilities*

	Heating facility	Type	Heating capacity	Control strategy
Room 1	Air source heat pump	Gree KFR-35GW	4500 W	On-off
Room 2	Radiator	/	Total area of 0.72 m^2, supply water temperature of 70 °C	By-pass control, i.e. control supply water volume flux
Room 3	Floor heating	Light thermal mass floor heating	3500 W	Control supply water temperature

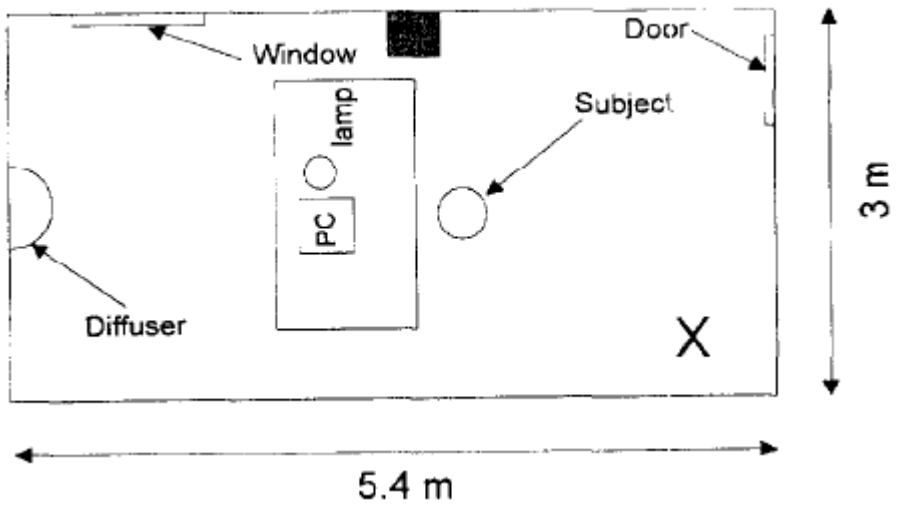

Fig. A6. *Plan of the experimental room*

APPENDIX B

Pannello attivo BLife tipo 1
Tagliando il pannello attivo tipo 1 lungo la linea evidenziata è possibile ricavare due pannelli con dimensione 2400x600 mm

Pannello attivo BLife tipo 2
Tagliando il pannello attivo tipo 2 lungo la linea evidenziata è possibile ricavare due pannelli con dimensione 1200x1200 mm

Pannello attivo BLife tipo 3
Tagliando il pannello attivo tipo 3 lungo le linee evidenziate è possibile ricavare quattro pannelli con dimensione 1200x600 mm

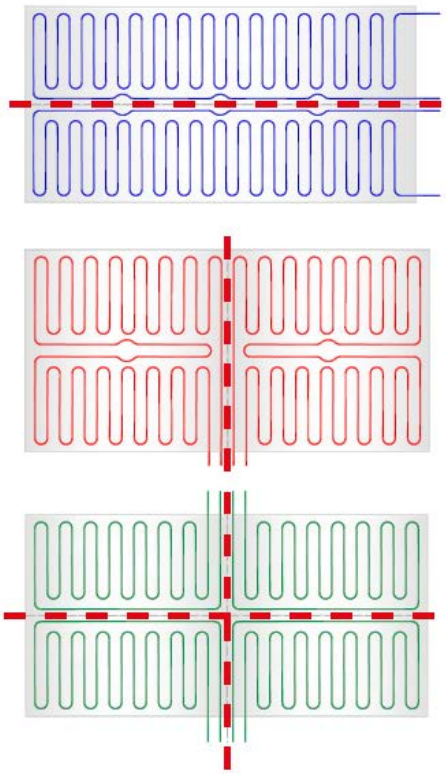

Fig. B1. *Typologies and possible separations of Loex radiant panels*

Riscaldamento
Diagramma di dimensionamento sistema BLife®
Diagramma ricavato da simulazioni FEM secondo UNI EN ISO 11855-2

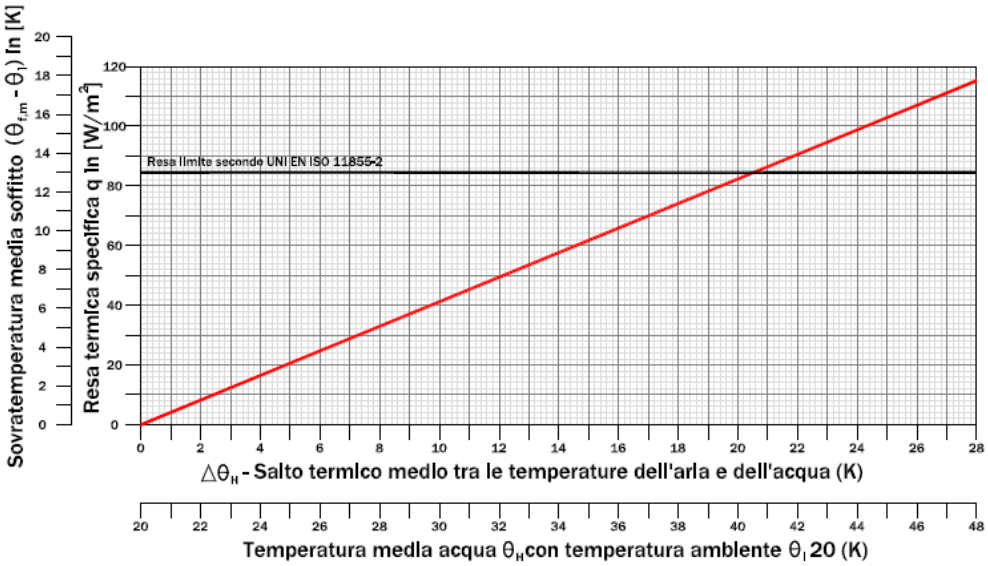

Fig. B2. *Diagram of thermal yield in heating conditions - Loex*

Raffrescamento

Diagramma di dimensionamento sistema BLife®

Diagramma ricavato da simulazioni FEM secondo UNI EN ISO 11855-2

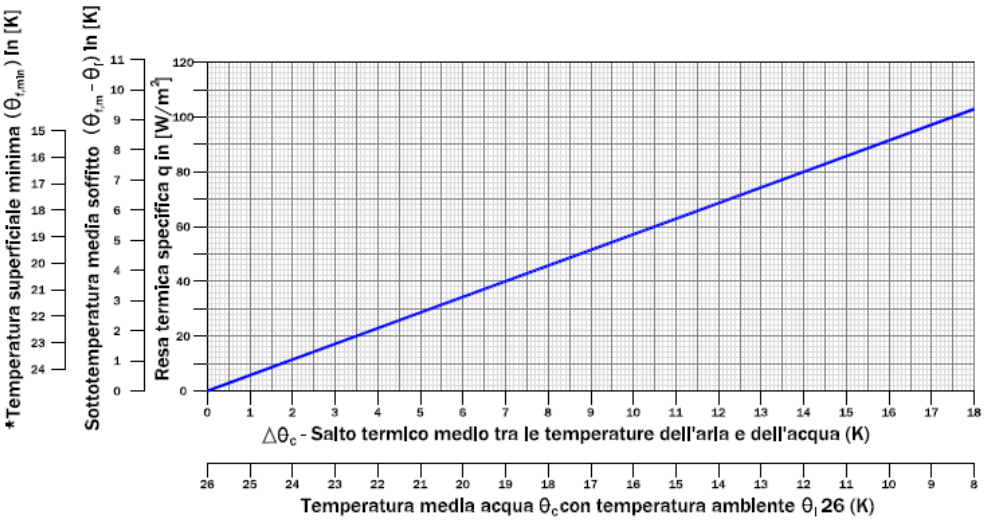

* Temperatura minima sulla verticale della prima tubazione con temperatura ambiente 26°C e differenza fra mandata e ritorno 4°C (da utilizzare per verifica assenza formazione di condensa)

Fig. B3. *Diagram of thermal yield in cooling conditions - Loex*

Resa sistema Plasterboard – riscaldamento a parete (rif. UNI EN ISO 11855-2)

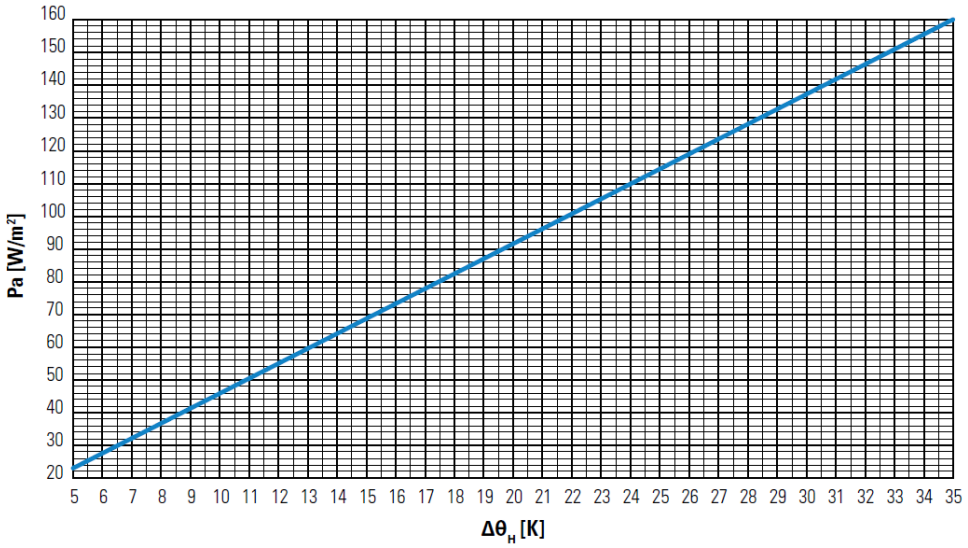

Fig. B4. *Diagram of thermal yield in heating conditions - Emmeti*

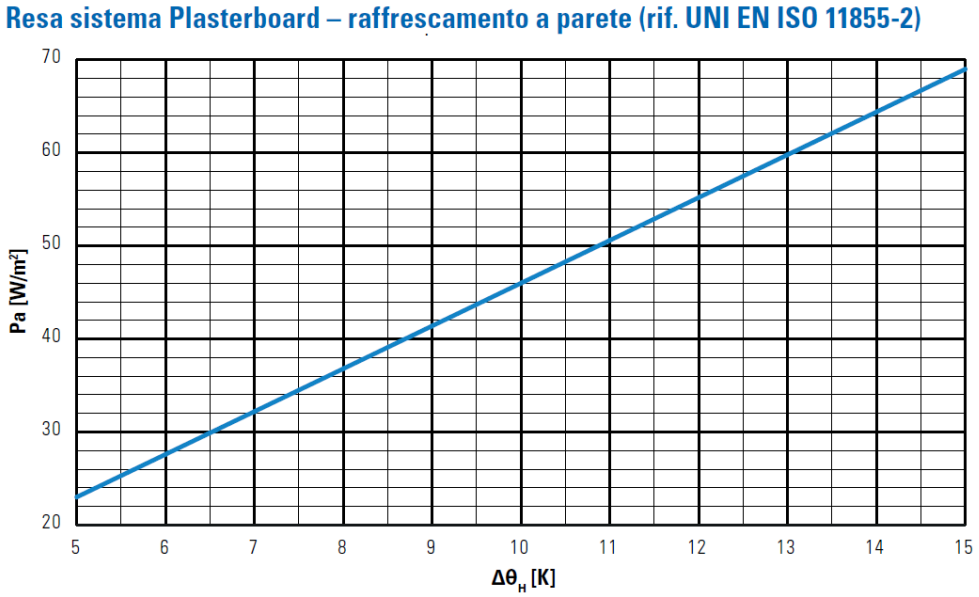

Fig. B5. *Diagram of thermal yield in cooling conditions - Emmeti*

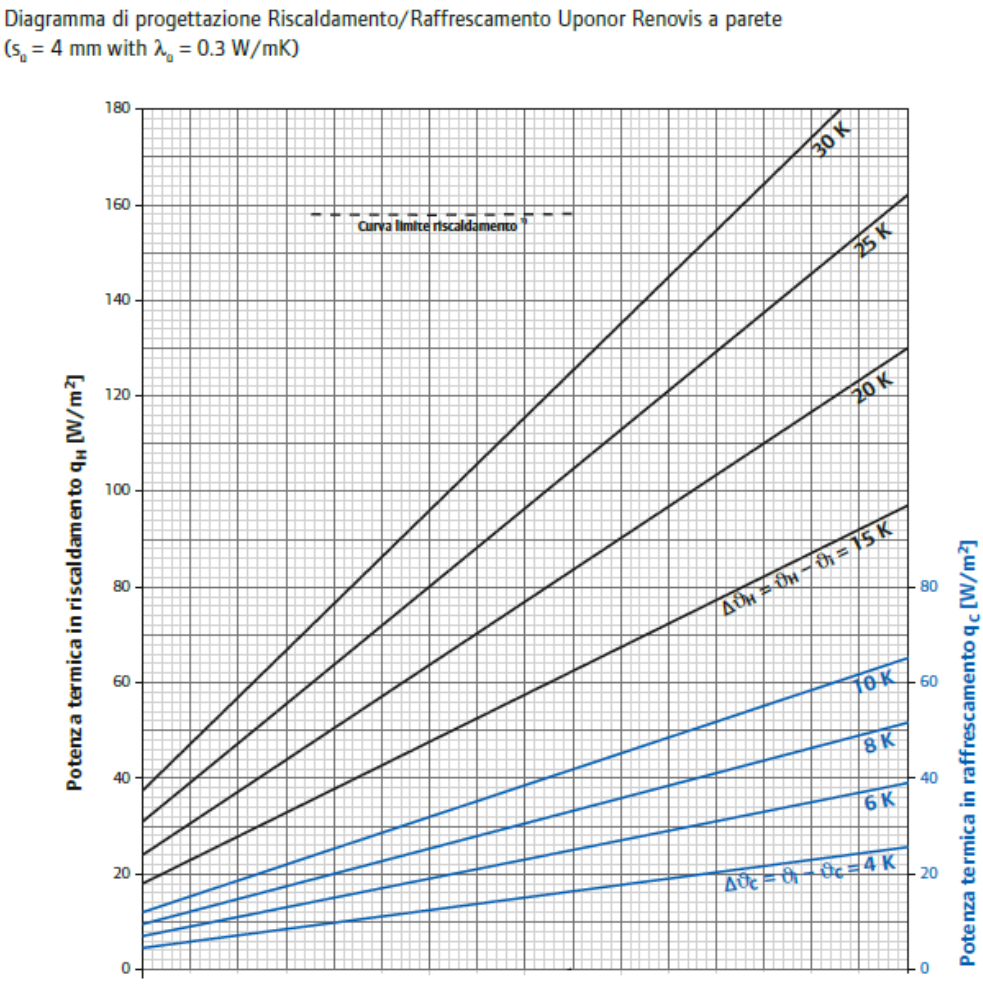

Fig. B6. *Diagrams of thermal yield in heating and cooling conditions - Uponor*

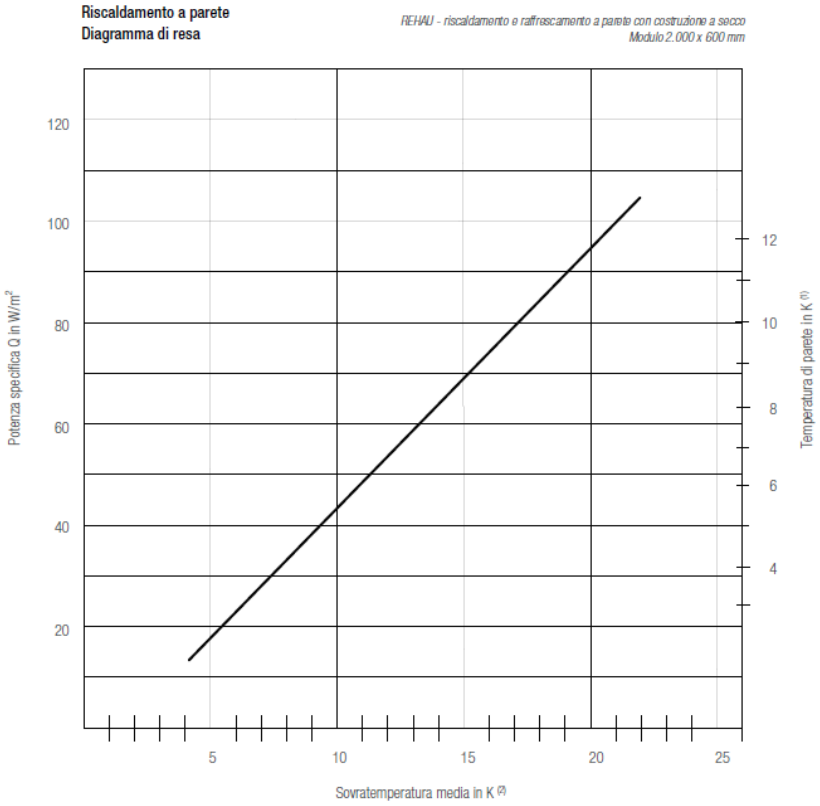

Fig. B7. *Diagram of thermal yield in heating conditions - Rehau*

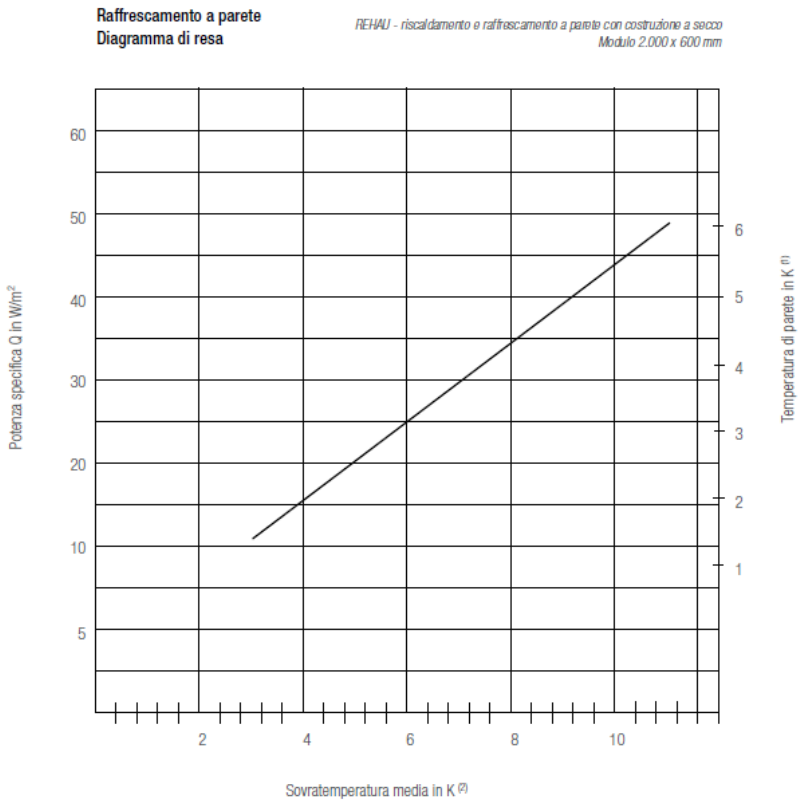

Fig. B8. *Diagram of thermal yield in cooling conditions - Rehau*

Tab. B1. *Technical characteristics of ventilation machine*

Table of technical characteristics **Tabella delle caratteristiche tecniche**			
Technical specifications	**Specifiche tecniche**		
Condensation (35°C - 50% - 200 m³/h)	Umidità condensata (35°C - 50% - 200 m³/h)	*l/day* l/giorno	38.7
Rated electrical power	Potenza elettrica nominale	W	460
Total max. power consumption of the fans	Potenza elettrica max. assorbita dai ventilatore	W	130
Nominal air flow rate	Portata aria nominale	m³/h	200
Fan performance	Prevalenza utile ventilatore	Pa	300
Unit water flow rate	Portata acqua unità	l/h	240
Condensation water supply	Attacchi alimentazione acqua		F1/2
Sound power level	Livello potenza sonora	dB(A)	44
Sound pressure level	Livello di pressione sonora	d(B(A)	36
Pre-cooling water head loss	Perdita di carico acqua pre-raffreddamento	DaPa	920
Refrigerant (R 134A)	Refrigerante (R 134A)	gr	250
Overall machine dimensions	**Ingombri macchina**		
Height	Altezza	mm	244
Width	Larghezza	mm	825
Depth	Profondità	mm	1118
Weight	Peso	kg	51
Overall machine dimensions	**Ingombri ventilatori**		
Height	Altezza	mm	200
Width	Larghezza	mm	327
Depth	Profondità	mm	385
Weight	Peso	kg	7

Tab. B2. *Performance of ventilation machine*

Yield during dehumidification, depending on room temperature, relative humidity, considering a unit supplied with water at 15°C.

Resa in deumidificazione, in funzione della temperatura ambiente, umidità relativa considerando l'unità alimentata con acqua a 15°C.

Performance in recirculation mode **Resa in ricircolo**							
Inlet air **Aria in ingresso**		***Outlet air*** **Aria in uscita**		***Latent cooling power*** **Pot. frig. latente**		***Sens. cooling power*** **Pot. frig. sensibile**	***Cooling power to be supplied to the unit*** **Potenza frigorifera da fornire all'unità**
°C	% UR	°C	% UR	W	l/g	W	W
100 m³/h							
33	50	26	35,1	729	25,2	374	560
35	50	26	36,9	859	29,7		650
150 m³/h							
33	50	26	44,0	855	29,5	561	710
35	50	26	46,7	1023	35,3		820
200 m³/h							
33	50	26	50,2	913	31,5	748	820
35	50	26	53,6	1121	38,7		940

APPENDIX C

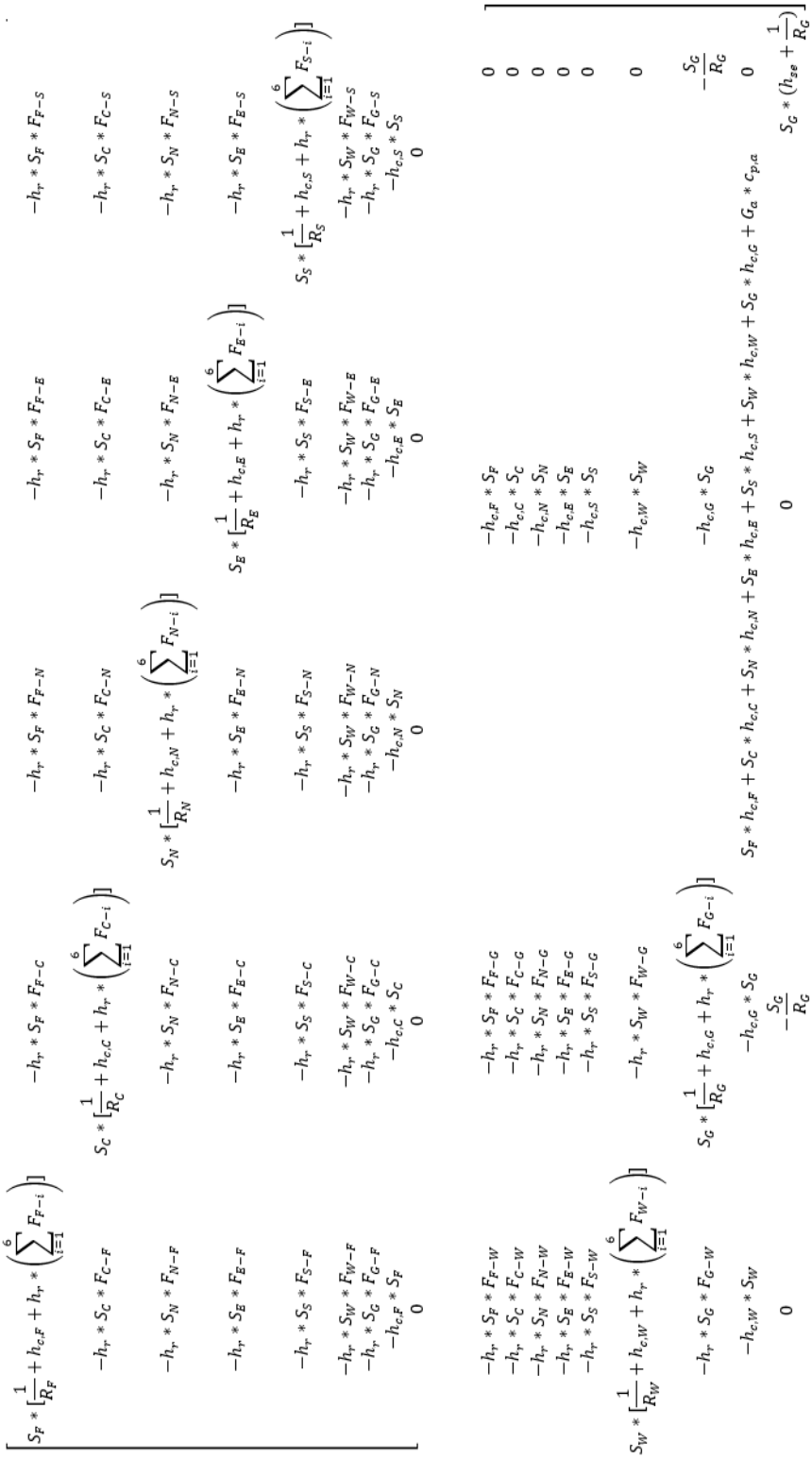

***Fig. C1**. Matrix of coefficients (dim: 9x9)*

$$
* \begin{pmatrix} t_{s,F} \\ t_{s,C} \\ t_{s,N} \\ t_{s,E} \\ t_{s,S} \\ t_{s,W} \\ t_{sG,i} \\ t_{air} \\ t_{sG,e} \end{pmatrix} = \begin{pmatrix} f_{r,F} * \sum_{k=1}^{f}(q_{s,k}) + f_{r,RAD} * f_{r,F} * \sum_{g=1}^{m}(q_{l,g}) + S_F * \frac{t_{w,F}}{R_F} \\ f_{r,C} * \sum_{k=1}^{f}(q_{s,k}) + f_{r,RAD} * f_{r,C} * \sum_{g=1}^{m}(q_{l,g}) + S_C * \frac{t_{w,C}}{R_C} \\ f_{r,N} * \sum_{k=1}^{f}(q_{s,k}) + f_{r,RAD} * f_{r,N} * \sum_{g=1}^{m}(q_{l,g}) + S_N * \frac{t_{w,N}}{R_N} \\ f_{r,E} * \sum_{k=1}^{f}(q_{s,k}) + f_{r,RAD} * f_{r,E} * \sum_{g=1}^{m}(q_{l,g}) + S_E * \frac{t_{w,E}}{R_E} \\ f_{r,S} * \sum_{k=1}^{f}(q_{s,k}) + f_{r,RAD} * f_{r,S} * \sum_{g=1}^{m}(q_{l,g}) + S_S * \frac{t_{w,S}}{R_S} \\ f_{r,W} * \sum_{k=1}^{f}(q_{s,k}) + f_{r,RAD} * f_{r,W} * \sum_{g=1}^{m}(q_{l,g}) + S_W * \frac{t_{w,W}}{R_W} \\ {}^{I_a}/_{2} \\ f_{r,CONV} * \sum_{g=1}^{m}(q_{l,g}) + G_a * c_{p,a} * t_{imm,air} \\ \frac{I_a}{2} + S_G * h_{se} * t_{ext} \end{pmatrix}
$$

Fig. C2. *Vector of unknown variables and vector of known terms*

In Fig. C1 e Fig. C2 are represented the terms that make up the resolution system of the detailed energy balance of our test room. The subscripts indicate respectively:

- *F : Floor;*
- *C : Ceiling;*
- *N : North wall;*
- *E : East wall;*
- *S : South wall;*
- *W : West wall;*
- *G : Glass;*

CONCLUSIONS

The present thesis work represents the first step of a research project for Indoor Environmental Quality (IEQ) analysis, aimed at recognizing the effects of environmental parameters on the productivity of people and their perception of the working environment through comfort parameters (thermal, acoustic, air quality, etc.). The objectives of the thesis can be summarized in the three macro-topics that comprise it:

- Research review;
- Detailed description of the laboratory and the technical room;
- Creation of a simulation model for the calibration of radiant systems.

The literary review carried out was particularly accurate and thorough, with the aim of investigating the research carried out in the past in terms of thermal comfort and indoor environmental quality. In particular, the focus was on the analysis of investigation methods and parameters evaluated. Of all the articles read, 74 papers were selected for more detailed analysis. From the literary research it emerged that measurements made in test chamber or in existing office with the presence of human subjects is not the most used method to assess comfort. Most research prefers numerical simulation and focuses solely on thermal comfort, neglecting other aspects of the IEQ, such as acoustic comfort, light, and air quality. However, we have to remember that for a global assessment of indoor environment quality, the analysis of hygrometric, acoustic and air quality parameters is also fundamental, because they are closely related to the well-being and health problems of people (e. g. Sick Building Syndrome). The psychological and productive aspects of the occupants are almost never taken into consideration. Therefore, the proposed multidisciplinary approach has no similar among all the research carried out. Thanks to this project in fact, the goal is to fill the gap emerged in the literature, due to the specificity of the research carried out so far. In parallel with the analysis of the most used research methods and the most evaluated parameters, a climate chambers research was carried out during the review. The objective of this investigation is to compare the characteristic dimensions (floor area and volume) of our test room with the others described in the analysed articles and then to select those geometrically similar in order to determine possible comparison terms with the results that will be obtained

in the future. From this comparison five climatic chambers geometrically similar to the one built in Padua were identified, four existing and one simulated.

The second part of this thesis consists of a detailed description of the laboratory and the technical room, analysing the geometry and the systems installed. All the drawings represented were made using the software AUTOCAD®, after having personally carried out measurements inside the two rooms. Radiant systems (floor, ceiling and walls), mechanical ventilation system and all the hydronic systems for managing flow rates and supply temperatures are carefully described and their main characteristics analysed. All the components present in the two rooms were designed, provided and installed by more than 20 companies from northern Italy. For this reason, the test room has no similar examples in Italian and European universities, due to the multidisciplinary nature of the aspects dealt with simultaneously.

Finally, following the method of the detailed energy balance of a room, the third part of this work aims at creating a simulation model in steady-state conditions that allows to determine the internal surface temperatures of the climate chamber (floor, ceiling, walls and windows) and the internal air temperature as a function of the external temperature, temperatures of the water into the six radiant systems and solar radiation (transmitted and absorbed). Furthermore, this model has been realized to carry out an analysis of the radiant asymmetry that occurs at different thermal conditions (hot / cold floor and hot / cold ceiling, according to the season considered). To do this, the hourly profile of the water temperature that flows inside floor or ceiling radiant systems was determined (depending on the thermal condition considered), respecting some conditions to be simulated, such as keeping constant the operative temperature inside the room, equal to the set-point value (26 °C in summer season, 20 °C in winter season).

It was decided to select three days characterized by the following conditions in order to simulate the model:

- Summer day: 18th July (5.00-20.00). High temperatures and high solar radiation;
- Winter day: 15th February (7.00-19.00). Low temperatures and high solar radiation;

- Winter day: 28th December (7.00-19.00). Low temperatures and low solar radiation.

By systematically repeating some data entry operations in the Excel spreadsheet, the hourly profiles of the water temperature were determined, useful for a future calibration of the radiant systems. This water temperature profile in fact substantially represents the compensation temperature values in order to satisfy the initial conditions imposed on the model (e. g. constant operative temperature) Comparing values and trends of the obtained profiles, it is possible to note the high influence that solar radiation has on the water temperature, so much that, in the simulation of the second day, temperatures fall below the neutrality condition of a surface (in heating conditions equal to 20 °C) for a short period of time.

Regarding the analysis of radiant temperature asymmetry, all the obtained values are within the limits established by the EN ISO 7730 standard, in particular the warm ceiling condition, considered the cause of maximum discomfort. The next step will be to determine the maximum temperature difference that can be reached in the hot ceiling / cold floor condition, keeping the operative temperature constant at the set point value, in order to exceed the limit values set by the standard.

Results obtained from the theoretical model will be verified by means of measurements as soon as the operation of the climate chamber is guaranteed. Moreover, they will be used to calibrate and set up the different radiant systems in order to perform experimental tests with human subject on radiant asymmetry and indoor environmental quality.

In future in fact, the test room will be used as a 4-person office to test the comfort and quality of the environment perceived by occupants changing environmental parameters. Participants will be required to perform typical tasks of a work environment (such as computer activities, etc.), in order to evaluate their productivity, and to give their opinion on the environmental conditions to which they are subjected.

REFERENCES

[1] "The Six Basic Factors." HSE. Accessed August 25, 2016. http://www.hse.gov.uk/temperature/thermal/factors.htm.

[2] U.S Department of Labor, Bureau of Labor Statistics, Occupational Outlook Handbook, 2012-13 Edition, Medical Assistants.

[3] B. Todorovic, Envelopes of building-the most influential factor of its energy efficiency, TTMD VI. International HVAC+R technology symposium, Istanbul, Turkey, 2004, p. 409-13.

[4] Department of Energy, Buildings energy databook, Office of Energy Efficiency & Renewable Energy.

[5] M. Tye-Gingras, L. Gosselin, Comfort and energy consumption of hydronic heating radiant ceilings and walls based on CFD analysis, Building and Environment 54 (2012) 1-13.

[6] ISO 7730, Ergonomics of the Thermal Environment-Analytical Determination and Interpretation of Thermal Comfort Using Calculation of the PMV and PPD Indices and Local Thermal Comfort Criteria, International Organization for Standardization, Geneva, Switzerland, 2005.

[7] EN 15251, Indoor Environmental Input Parameters for Design and Assessment of Energy Performance of Buildings Addressing Indoor Air Quality, Thermal Environment, Lighting and Acoustics, European Committee for Standardization, B-1050 Brussels, 2007.

[8] O. Fanger, Thermal comfort, Copenhagen: Danish Technical University, 1970.

[9] ASHRAE, Standard 55: Thermal environmental conditions for human occupancy, Atlanta, GA, USA: American Society for Heating, Refrigerating and Air Conditioning Engineers; 2010.

[10] PO. Fanger, Thermal comfort analysis and applications in environment engineering, 1972.

[11] C. Huizenga, Z. Hui, E. Arens, A model of human physiology and comfort for assessing complex thermal environments, Building and Environment 36 (6) (2001) 691-699.

[12] P. Roelofsen, The impact of office environments on employee performance: the design of the workplace as a strategy for productivity enhancement, Journal of Facilities Management 1 (3) (2002) 247-64.

[13] L. Lan, Z. Lian, L. Pan, Q. Ye, Neurobehavioral approach for evaluation of office workers' productivity: The effects of room temperature, Building and Environment 44 (2009) 1578-1588.

[14] L.M. Domínguez, O.B. Kazanci, N. Rage, B.W. Olesen, Experimental and numerical study of the effects of acoustic sound absorbers on the cooling performance of Thermally Active Building Systems, Building and Environment 116 (2017) 108-120.

[15] B.W. Olesen, E. Mortensen, J. Thorshauge, B. Berg-Munch, Thermal comfort in a room heated by different methods, ASHRAE Trans. 86 (1) (1980) 34-48.

[16] R.W. Kulpmann, Thermal comfort and air quality in rooms with cooled ceilings: Results of scientific investigations, ASHRAE Trans. 99 (2) (1993) 488-502.

[17] S. Schiavon, F. Bauman, B. Tully, J. Rimmer, Room air stratification in combined chilled ceiling and displacement ventilation systems, HVAC&R Res. 18 (1-2) (2012) 147-159.

[18] S. Schiavon, F.S. Bauman, B. Tully, J. Rimmer, Chilled ceiling and displacement ventilation system: Laboratory study with high cooling load, Science and Technology for the Built Environment 21 (7) (2015) 944-956.

[19] P. Mustakallio, Z. Bolashikov, K. Kostov, A. Melikov, R. Kosonen, Thermal environment in simulated offices with convective and radiant cooling systems under cooling (summer) mode of operation, Building and Environment 100 (2016) 82-91.

[20] H. Jia, X. Pang, P. Haves, Experimentally-determined characteristics of radiant systems for office buildings, Applied Energy 221 (2018) 41-54.

[21] C. Karmann, F.S. Bauman, P. Raftery, S. Schiavon, W.H. Frantz, K.P. Roy, Cooling capacity and acoustic performance of radiant slab systemswith free-hanging acoustical clouds, Energy and Buildings 138 (2017) 676-686.

[22] B. Ning, Y. Chen, H. Liu, S. Zhang, Cooling capacity improvement for a radiant ceiling panel with uniform surface temperature distribution, Building and Environment 102 (2016) 64-72.

[23] F. Bauman, J.D. Feng, S. Schiavon, Cooling load calculations for radiant systems: are they the same traditional methods?, ASHRAE Journal, December 2013.

[24] J.D. Feng, S. Schiavon, F. Bauman, Cooling load differences between radiant and air systems, Energy and Buildings 65 (2013) 310-321.

[25] J.D. Feng, S. Schiavon, F. Bauman, Experimental comparison of zone cooling load between radiant and air systems, Energy and Buildings 84 (2014) 152-159.

[26] J. Miriel, L. Serres, A. Trombe, Radiant ceiling panel heating–cooling systems: experimental and simulated study of the performances, thermal comfort and energy consumptions, Applied Thermal Engineering 22 (2002) 1861-1873.

[27] F. Causone, S.P. Corgnati, M. Filippi, B.W. Olesen, Experimental evaluation of heat transfer coefficients between radiant ceiling and room, Energy and Buildings 41 (2009) 622-628.

[28] M. Rahimi, A. Sabernaeemi, Experimental study of radiation and free convection in an enclosure with a radiant ceiling heating system, Energy and Buildings 42 (2010) 2077-2082.

[29] F.R. d'Ambrosio Alfano, M. Dell'Isola, B.I. Palella, G. Riccio, A. Russi, On the measurement of the mean radiant temperature and its influence on the indoor thermal environment assessment, Building and Environment 63 (2013) 79-88.

[30] P. Mustakallio, Z. Bolashikov, K. Kostov, R. Kosonen, A. Melikov, Thermal Conditions in a Simulated 6-person Meeting Room with Convective and Radiant Cooling Systems, Proceedings of 11th REHVA World Congress and the 8th International Conference on Indoor Air Quality, Ventilation and Energy Conservation in Buildings, 2013.

[31] A. Casale, F. Arpino, M. Dell'Isola, A. Massimo, A. Russi, Caratterizzazione del metodo di misura della temperatura media radiante e dell'assimmetria radiante mediante tecnica termografica, 15th CIRIAF National Congress, Perugia, Italy, April 9-11, 2015.

[32] B. Yang, S. Schiavon, C. Sekhar, D. Cheong, K.W. Tham, W.W Nazaroff, Cooling efficiency of a brushless direct current stand fan, Building and Environment 85 (2015) 196-204.

[33] M. Klemke, B.S. Gilani, M. Kriegel, Dynamic simulation and experimental validation of unsteady state operation of floor heating systems, CLIMA 2016 - proceedings of the 12th REHVA World Congress.

[34] S.J. Rees, P. Haves, An experimental study of air flow and temperature distribution in a room with displacement ventilation and a chilled ceiling, Building and Environment 59 (2013) 358-368.

[35] M. Behne, Indoor air quality in rooms with cooled ceilings. Mixing ventilation or rather displacement ventilation?, Energy and Buildings 30 (199) 155-166.

[36] T. Kim, S. Kato, S. Murakami, J. Rho, Studyon indoor thermal environment of office space controlled by cooling panel system using field measurement and the numerical simulation, Building and Environment 40 (2005) 301-310.

[37] E.M. Saber, R. Iyengar, M. Mast, Forrest Meggers, K.W. Tham, H. Leibundgut, Thermal comfort and IAQ analysis of a decentralized DOAS system coupled with radiant cooling for the tropics, Building and Environment 82 (2014) 361-370.

[38] J. Kolarik, J. Toftum, B.W. Olesen, Operative temperature drifts and occupant satisfaction with thermal environment in three office buildings using radiant heating/ cooling system, Proceedings of the Healthy Buildings Conference Europe, Eindhoven, The Netherlands, 2015.

[39] N. Rage, O.B. Kazanci, B.W. Olesen, Validation of a numerical model of acoustic ceiling combined with TABS, Conference: 12th REHVA World Congress CLIMA 2016, Aalborg, Denmark.

[40] E. Pittarello, "Influence of acoustical panels on cooling of Thermo-Active Building Systems (TABS)". MSc thesis, Technical University of Denmark, 2006.

[41] N. Rage, O.B. Kazanci, B.W. Olesen, Numerical simulation of the effects of hanging sound absorbers on TABS cooling performance, Conference: 12th REHVA World Congress CLIMA 2016, Aalborg, Denmark.

[42] A.A. Chowdhury, M.G. Rasul, M.M.K. Khan, Thermal-comfort analysis and simulation for various low-energy cooling-technologies applied to an office building in a subtropical climate, Applied Energy 85 (6) (2008) 449-462.

[43] B.W. Olesen, L. Mattarolo, Thermal comfort and energy performance of hydronic radiant cooling systems compared to convective systems, Proceeding of Healthy Buildings, 2009.

[44] CEN, 15251, Criteria for the Indoor Environment Including Thermal, Indoor Air Quality, Light and Noise, European Committee for Standardization, Brussels, Belgium, 2007.

[45] G. Salvalai, J. Pfafferott, M.M. Sesana, Assessing energy and thermal comfort of different low-energy cooling concepts for non-residential buildings, Energy Conversion and Management. 76 (2013) 332-341.

[46] S.P. Corgnati, M. Perino, G.V. Fracastoro, P.V. Nielsen, Experimental and numerical analysis of air and radiant cooling systems in offices, Building and Environment 44 (4) (2009) 801-806.

[47] B. Ning, S. Schiavon, F.S. Bauman, A novel classification scheme for design and control of radiant systembased on thermal response time, Energy and Buildings 137 (2017) 38-45.

[48] Q. Jin, M. Overend, P. Thompson, Towards productivity indicators for performance-based façade design in commercial buildings, Building and Environment 57 (2012) 271-281.

[49] L.T. Wong, K.W. Mui, P.S. Hui, A multivariate-logistic model for acceptance of indoor environmental quality (IEQ) in offices, Building and Environment 43 (2008) 1-6.

[50] A. Kawamura, S. Tanabe, N. Nishihara, M. Haneda, M. Ueki, Evaluation method for effects of improvement of indoor environmental quality on productivity, Proceedings of Clima 2007 WellBeing Indoors.

[51] Z. Wang, H.Ph.D. Zhang, E. Arens, D. Lehrer, C. Huizenga, T. Yu, S. Hoffman, Modeling thermal comfort with radiant floors and ceilings, 4th International Building Physics Conference, 2009, June 15-18, Istanbul.

[52] V. Gooje, Impact of radiant asymmetry of thermal comfort: Comparison of real data with simulated data, PLEA2013 - 29th Conference, Sustainable Architecture for a Renewable Future, Munich, Germany 10-12 September 2013.

[53] I. Atmaca, O. Kaynakli, A. Yigit, Effects of radiant temperature on thermal comfort, Building and Environment 42 (2007) 3210-3220.

[54] S. Moslehi, M. Maerefat, R. Arababadi, Applicability of Radiant Heating-Cooling Ceiling Panels in Residential Buildings in Different Climates of Iran, Procedia Engineering 145 (2016) 18-25.

[55] X. Hao, G. Zhang, Y. Chen, S. Zou, D.J. Moschandreas, A combined system of chilled ceiling, displacement ventilation and desiccant dehumidification, Building and Environment 42 (2007) 3298-3308.

[56] W.-H. Chiang, C.-Y. Wang, J.-S. Huang, Evaluation of cooling ceiling and mechanical ventilation systems on thermal comfort using CFD study in an office for subtropical region, Building and Environment 48 (2012) 113-127.

[57] J.A. Myhren, S. Holmberg, Flow patterns and thermal comfort in a room with panel, floor and wall heating, Energy and Buildings 40 (2008) 524-536.

[58] J. Niu, J.v.d. Kooi, Indoor climate in rooms with cooled ceiling systems, Building and Environment, Vol. 29, No. 3, pp. 283-290, 1994.

[59] H. Khorasanizadeh, G.A. Sheikhzadeh, A.A. Azemati, B. Shirkavand Hadavand, Numerical study of air flow and heat transfer in a two-dimensionalenclosure with floor heating, Energy and Buildings 78 (2014) 98-104.

[60] M. Maerefat, A. Zolfaghari, A. Omidvar, On the conformity of floor heating systems with sleeping in the eastern-style beds; physiological responses and thermal comfort assessment, Building and Environment 47 (2012) 322-329.

[61] J. Le Dréau, P. Heiselberg, Sensitivity analysis of the thermal performance of radiant andconvective terminals for cooling buildings, Energy and Buildings 82 (2014) 482-491.

[62] C. Leung, H. Ge, Sleep thermal comfort and the energy saving potential due to reduced indoor operative temperature during sleep, Building and Environment 59 (2013) 91-98.

[63] R. Zmeureanu, P. Fazio, Thermal performance of a hollow core concrete floor system for passive cooling, Building and Environment, Vol. 23, No. 3, pp. 243-252, 1988

[64] K.N. Nkurikiyeyezu, Y. Suzuki, G.F. Lopez, Heart Rate Variability as a Predictive Biomarker of Thermal Comfort, Journal of Ambient Intelligence and Humanized Computing, 2017.

[65] L. Schellen, M. Loomans, M.H. de Wit, B.W. Olesen, W.D. van Marken Lichtenbelt, The influence of local effects on thermal sensation under non-uniform environmental conditions - Gender differences in thermophysiology, thermal comfort and productivity during convective and radiant cooling, Physiology & Behavior 107 (2) (2012) 252-261.

[66] L. Schellen, M.G.L.C. Loomans, M.H. de Wit, B.W. Olesen, W.D. van M. Lichtenbelt, Effects of different cooling principles on thermal sensation and physiological responses, Energy and Buildings 62 (2013) 116-125.

[67] T. Imanari, T. Omori, K. Bogaki, Thermal comfort and energy consumption of the radiant ceiling panel system. Comparison with the conventional all-air system, Energy and Buildings. 30 (2) (1999) 167-175.

[68] B. Lin, Z. Wang, H. Sun, Y. Zhu, Q. Ouyang, Evaluation and comparison of thermal comfort of convective and radiant heating terminals in office buildings, Building and Environment 106 (2016) 91-102.

[69] T. Akimoto, S. Tanabe, T. Yanai, M. Sasaki, Thermal comfort and productivity - Evaluation of workplace environment in a task conditioned office, Building and Environment 45 (2010) 45-50.

[70] A.C. Boerstra, M. te Kulve, J. Toftum, M.G.L.C. Loomans, B.W. Olesen, J.L.M. Hensen, Comfort and performance impact of personal control over thermal environment in summer: Results from a laboratory study, Building and Environment 87 (2015) 315-326.

[71] X. Shan, J. Zhou, V.W.C. Chang, E. Yang, Comparing mixing and displacement ventilation in tutorial rooms: Students' thermal comfort, sick building syndromes, and short-term performance, Building and Environment 102 (2016) 128-137.

[72] L. Lan, Z. Lian, L. Pan, The effects of air temperature on office workers' well-being, workload and productivity-evaluated with subjective ratings, Applied Ergonomics 42 (2010) 29-36.

[73] L. Lan, P. Wargocki, Z. Lian, Quantitative measurement of productivity loss due to thermal discomfort, Energy and Buildings 43 (2011) 1057-1062.

[74] L. Lan, Z. Lian, Use of neurobehavioral tests to evaluate the effects of indoor environment quality on productivity, Building and Environment 44 (2009) 2208-2217.

[75] S.G. Hodder, D.L. Loveday, K.C. Parsons, A.H. Taki, Thermal comfort in chilled ceiling and displacement ventilation environments: vertical radiant temperature asymmetry effects, Energy and Buildings 27 (1998) 167-173.

[76] S. Olesen, Dr.P.O. Fanger, P.B. Jensen, O.J. Nielsen, Comfort limits for man exposed to asymmetric thermal radiation, Building Research Station, London, September, 1972.

[77] Dr.P.O. Fanger, L. Banhidi, B.W. Olesen, G. Langkilde, Comfort limits for heated ceilings, ASHRAE No. 2596.

[78] P.O. Fanger, B.M. Ipsen, G. Langkilde, B.W. Olesen, N.K. Christensen, S. Tanabe, Comfort limits for asymmetric thermal radiation, Energy and Buildings 8 (1985) 225-236.

[79] U. Satish, M.J. Mendell, K. Shekhar, T. Hotchi, D. Sullivan, S. Streufert, W.J. Fisk, Is CO2 an indoor pollutant? Direct effects of low-to-moderate CO2 concentrations on human decision-making performance, Environmental Health Perspectives, volume 120, number 12, December 2012.

[80] Z. Tian, J.A. Love, A field study of occupant thermal comfort and thermal environments with radiant slab cooling, Building and Environment 43 (2008) 1658-1670.

[81] C. Karmann, S. Schiavon, L.T. Graham, P. Raftery, F. Bauman, Comparing temperature and acoustic satisfaction in 60 radiant and all-air buildings, Building and Environment 126 (2017) 431–441.

[82] A.F. Neto, I. Bianchi, F. Wurtz, B. Delinchant, Thermal Comfort Assessment, Federal Institute of Santa Catarina - IFSC, Florianópolis, Brazil, September 12-14, 2016.

[83] J. Pfafferott, S. Herkel, D.E. Kalz, A. Zeuschner, Comparison of low-energy office buildings in summer using different thermal comfort criteria, Energy and Buildings 39 (7) (2007) 750-757.

[84] L. Zagreus, C. Huizenga, E. Arens, D. Lehrer, Listening to the occupants: a Web-based indoor environmental quality survey, Indoor Air 14 (s8) (2004) 65-74.

[85] J. Kim, C. Candido, L. Thomas, R. de Dear, Desk ownership in the workplace: The effect of non-territorial working on employee workplace satisfaction, perceived productivity and health, Building and Environment 103 (2016) 203-214.

[86] BS EN ISO 10077-1:2006, Thermal performance of windows, doors and shutters. Calculation of thermal transmittance. Part 1: General;

[87] ISO 11855:2015, Design, Dimensioning, Installation and Control of Embedded Radiant Heating and Cooling Systems, International Standards Organization, Geneva, Switzerland, 2012.

[88] CEN 15377, Heating Systems in Buildings. Design of Embedded Water Based Surface Heating and Cooling Systems, European Committee for Standardization, Brussels, Belgium, 2008.

[89] ASHRAE, Handbook HVAC Systems and Equipment, American Society of Heating, Refrigerating and Air-Conditioning Engineers, Inc., Atlanta, GA, USA, 2012.

[90] J. Babiak, B.W. Olesen, D. Petras, REHVA Guidebook No 7: Low Temperature Heating and High Temperature Cooling, first ed., Federation of European Heating and Air-conditioning Associations, Belgium, 2009.

[91] BS EN 1264-1:2011, Water based surface embedded heating and cooling systems - Part 1: Definitions and symbols.

[92] BS EN 1264-2:2008, Water based surface embedded heating and cooling systems - Part 2: Floor heating: Prove methods for the determination of the thermal output using calculation and test methods.

[93] CEN Standard TR 1752 1998. Ventilation for buildings: design criteria for the indoor environment; CEN.

[94] D. Müller, C. Kandzia, R. Kosonen, A. Melikov, P.V. Nielsen. Mixing ventilation - guidebook on mixing air distribution design. No.19. REHVA guidebook;2013.

[95] ASHRAE Standard 70-2006 (RA 2011). Method of testing the performance of air outlets and air inlets. Atlanta, GA, USA: American Society of Heating, Refrigerating and Air- Conditioning Engineers, Inc.; 2011.

[96] ANSI/ASHRAE Standard 113-2013. Method of testing for room air diffusion. Atlanta, GA, USA: American Society of Heating, Refrigerating and Air-Conditioning Engineers, Inc.; 2013.

[97] https://energyplus.net/weather-location/europe_wmo_region_6/ITA//ITA_Venezia-Tessera.161050_IGDG.

[98] P.O. Fanger, B.M. Ipsen., G. Langkilde, B.W. Olesen, N.K. Christinsn, S. Tanabe, (1985). “Comfort Limits for Asymmetric Thermal Radiation”. Energy and Buildings, 8, 225-236

SITOGRAPHY

- https://www.energyplus.net/sites/default/files/docs/site_v8.3.0/EngineeringReference/03-SurfaceHeatBalance/index.html#inside-heat-balance
- https://bigladdersoftware.com/epx/docs/8-4/engineering-reference/window-heat-balance-calculation
- http://biblus.acca.it/focus/benessere-termoigrometrico-e-comfort-termico/
- https://www.repubblica.it/salute/2017/07/02/news/aria_condizionata_regole_galateo_ufficio-166991332/?refresh_ce
- https://www.quotidianosicurezza.it/sicurezza-sul-lavoro/esperto-risponde/microclima-salute-ambienti-lavoro.htm